Universiteit Utrecht

Commercial astaxanthin production derived by green alga *Haematococcus pluvialis*: A microalgae process model and a techno-economic assessment all through production line

Georgios Panis

Utrecht University

Master Thesis (45 EC), 2015

Commercial astaxanthin production derived by green alga *Haematococcus pluvialis*: A microalgae process model and a techno-economic assessment all through production line

Author:
Georgios Panis
Franciscusdreef 28, 3565 AC Utrecht
g.panis@students.uu.nl/panis.george@gmai.com
Master: Sustainable Development; Track: Energy and Resources
Student number: 4113977

Supervisor:
Dr. Jesus Rosales Carreon
Department of Sustainable Development
Heidelberglaan 2, 3584 CS Utrecht
Room 9.11
J.RosalesCarreon@uu.nl

Second reader:
Dr. Robert Harmsen
Department of Sustainable Development
Heidelberglaan 2, 3584 CS Utrecht
Room 10.18
R.Harmsen@uu.nl

Hosting Institute:
Utrecht University
Department of Sustainable Development
Track: Energy & Resources
Heidelberglaan 2, 3584 CS Utrecht
Course Code: GEO4-2321
Period: November 2014-July 2015

To my family and George R.

Acknowledgements

This thesis constitutes the grand finale of my academic journey in Utrecht University. It is a product of my passion on the potentiality of microalgae in the food and feed sector in the years to come. Although the completion of this thesis involved countless sleepless nights in front of the computer and my abilities on conducting a research were tested to the limits, I highly enjoyed the process all through the past 8 months. A number of people helped me in order to carry through with this research and I would like to thank them individually in this section.

I would like to express my special appreciation and thanks to my supervisor Dr. Jesus Rosales Carreon for being a tremendous mentor for me. Jesus, I would like to thank you for encouraging my research and for allowing me to grow as a research scientist. Your advice on both the individual research as well as the personal values a scientist should acquire and develop, have been priceless. I consider myself fortunate that you highly contributed on developing the most fruitful relationship with a professor that I have ever experienced so far.

For the construction of the process model, environmental data and more specifically solar radiation and temperature data were necessary. I would like to thank my cousin, George Panetas, Sales Director of ETHER, for providing me confidentially detailed hourly solar radiation data for Livadeia.

Furthermore, I would like to express my deepest appreciation to my former water-polo teammate and venerated friend, George Reppas, Vice President of R^2 Strom GmbH/R Energy SA, for his valuable advice on how to conduct and present a Profit and Loss analysis associated with a microalgae production venture. Thanks to your advice back in 2010, I chose to enter the MSc of Sustainable Development and conduct a research on potentiality of microalgae.

Last but not least, a special thanks to my family. Words cannot express how grateful I am to my mother, father and my two sisters for all of the sacrifices that you've made on my behalf. You were always my support in the moments when there was no one nearby, providing me with the mental strength never to give up.

Abstract

The freshwater green microalgae strain *Haematococcus pluvialis* is the richest source for the production of natural astaxanthin. Astaxanthin is a pigment and member of the xanthophyll family of carotenoids that constitutes the highest value product derived by microalgae with a vast range of applications in the food, feed and pharmaceutical sector. So far, natural astaxanthin derived by microalgae amounts to <1% of the global market, since the synthetic alternative derived by petrochemicals involves lower production costs.

In this study, the technical and economic performance all through large scale production of natural astaxanthin, for two European cities (Livadeia, Greece and Amsterdam, the Netherlands) with different environmental conditions for cultivation, is investigated. The techno-economic assessment was facilitated by creating a process model, which simulated all phases of the production process. A hybrid system for photoautotrophic cultivation, comprising by a photobioreactor (PBR) for the 'green' stage and a raceway pond for the 'red' stage, was assumed. The area covered by the PBR and the raceway pond was assumed as 1 hectare respectively.

The technical part included the mass-energy flows during the production process. According to the results, the most important inflow in the system refers to freshwater. More specifically, 81662 (m^3/year) and 34281 (m^3/year) without recycling are needed for the production of 471 (kg/year) and 158 (kg/year) astaxanthin in Livadeia and Amsterdam respectively. The total energy needs were calculated at 494.8 (MWh/year) and 225.9 (MWh/year) for the Greek and the Dutch city respectively. This study investigated also the energy self-sufficiency of the production process by exploiting electricity generated by residual biomass gasification, after the pigment is recovered. It was found that only 12% for Livadeia and 9% for Amsterdam of the total energy needs were offset by residual biomass gasification.

As for economic performance, a Profit and Loss (P&L) analysis was conducted. The analysis involved the calculation of the CAPEX and annual OPEX that led to the determination of the return of investment (ROI) for different market prices of astaxanthin. It was found that only in Livadeia viability of a microalgae company can be achieved for all market prices. The costs for Livadeia and Amsterdam were calculated at €1122/kg and €3247/kg respectively, rendering only the Greek city as a decent site in order to compete with the synthetic alternative (costs of synthetic astaxanthin are €880/kg).

Table of Contents

1 Introduction

1.1 General

As global population and consequently energy demand increase over time, the introduction and commercialization of renewable sources of energy becomes a critical issue. Microalgal biomass as feedstock for bio-energy production (electricity, heat, biofuels) is an attractive alternative to bio-energy derived from terrestrial plant utilization (Mata et al., 2010). The major advantages that render microalgae a promising solution in the global energy agenda are their high growth rates, high lipid accumulation in the intracellular environment and their sturdiness against harsh conditions (Duan & Savage 2010; Mata et al., 2010; Bucy et al., 2012; Borowitzka, 2013). Nevertheless, recent researches have shown that microalgae cultivation solely for bio-energy production purposes seems not yet to be economically feasible (Clarens et al., 2010; Razon & Tan, 2011; Borowitzka, 2013; Koller et al., 2014). Therefore, other applications of microalgae have been investigated. Microalgae, cultivated under specific stress conditions (e.g. nutrient starvation, light stress, high acidity, temperature variations etc.), can accumulate, along with the lipids and carbohydrates, considerable amount of secondary metabolites. These metabolites constitute valuable compounds with an enormous range of industrial applications that strongly enhance a bio-based economy. (Markou & Nerantzis, 2013).

Among these metabolites, the carotenoid pigment astaxanthin is considered to be one of the most valuable compounds with a wide range of applications in the food, feed, cosmetics and pharmaceutical industry (Cardozo et al., 2007; Borowitzka, 2013; Koller et al., 2014; Pérez-López et al., 2014). Astaxanthin derived by microalgae corresponds to less than 1% of the commercialized quantity, since synthetic astaxanthin from petrochemicals is reported to involve lower production costs (Koller et al., 2014). Nonetheless, along with the transition towards natural products, it is expected that in the foreseeable future after the optimization of the production technology, the production costs of the natural astaxanthin should be more competitive to these of the synthetic alternative (Pérez-López et al., 2014).

There are only a few companies that produce natural astaxanthin from microalgae at commercial scale. Two of them are Cyanotech in USA and Algaetechnologies in Israel. Both cultivate photoautotrophically the alga strain *Haematococcus pluvialis* with a different combination of cultivation systems (Borowitzka, 2013). Natural photoautotrophic cultivation involves the use of sunlight as the energy carrier for photosynthesis and consequently microalgae blooming. Different values of light intensity, along with other climatic parameters, may have an adverse or favorable impact on algae growth. Thus, an investigation of this impact all through production line of astaxanthin for locations with different environmental regimes is of particular interest.

1.2 Background of the research

1.2.1 What are microalgae?

Microalgae are prokaryotic or eukaryotic photosynthetic aquatic microorganisms, which are naturally found in freshwater and marine environments, inhabiting a vast range of ecosystems, from the extremely cold (Antarctic) to extremely hot (deserts) regions of the Earth (Guschina & Harwood, 2006). They are considered to be one of the oldest living organisms in our planet representing a big variety of species; more than 300.000 (Alam et al., 2012). Nevertheless, only a small fraction of around 30.000 species has been studied and analyzed (Mata et al., 2010). Unlike normal plants, microalgae lack roots, stems and leaves, while their basic composition involves the elements: Carbon (C), Oxygen (O), Hydrogen (H), Nitrogen (N), Phosphorus (P) and sometimes Iron (Fe) and silicon (Si) (Brennan & Owende, 2010; Chisti, 2007). These elements constitute the building blocks of the different products that can be extracted by microalgae (see section 1.2.2).

In general, microalgae are classified in accordance with their color (Alam et al., 2012). The current systems of classification of microalgae are based on a) kinds of pigments, b) chemical nature of the stored products, and c) cell wall components, which define the different groups of species of microalgae (Dragone et al., 2010). Some additional criteria involve cytological and morphological characteristics: presence of flagellate cells, structure of the flagella, scheme and path of nuclear and cell division, presence of an endoplasmic reticulum envelope around the chloroplast and possible connection between the endoplasmic reticulum and the nuclear membrane (Tomaselli, 2004). Table 1 portrays some major groups of microalgae in terms of color (Alam et al., 2012).

Colour	Group
Yellow-green algae	Xanthophyceae
Red algae	Rhodophyceae
Golden algae	Chrysophyceae
Green algae	Chlorophyceae
Brown algae	Phaeophyceae
Cyanobacteria	Cyanophyceae

Table 1: Major microalgae groups based on their colors (Alam et al., 2012)

1.2.2 Applications

Microalgae constitute very promising bio-catalysts to be implemented in the increasing field of biotechnology. This is valid for the production of food, feed, fine chemicals and biofuels (Milledge, 2012; Wijffels et al., 2013) due to various reasons:

- Microalgae commonly double their biomass within 24 hours, with the shortest duration of this exponential growth be 3.5 hours (Bucy et al., 2012). Moreover, it is estimated that algae could yield 61000 liters of lipid oil per hectare (l/ha) compared to crop-based biofuels (e.g. derived from soybean, rapeseed, sunflower and palm) which vary from 200-450 (l/ha) (Duan and Savage, 2010).
- Microalgae are characterized by greenhouse gas fixation ability, meaning that the life-cycle of the product is characterized by carbon neutrality (net zero emission balance) (Alam et al., 2012). In this realm, CO_2 removal from industrial flue gases by algae bio-fixation is a promising alternative in order to reduce GHG emissions (Wang et al., 2008).

- Microalgae are characterized by sturdiness against harsh conditions (Mata et al., 2010). Wastewater treatment is a significant application, which takes advantage of this attribute. Microalgae can be employed for removal of inorganic nitrogen (N) and phosphorus (P) from wastewater as ammonium (NH_4^+) and phosphate (PO_4^{3-}), and from (nitrified) wastewater effluent as nitrate (NO_3^-) and (PO_4^{3-}), by assimilating these nutrients into their biomass (Wang et al., 2008).
- Microalgae are characterized by higher efficiency conversion of solar energy than higher plants (conventional forestry, agricultural crops, and other aquatic plants) in the natural chain due to their unicellular or simple multi-cellular structure (Mata et al., 2010).
- Microalgae cultivation result in high production capacity of dry biomass, since the feedstock does not compete with human and animal crops (Alam et al., 2012).

Although microalgal biomass is considered as the next generation of feedstock for biofuel production, their cultivation for sole biofuel production in commercial scale appears not yet to be economically feasible (Clarens et al., 2010; Razon & Tan, 2011; Borowitzka, 2013). More specifically, the general market price for biodiesel currently amounts to less than $0.5/kg with a production cost of $4/kg and even more (Sun et al., 2011). Nevertheless, some microalgal species cultivated under specific stress conditions (e.g. nutrient starvation, high acidity, temperature variations, light stress etc.) accumulate, along with the lipids and carbohydrates that could be used for biofuel production, specific secondary metabolites, such as sugars, pigments, vitamins, proteins and bioplastics (Markou & Nerantzis, 2013). These secondary metabolites constitute high-value products that could be applied on the cosmetic, food or pharmaceutical sector (Skjånes et al., 2012).

1.2.2.1 Pigments

Among these secondary metabolites, pigments are considered as the algal products of highest potential for commercial success in the near future (Spolaore et al., 2006). Algal pigments serve a very important role in order microalgae to thrive: They are responsible for light harvesting, CO_2 fixation, protection of algal cells against damage by excessive illumination, and, macroscopically, the coloration of the algal culture (Koller et al., 2014). Three major groups of pigments are found in microalgae, namely carotenoids (among them, carotenes provide an orange coloration, whereas xanthophylls are responsible for yellowish shade), phycobilins (red or blue coloration), and chlorophylls (green coloration) (Spolaore et al., 2006). Table 2 illustrates an overview of the different pigments derived by various microalgae species as well as their potential fields of application (Koller et al., 2014).

Pigment Group	Pigment name	Microalgal representatives	Color of pigment	Applications
Carotenoids (Carotenes)	ß-Carotene	Dunaliella salina, Dunaliella bardawil, Botryococcus braunii	Yellow	Pro-vitamin A; antioxidant; food additive E160a; coloration of egg yolk
Carotenoids (Tocopherol)	α-Tocopherol	Chlorella sp., Nannochloropsis oculata, Stichococcus bacillaris, Euglena gracilis	Brown	Vitamin E; food additive E306, E307, E308; antioxidant in cosmetics and foods
Carotenoids (Carotenes)	Bixin	Dunaliella salina	Yellowish to peach-color	Food additive E160b (colorant); cosmetics
Carotenoids (Xanthophylls)	Violaxanthin	Botryococcus braunii, Dunaliella tertiolecta, Nannochloropsis sp.	Orange	Food additive E161e
Carotenoids (Xanthophylls)	Astaxanthin	Haematococcus pluvialis, Botryococcus braunii	Reddish-salmon	Food additive E161j; antioxidant; farming of salmon and trout (color, immuno-response)
Carotenoids (Xanthophylls)	Fucoxanthin	Phaeophyceae	Brown to olive	Anti-adipositas
Carotenoids (Xanthophylls)	Lutein	Chlorella protothecoides, Chlorella zofingiensis, Botryococcus braunii, Chlorococcum citriforme, Dunaliella salina, Muriellopsis sp., Neospongiococcum gelatinosum	Yellow-orange	Food additive E161b; yellow coloration of egg yolk (feed additive); pigmentation of animal tissues; pharmaceutical: anti-macular degeneration, anti-colon cancer; cosmetics: coloration
Carotenoids (Xanthophylls)	Zeaxanthin	Botryococcus braunii, Dunaliella salina, Nannochloropsis oculata, Nannochloropsis gladitana	Orange-yellow	Food additive E 161h; animal feed; pharmaceutical: anti- colon cancer, eye health
Carotenoids (Xanthophylls)	Canthaxanthin	Nannochloropsis oculata, Nannochloropsis salina, Nannochloropsis gladitana	Golden-orange	Food additive E 161g; farming of salmonids and chickens; tanning pills
Phycobilins	Phycocyanin	Arthrospira, Spirulina	Blue-green (“cyano”)	Food colorant (beverages, ice cream, sweets); cosmetics; immunofluorescence techniques; antibody labels; receptors and other biological molecules
Phycobilins	Phycoerythrin	Cyanobacteria, Porphyridium	Red	Immunofluorescence techniques; labels for antibodies; receptors and other biological molecules
Chlorophylls	Chlorophyll a	All photoautotrophic oxygenic algae	Green	Pharmaceutical and cosmetical (deodorant)

Table 2: Microalgal pigments and potential fields of application — an overview (Koller et al., 2014).

1.2.2.2 Astaxanthin

Astaxanthin ($C_{40}H_{52}O_4$, 3,3'-dihydroxy-β,β'-carotene-4,4'-dione, see figure 1) is a member of the xanthophyll family of carotenoids and constitutes a high value product with high commercial potential that is ubiquitous in the watery nature (Markou & Nerantzis, 2013; Zhang et al., 2014). It is a substance best known for giving the pinkish-red hue to the flesh of salmonids (salmons and trouts), as well as shrimps, lobsters and crayfishes (Koller et al., 2014). These animals cannot synthesize astaxanthin *de novo,* since only plants, algae and some fungal-bacterial species synthesize astaxanthin among other carotenoids. Therefore, they have to introduce this pigment in their diet in order to absorb it (Goodwin, 1984). In the watery environment, astaxanthin is introduced in the food chain via biosynthesis in the microalgae (phytoplankton). This is the primary production level. Zooplankton consumes these microalgae and, in turn, is ingested by the abovementioned aquatic animals (Lorenz & Cysewski, 2000). Besides the colorant properties, astaxanthin displays a central role for the immune-system of these fishes and positively impacts their fertility (Koller et al., 2014).

Furthermore, astaxanthin is considered as the most powerful antioxidant in the nature. It is claimed to possess as much as 10 times the antioxidant potential of other carotenoids such as β-carotene, canthaxantin, zeaxanthin and lutein; and 100 times more that α-tocopherol. In other words it serves the role of a highly efficient scavenger of free radicals build up within the human body (Cyanotech, 2015; Koller et al., 2014). These antioxidant properties are of great significance in the human metabolism, since it is believed to play a key role in the amelioration/prevention of several human pathological processes: Astaxanthin is a substance that protects the skin against UV-induced photo-oxidation and that is used for anti-tumor therapies, inflammation and age-related diseases (Cardozo et al., 2007).

Figure 1 displays the chemical structure of astaxanthin with a numbering scheme.

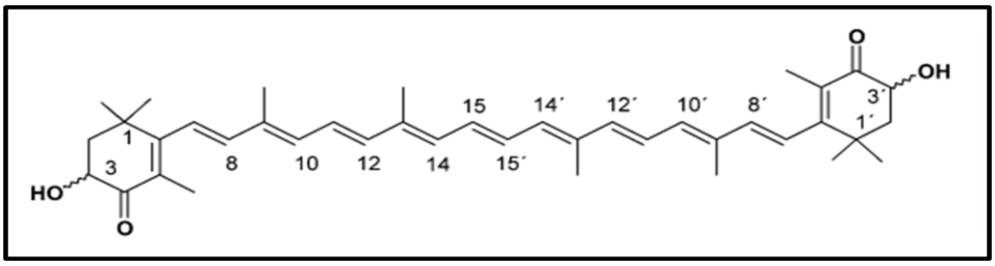

Figure 1: Chemical structure of astaxanthin with a numbering scheme (Zhang et al., 2014).

Astaxanthin has a great potential in the market. Nowadays, the estimated market value of astaxanthin depending on products' purity varies usually from $2500-7000/kg and may reach in special occasions $100000/kg, while its global market potential was estimated at 280 metric tons and was valued at $447 million in 2014 for synthhetic and natural astaxanthin (Milledge, 2010; Borowitzka, 2013; Koller et al., 2014; Pérez-López et al., 2014; Industry Experts, 2015). Of this market, more than 95% consumes synthetically derived astaxanthin, while astaxanthin derived from microalgae amounts to less than 1% of the commercialized quantity (Koller et al., 2014; Pérez-López et al., 2014). Synthetic astaxanthin is derived from petrochemical sources. This attribute raises the issues of food safety, pollution, and sustainability (Milledge, 2010). Furthermore, the production costs of the synthetic version are considerably high ($1000/kg) (Olaizola, 2003; Li et al., 2011). Therefore, as society, nowadays, stimulates a transition towards less expensive 'green' solutions, synthetic astaxanthin seems to be much less desirable (Pérez-López et al., 2014). In this realm, Li et

al. (2011) estimated a production cost of $718/kg astaxanthin, by conceptually scaling up a pilot plant, which resulted in an annual astaxanthin yield of 900 kg. These production costs are significantly lower than the ones from the synthetic version, posing clear market opportunities for natural astaxanthin derived by microalgae. In fact, studies have predicted the potential market value to be over 1.5 billion dollars by 2020 (Nguyen, 2013).

1.2.2.3 Bio-energy from residual biomass

After the extraction of the desired compound(s), the remaining unexploited microalgae biomass could be utilized by one of the current biomass energy conversion technologies, such as anaerobic digestion, anaerobic fermentation, pyrolisis, direct combustion, gasification etc. in order to produce bio-energy (Markou & Nerantzis, 2013). The criteria to choose one of these technologies depends on the composition of the remained biomass and the desired type of bio-energy (heat, electricity, biofuels) to be produced (Mohan et al., 2014). For instance, in the study of Nobre et al. (2013) the strain *Nannochloropsis sp*. was used for the production of fatty acids for biodiesel and high added-value compounds, while the leftover biomass was used as feedstock for biohydrogen production implementing dark fermentation. In another study, Alzate et al. (2014) show that after the extraction of lipids using again the strain *Nannochloropsis sp*, biochemical methane was produced through anaerobic digestion. Studies that focus on this binary perspective of microalgae are scarce.

1.2.3 Energy consumption during microalgae production process

The production process of microalgae in a production line consists of 3 phases: cultivation, harvesting and extraction (see sections 3, 4 and 5). These three phases involves various others steps, which all can be integrated in one facility called bio-refinery. The aim of a bio-refinery is to combine various processes and equipment to recover in the most sustainable way the desired compounds from the same batch of biomass, in a manner of production of intact commercial products (Vanthoor-Koopmans et al., 2013). One of the most important steps is the selection of the appropriate cultivation system. There are three alternatives for cultivating microalgae: open pond systems, closed systems called photobioreactors (PBRs) and hybrid systems, which combine distinct growth stages in PBRs and in open ponds (Brennan & Owende, 2010; Robert et al., 2012) (see section 3.3 and 3.5).

In order to reflect the extent of the energy needs through the production process of microalgae, Sudhakar et al. (2012a) portray a net energy balance assessment of large scale raceway open ponds. More specifically, the total electricity consumption in cultivation in open ponds was calculated 149000 (MJ/ha/year). The total electricity consumption in biomass harvesting phase was calculated 110000 (MJ/ha/year). Last but not least the total electricity consumption during the extraction phase was calculated 187000 (MJ/ha/year). The total electricity consumption of the three phases amounts consequently to approximately 446000 (MJ/ha/year). A large scale production line for microalgae cultivated in open ponds often involves areas of more than 100ha. Slade & Bauen (2013) give an example of 400ha for cultivation. For this area the total energy consumption during the three phases would then amount to 179200 (GJ/year). In UK, the average electricity consumption per household in 2013 was 4,192 kilowatt hours (kWh) or 15091 (MJ) (Prime et al., 2014).This means that the energy needs during the microalgae production process cultivated in open ponds in an area of 400ha are equivalent to the annual energy needs of 11874 households in UK.

1.3 Problem Description

In case of large scale astaxanthin production, these numbers have not been yet investigated in deep. This pigment seems to have high economic potential in the market (see section 1.2.2.2). In order to reflect on this potential, however, a detailed analysis on the associated mass-energy flows and costs is essential. Hitherto, there is little scientific research on the performance and viability of large scale astaxanthin production lines, and most publications focus on either laboratory or pilot scale. This constitutes a knowledge gap that this Master thesis aims to fill. The mass-energy flows as well as the economic performance during the production process of microalgae for the scaling up of astaxanthin constitute the core of this Master Thesis.

Furthermore, as already mentioned in section 1.2.2.3, along with the production of astaxanthin, the remaining unexploited microalgae biomass could be used for bio-energy production. This bio-energy could be carried by biogas, which in turn could be converted into electricity in order to power the bio-refinery, stimulating that way sustainable development and circular economy. Therefore, it is worth exploring, which amount of bio-energy from residual biomass can be generated in order to compensate the energy needs during microalgae life-cycle in a bio-refinery. Such investigation will exhibit the potential of a low carbon operation and self-sufficiency of the system. The investigation on the residual bio-energy constitutes the second aim of the Master thesis. The aim is to fill the knowledge gap regarding fossil fuel energy independence in terms of electricity during the production process in a large scale microalgal bio-refinery.

1.3.1 Research Questions

1.3.1.1 Main research question

What are the expected mass-energy flows as well as economic performance involved in large scale production of astaxanthin derived by microalgae?

1.3.1.2 Sub research questions

- *What is the most suitable microalgae species to cultivate?*
- *What is the optimal yield of astaxanthin recovered?*
- *What is the amount of bio-energy (electricity) derived by the by-products after recovery of astaxanthin?*
- *To what extent can the energy needs of the system be met by bio-energy (electricity) derived by residual biomass after recovery of astaxanthin?*

1.3.2 Problem Limitations

This research focuses only on microalgae life-cycle for the production of astaxanthin. The production of other chemical compounds that could be introduced in the food, feed, cosmetics and pharmaceutical sector will not be investigated. Furthermore, this research will examine the potential of biogas production that could be converted into electricity in order to satisfy the energy needs all through production line. The possibilities for heat and biofuel production will not be taken into account. Last but not least, since large scale biorefineries for the production of astaxanthin are yet at initial stage, assumptions have to be made in the process model, mass and energy balances and economic calculations as well. These assumptions will be based mainly on literature research.

2 Methods

2.1 General

This research was based on four elements: 1) a process model; 2) mass-energy flows; 3) bio-energy (electricity) generation and energy balance ratios (EBRs); and 4) economic evaluation for large scale astaxanthin production. In figure 2, the multi-path and the dynamic interdependence of the four elements are depicted. For cultivation phase, the performance of a hybrid system is investigated. Regarding harvesting and extraction phases, there are different techniques to follow. Hence, a comparative research was conducted in order to select the most suitable process regarding three aspects: costs, energy intensity and risks.

2.2 Microalgae process model

Due to the limited studies that investigate adequately all phases (cultivation, harvesting and extraction) regarding astaxanthin production, a model was constructed to simulate the production chain. The first and most important step of the astaxanthin production chain is the cultivation of a microalgae strain, since harvesting and extraction phases performance depends on the algal biomass developed during cultivation. Thus, the core of the process model refers to microalgae cultivation. In this thesis, modelling of cultivation phase is based on previous attempts to simulate algae growth, scientific literature on micro-algae growth and cultivation systems and other publications related to microalgae growth parameters.

After cultivation, harvesting and extraction take place. The goal of these phases revolves around the dewatering of the 'wet' biomass and the recovery of the desired metabolite (see sections 4 and 5). There is an abundance of methods that can be employed during harvesting and extraction. A comparative research was conducted to end with the most appropriate combination of methods for the production of astaxanthin. These methods were then introduced into the process model, which in turn calculated the yield of astaxanthin for the selected locations.

2.2.1 Samples

There are different nutritional modes to cultivate microalgae. In this thesis, natural photoautotrophic metabolism is investigated. The most crucial parameter for natural photoautotrophic microalgae cultivation is solar irradiance, since light is the main input for photosynthesis (see sections 3.2.1 and 3.6.2). Algae cells proliferation depends directly on the levels of solar irradiance, and significantly high or low values may result in an adverse impact on algal biomass productivity and the desired metabolite accumulation. For instance, microalgae cannot bear temperatures higher than 15–35°C, which means that high solar irradiance values that lead to increased temperatures, may hinder optimal microalgae growth (Arnold, 2013). Therefore, regional scenarios are necessary. In this thesis, two cities of two countries of different latitude are selected for investigation. These cities are Livadeia, Greece (38°43'33'' N/22°86'67'' E) and Amsterdam, the Netherlands (52°36'67'' N, 4°90'00'' E). As main model input, detailed climate data (irradiance and temperature data) throughout a calendar year (2014) were used in order to determine 'wet' biomass productivity in the two cities. For Livadeia, ETHER, a company focused on photovoltaic parks, provided the appropriate climate data. For Amsterdam, the climate data were derived by the official website of Royal Netherlands Meteorological Institute (in Dutch Koninklijk Nederlands Meteorologisch Instituut). All other data that play a role in algae growth were assumed as constants and they were determined conducting literature research.

2.3 Mass - Energy Flows

The annual biomass productivity determined by the process model is input for the mass and energy flows all through production line. The mass flows refer to the in- and outflows of the different substrates, while the energy flows refer to the direct energy consumption of equipment within the system boundaries. Relevant mass-energy reference values associated with the different phases were sourced by experts and scientific publications on the already existing large scale production lines or laboratory/pilot plants that were scaled up conceptually. When needed, assumptions have been made.

2.4 Residual bio-energy generation and Energy Balance Ratio (EBR)

After astaxanthin recovery, the residual biomass could be exploited for the production of bio-energy. In this thesis, the potential of electricity generation is investigated. This process involves a comparative research on the different technologies that can convert the calorific value of algal biomass into electricity. The selection of the most appropriate bio-energy conversion technology is based mainly on the conversion and cost efficiency point of view. Taking into account the bio-energy produced as well as the energy flows (requirements) all through production line, the energy balance ratio (EBR) can be determined. The energy balance ratio is defined as the ratio of total energy inputs to the total energy outputs inside the boundaries selected for a system (Shirvani et al., 2011; Khoo et al., 2013):

$$(\text{EBR}) = \frac{\sum \text{Energy input}}{\sum \text{Energy output}} \quad (\mathbf{1})$$

The EBR reflects the potential of energy efficiency inside the boundaries of a system. In this thesis, the EBR delineated the potential of meeting the energy needs all through production line. Furthermore, the EBR was calculated for each individual step of the production chain that consumes electricity. In such way the extent of compensation for each step can be depicted.

2.5 Economic Performance

In the economic evaluation, a Profit and Loss (P&L) analysis took place. The costs involved in all three phases of the production chain of astaxanthin in the selected locations referred to the capital expenditures (CAPEX) and operational expenditures (OPEX). CAPEX included equipment costs and fixed capital costs (i.e. all processes needed in order to construct the bio-refinery) and was determined using data found in the literature for large scale microalgae production lines. OPEX refers to all costs in order the bio-refinery to operate, and was derived from cost analysis based on the mass-energy flows associated with the system selected. The profits were determined by the market prices for astaxanthin and residual biomass if energy needs compensation is not an attractive option. The P&L analysis resulted in a financial statement that summarized the revenues, operational costs and other expenses incurred in an annual basis for the selected locations. The cornerstone of this statement refers to the return of investment (ROI). ROI reflects the potential of a microalgae production company to offset the CAPEX, and constitutes a valuable tool to assess its viability from a business point of view. The formula to calculate ROI is given below:

$$\text{ROI} = \frac{\text{CAD}}{\text{CAPEX}} * 100\% \quad (\mathbf{2})$$

CAD is the abbreviation for cash available for distribution to shareholders and its calculation is presented in detail in section 10.3.

Besides ROI, the determination of costs per kg of natural astaxanthin shows the potential in the market over the synthetic alternative. Thus in this thesis, OPEX was divided with the annual astaxanthin yield calculated by the process model in order to calculate costs per kg of natural astaxanthin.

Figure 2 illustrates the flow diagram of the methods.

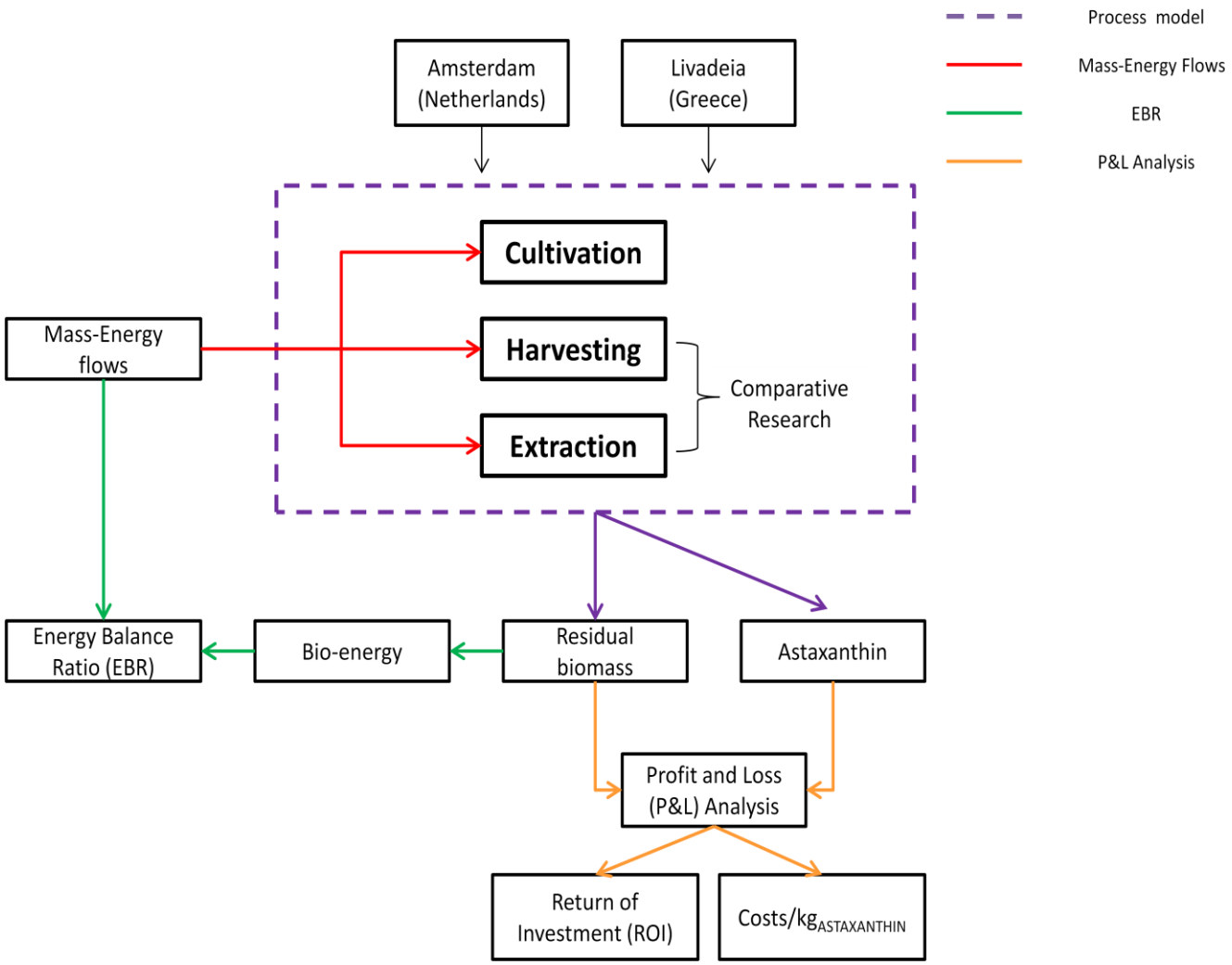

Figure 2: Flow diagram of the methods.

3 Cultivation phase

3.1 Introduction

Microalgae cultivation constitutes the most important phase among the three phases (i.e. cultivation, harvesting and extraction) that build the production line. A successful cultivation results in a 'healthy' highly concentrated algal broth, which can be further processed for the extraction of the desired metabolite. In this chapter all parameters that play a role in microalgae cultivation are analyzed, targeting to astaxanthin accumulation inside the algal cells. This analysis was the base in order to construct and run the microalgae process model, which calculated the annual astaxanthin productivity for the selected locations.

3.2 Nutritional Modes of Microalgae

Microalgae may assume four types of metabolisms and are capable of a metabolic shift as a response to changes in the environmental conditions. These modes are discussed in detail in the following sections.

3.2.1 Photoautotrophic Metabolism

Photoautotrophic metabolism is the most common procedure to cultivate microalgae in open ponds and photobioreactors. It involves the use of light (either sunlight or artificial light) as energy source and inorganic carbon (e.g. derived from CO_2) as the carbon source for the formation of biochemical energy through photosynthesis (Huang et al., 2010). This mode has three major advantages: First, autotrophic cultivation enhances sustainable development, since it requires large quantities of CO_2 as a carbon source, which could be derived from factories and power plants (Chen et al., 2011). Second, this mode is involved in less severe contamination problems compared to other modes (Chiu et al., 2008). Third, the simplicity of growing microalgae photoautotrophically makes this option the most cost-efficient among the different nutritional modes (Mohan et al., 2014). However, since photoautotrophic cultivation requires large quantities of CO_2 as a carbon source, the cultivation site should be close to industrial areas that can supply a large amount of CO_2 for microalgal growth (Mata et al., 2010). Besides the site limitation, there is a limitation in biomass productivity as well. In photoautotrophic cultivation the algal cells are most of the times subjected to stress conditions, in order to force the cells to accumulate the desirable metabolite (see sections 1.2.2 and 3.4). Achieving higher concentrations of the desirable product photoautotrophically is usually at the expense of lower biomass productivity (Chen et al., 2011).

3.2.2 Heterotrophic Metabolism

Heterotrophic metabolism is the mode of nutrition, where microalgae utilize solely organic carbon or substrates (such as such as glucose, acetate, glycerol and fructose) as primary energy and carbon source for their growth (Mata et al., 2010; Chen et al., 2011). Unlike photoautotrophic metabolism, heterotrophic metabolism takes place in absence of light in conventional fermentors, since the growth of the microalgae in the dark heterotrophic operation is enhanced by a carbon source, which replaces light energy (Chen et al., 2011; Perez-Garcia et al., 2011). The two major advantages of this mode are the possibility to obtain extreme biomass productivity - cell density (the highest among the different modes and nearly 20 times higher than that obtained under photoautotrophic cultivation and the facilitation of wastewater as a base environment for cultivation (Chen et al., 2011; Perez-Garcia et al., 2011). However, a heterotrophic system frequently suffers from contamination

problems (Olguin et al., 2012). Furthermore, the costs are higher than in photoautotrophic metabolism, mainly due to the high costs of organic carbon used for the algal cultivation (Chen et al., 2011).

3.2.3 Mixotrophic Metabolism

Mixotrophic metabolism is a variant of the heterotrophic metabolism and constitutes the combination of photoautotrophic and heterotrophic metabolisms. Photosynthesis is the main energy source, however, in the absence of light organic carbon could serve the role of energy carrier. Regarding carbon assimilation, both organic compounds as well as inorganic carbon (CO_2) facilitate the process (Chang et al., 2011). In other words, this technique takes advantage of an attribute that microalgae possess, which is their flexibility to switch their nutritional mode (thriving under either photoautotrophic or heterotrophic conditions, or both) based on substrate availability and light conditions (Mohan et al., 2014). Highly controlled environmental conditions are essential for successful mixotrophic cultivation. Therefore, photobioreactors (PBRs) are deemed to be the most suitable cultivation systems (Chen et al., 2011). The main advantage of this nutritional mode refers to its independence in terms of both photosynthesis and growth substrates (Kong et al., 2012). On the other side, mixotrophic culture systems are more sophisticated and the equipment used is more expensive than photoautotrophic and heterotrophic systems. Operational costs increase more if high substrate costs are taken into account. Last but not least, contamination issues have been reported as well (Chen et al., 2011).

3.2.4 Photoheterotrophic Metabolism

In this mode, the microalgae require light as energy source, while using organic compounds as the carbon source (Chen et al., 2011). The difference between mixotrophic and photoheterotrophic cultivation is that the latter requires light as the energy source, while mixotrophic cultivation can use either light or organic compounds to serve this purpose. Thus, photoheterotrophic cultivation needs both sugars and light simultaneously (Chojnacka and Marquez-Rocha, 2004). This mode is suitable for a few algal strains, which accumulate high quality of specific metabolites developed only under photoheterotrophic conditions (Mata et al., 2010). Like mixotrophic culture systems, photoherotrophic systems are highly sophisticated, which leads to high operational costs (Chen et al., 2011).

3.2.5 Comparison of the different nutritional modes

There is little information on the commercial potential of mixotrophic and photoheterotrophic cultivation (Mata et al., 2010). This means that the design of a special cultivation system might be required having as a consequence the increase of operational costs. On the other hand, a heterotrophic system seems to be promising for massive microalgae growth combined with biological cleaning. Nonetheless, there are two major limitations. Heterotrophic culture can get contaminated very easily causing problems in large-scale production (Olguin et al., 2012) and the cost of an organic carbon source is also a major concern from the commercial point of view (Chen et al., 2011). In photoautotrophic cultivation, even though the biomass productivity is the lowest among the different nutritional modes, lower costs for scaling up, potential uptake of CO_2 from flue gases and fewer contamination problems render this mode the most preferable for large scale

production lines (Mata et al., 2010). In this realm, Brennan & Owende (2010) state explicitly that microalgae cultivation under photoautotrophic metabolism is the only method, which is technically and economically feasible for large-scale production of algae biomass in order to exctract non-energy products. Furthermore, this research aims to investigate the microalgae life-cycle for the production of natural astaxanthin, by constructing a model that employs solar irradiation data as the energy source for microalgae growth. In other words, the potential productivity due to different solar irradiation values is calculated (see section 6). Therefore, among the different nutritional modes of microalgae, photoautotrophic metabolism is chosen throughout cultivation phase.

Table 3 portrays concisely the findings on the different nutritional modes discussed in sections 3.2.1-3.2.5.

Nutritional mode	**Energy source**	**Carbon source**	**Biomass productivity**	**Culture system**	**Advantages**	**Disadvantages**
Photoautotrophic	Light	Inorganic	Low	Open pond or PBR	Industrial CO_2 uptake; Less contamination; cost-efficient;	Low Cell density; Site limitation
Heterotrophic	Organic	Organic	High	Conventional fermentor	High biomass productivity; wastewater facilitation	Contamination; High substrate cost
Mixotrophic	Light and Organic	Inorganic and organic	Medium	Sophisticated PBR	Growth parameters independence	Contamination; High operational costs;
Photoheterotrophic	Light	Organic	Medium	Sophisticated PBR	High quality metabolites	High operational costs;

Table 3: Overview of the different types of nutritional modes for microalgae cultivation

3.3 Microalgae Culture systems

3.3.1 Introduction

In this research, microalgae biomass productivity is determined using solar irradiation and temperature data as the main input in the microalgae process model (see section 6.2). Consequently, the chosen culture system should be installed outdoors (i.e. light permeable) and should facilitate high biomass productivity with high concentration of astaxanthin as well. Along with the growth requirements, the cultivation system characteristics play a crucial role on microalgae growth. Depending on the local conditions and the available materials, different culture systems can be used, which vary in size, shape, construction materials, inclination and agitation type (Mata et al., 2010). These systems are divided into three main categories: open pond systems, closed systems called photobioreactors (PBRs) and hybrid systems (Brennan & Owende, 2010; Robert et al., 2012). According to Maity et al. (2014), these categories may assume an abundance of different types. Admittedly, not all types are described, since that would be outside the scope of this research. In this section a general overview of the three main categories for cultivation is presented. The most important types for each category that refer to photoautotrophic cultivation are exhibited as well.

3.3.2 Open Pond Systems

The vast bulk of microalgae cultivated today are grown in open ponds. Cultivation of microalgae in open pond systems imitates the natural way (in lakes, lagoons, ponds etc.) of algae growth (Chisti, 2007). Among the various sizes and shapes of ponds, the major designs for microalgae biomass production include (Chisti, 2007; Mata et al., 2010; Mohan et al., 2014; Schenk et al., 2008): 1) Raceway ponds, which include a closed loop recirculation channel driven by paddle wheels; 2) Circular ponds with agitation provided by a rotating arm; 3) shallow natural ponds (large in size), which are characterized by the absence of any mixing/circulation technique; 4) inclined systems, in which mixing is achieved through pumping and gravity flow.

Compared to PBRs, open pond systems are a cheaper method (3-10 times lower) of large-scale algal biomass production in terms of construction and operation costs (Mohan et al., 2014). Although open pond systems occupy more extensive land areas than PBRs, they do not necessarily compete for land with high-value lands and crop-producing areas, since they can be constructed on degraded and nonagricultural lands with marginal crop production potential (Brennan & Owende, 2010, Harun et al., 2010). Open pond systems require lower energy input, while regular maintenance and cleaning are easier than PBRs, since there is large open access to remove the bio-film that builds up on the surface (Schenk et al., 2008).

On the contrary, open pond cultivation inherits a variety of drawbacks as well. Uncontrolled environmental conditions in and around the open pond systems pose multiple of constraints, which may directly or indirectly affect microalgae growth, leading to less biomass productivity compared to PBRs (Mohan et al., 2014). Being open to the atmosphere, open pond systems are more susceptible to weather conditions, which result in loss of water by evaporation similar to land crops and in poor light and CO_2 diffusion from the atmosphere (Schenk et al., 2008; Mata et al., 2010; Perez-Garcia et al., 2011). Furthermore, contamination is a major problem during open pond cultivation: Generally, a new open pond system is vaccinated with the desired algal culture, which thrives and dominates the pond flora (Schenk et al., 2008). However, predators and other undesired algal species may invade into the pond reducing severely biomass yields and even out-competing the vaccinated species (Brennan & Owende, 2010). Last but not least, due to large area of open pond systems and uncontrolled environmental conditions, temperature control constitutes a challenging process: In open pond systems, any cooling is achieved only by evaporation, while temperature of the growth medium fluctuates within a diurnal cycle and seasonally (Chisti, 2007).

3.3.3 Closed systems - Photobioreactors (PBRs)

Microalgae cultivation in PBRs aims to overcome some of the major problems associated with the open pond systems described above. PBRs are closed flexible systems, which provide more controlled environment conditions than open pond systems, since microalgae in PBRs are isolated from the ''threats'' of the open atmosphere (Chisti, 2007). More specifically, in a PBR, direct exchange of gases and contaminants (e.g. microorganisms, invasive algae species, dirt) between the algal cells and the atmosphere is prevented by the reactor's walls (Mata et al., 2010). Besides the protected environment, PBRs are considered to point up more advantages over open pond systems (Mohan et al., 2014): PBRs facilitate better control over culture conditions and growth parameters such as PH levels, optimal temperature, nutrients, water supply, solar irradiation absorption, CO_2 supply and mixing regime. But the biggest advantage of PBRs over open pond systems is the biomass productivity that can be achieved (Ramanathan et al., 2011). Chisti (2007) mentions that the typical

biomass concentration that is produced in PBRs is up to 30 times the biomass concentration, which is generally produced in open pond systems, while volumetric biomass productivity of PBRs is more than 13-fold greater.

The most popular designs of PBRs involve flat plate, vertical column and tubular PBRs (Mohan et al., 2014):

Flat plate PBRs are the oldest form of PBRs and have received much research attention due to the large surface area exposed to illumination (Ugwu et al., 2008) and high densities of photoautotrophic microalgal cells observed. In some cases these densities may exceed 80gr/l (Brennan & Owende, 2010). On the other hand, it is difficult to control the culture temperature and there is some degree of wall growth, while scaling-up requires an abundance of compartments and materials. Therefore, microalgae cultivation using a flat plate PBR is a rather expensive alternative (Mohan et al., 2014).

Vertical column PBRs have a low surface/volume but they offer the most efficient mixing, the highest volumetric mass transfer rates, and the best controllable growth conditions (Ugwu et al., 2008). Consequently, cultures suffer less from photo-inhibition and photo-oxidation, and experience a more adequate light–dark cycle (Janssen et al., 2003). Limitations involve the high costs of construction and operation, the sophisticated construction and the shear stress to algal cultures (Mata et al., 2010).

Tubular PBRs are divided into horizontal, vertical, inclined and helix (Mata et al., 2010). They have design limitations on length of the tubes (Eriksen, 2008), and thus, large-scale production plants are based on the integration of multiple reactor units, which require large land space (Brennan & Owende, 2010). Further limitations involve fouling, some degree of wall growth, dissolved oxygen and CO_2 along the tubes, and the pH gradients (Mata et al., 2010). Nonetheless, compared to the different PBRs, tubular PBRs are relatively cheaper to construct and operate and constitute the most appropriate alternative for outdoor cultivation (Chisti, 2007).

Table 4 illustrates a comparison among open pond systems and PBRs adapted from Mata et al. (2010) and Iersel et al. (2009):

Culture Parameters	Closed systems (PBRs)	Open ponds systems
Contamination control	Easy	Difficult
Contamination risk	Reduced	High
Process control	Easy	Difficult
Species control	Easy, switching possible	Difficult to switch
Mixing	Uniform	Poor
Operation regime	Batch or semi-continuous	Batch or semi-continuous
Space required	A matter of system selected	PBRs < Ponds
Weather dependence	Medium (light intensity, cooling required)	High (light intensity, temperature, rainfall)
Space required	In general small	Big
Population density (algal cell)	High	Low
Capital/operating costs	High	Low (3-10 times lower)
Light utilization efficiency	High	Poor
Temperature control	More uniform temperature, cooling often required	Difficult (temperature is highly variable)
Volumetric Productivity	13 times more	Low
Water losses	Depends upon cooling design	Open Ponds > PBRs
Hydrodynamic stress on algae	Low–high	Very low
Evaporation of growth medium	Low	High
Gas transfer control	High	Low
CO_2 losses	Low	High
O_2 concentration	O2 must be removed to prevent inhibition of photosynthesis and photo-oxidative damage	Usually low enough because of continuous spontaneous outgassing
Biomass concentration	up to 30 times more in PBRs	PBRs > Ponds
Scale-up	Difficult	Easy

Table 4: General comparison between open pond systems and PBRs (adapted from Mata et al., 2010; Iersel et al., 2009)

PBRs cultivation constitutes a very promising way for massive algal biomass production. However, despite their advantages, there is still the need to fill the gap between designing a high-end reactor, which meets all demands of the algal cells on the one hand, and a cheap reactor on the other hand, which enhances the economic viability of the process.

3.3.4 Hybrid systems

Hybrid cultivation constitutes a method that combines different cultivation systems. This method involves usually distinct growth stages in one open pond system and in one PBR (Brennan & Owende, 2010). More specifically, the first stage takes place in a PBR, where controllable conditions minimize contamination from other organisms and facilitate continuous cell division (see advantages of PBRs in section 3.3.3). The second stage refers to the exposition of microalgae to stress environmental and nutritional conditions, which enhance the synthesis of the desirable metabolite. This stage is ideally suited to open pond systems, as environmental stresses can occur naturally, when transferring the culture from the PBR to the open pond system (Huntley & Redalje, 2007; Rodolfi et al., 2008).

In this thesis a hybrid culture system comprised of a tubular PBR and a raceway pond was chosen to be used in the microalgae process model. More information that justifies the selection of a hybrid culture system is presented in sections 3.4 and 3.5.

3.4 Species

There are several microalgae strains that are reported as potential feedstock to produce astaxanthin, such as *Chlorella sp*., *Chlorococcum sp*. and *Scenedesmus sp*. (Del Campo et al., 2004; Ma and Chen, 2001; Qin et al., 2008). Nevertheless, the accumulation of astaxanthin inside *Haematococcus pluvialis* cells exceeds any other known microalgae strain (up to 4% of dry biomass) and thus it is the most preferred species for large scale natural astaxanthin production (Zhekisheva et al., 2005).

Haematococcus pluvialis is a freshwater strain of green microalgae with a very unique life, which is divided in two stages (Boussiba, 2000): The first refers to a green, motile vegetative stage, in which the microalgal cells continuously divide and proliferate (following specific growth kinetics), synthesizing chlorophyll. The second refers to a red, non-motile resting stage, in which cell division stops and chlorophyll levels do not fluctuate, resulting in a continuous increase of astaxanthin content and cellular dry weight (see figure 3). In order *Haematococcus pluvialis* to transit from stage one ('green stage') to stage two ('red stage'), specific stress conditions during cultivation are needed. This means that the accumulation of astaxanthin can be induced by any factor that inhibits cell proliferation.

Figure 3 illustrates the microscopic depiction of the two stages of *Haematococcus pluvialis* cultivation (Lorenz & Cysewski, 2000).

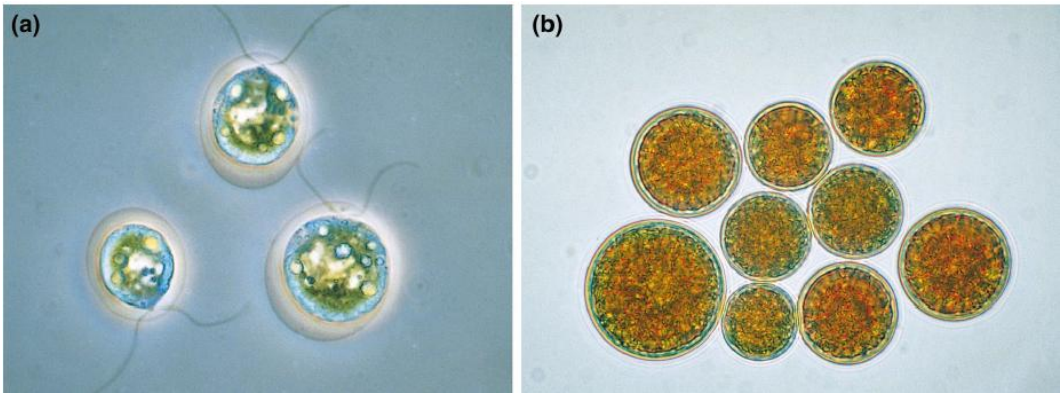

Figure 3: (a) 'Green stage': Vegetative actively growing *Haematococcus pluvialis* cells. (b) 'Red stage': *Haematococcus pluvialis* that have accumulated astaxanthin as a result of nutrient starvation and adverse environmental conditions (Lorenz & Cysewski, 2000).

The optimal environmental and nutritional conditions for each stage are quite different (Del Rio et al., 2007). Many studies report that during 'green stage' full nutrient medium and moderate light intensity, temperature and pH are required (Boussiba, 2000; Aflalo et al., 2007; Del Rio et al., 2007;). In the 'red stage', the inhibition of cell proliferation and, thus, the accumulation of astaxanthin using *Haematococcus pluvialis,* are triggered, when microalgal cells experience nutrient starvation, such as nitrogen, phosphorus and sulfur. Further adverse environmental conditions involve salt stress, high temperature and high light intensity (Boussiba and Vonshak, 1991; He et al., 2007; Markou & Nerantzis, 2013).

Due to such discrepancies, it is reported that the two stages should be separated into different cultivation systems: First producing green biomass under optimal growth conditions ('green stage') and next exposing algal cells into the abovementioned stress environmental conditions to induce astaxanthin accumulation ('red stage') (Boussiba, 2000; Orosa et al., 2005; Aflalo et al., 2007).

Nevertheless, recent studies proposed the implementation of a simpler one-step strategy for the production of astaxanthin processing *Haematococcus pluvialis*. This strategy involves the imposition of nitrate starvation and specific average irradiance in the fresh medium, resulting in simultaneous algal cell growth and astaxanthin accumulation (Del Rio et al., 2007). Although the one-stage cultivation seems attractive, since it is less complicated than the two-stage cultivation and the production of astaxanthin takes place in a continuous mode, it has two serious drawbacks (Aflalo et al., 2007): First, the actual astaxanthin production is significantly lower compared to the two-stage cultivation. Second and more important, the one-stage cultivation is unsuitable to outdoors setting, since it requires incessant illumination. This means that one-step cultivation needs illumination during night as well. This can be achieved only by using artificial light (the most common are fluorescent lamps and tungsten-halogen lamps), something that is out of the scope of this research. Thus, this research focuses on the two-stage cultivation.

3.5 Selection of culture system

3.5.1 Introduction

Taking into account the need of a two-stage cultivation (see section 3.4), this research investigated the performance of a hybrid culture system, which consists of one horizontal tubular photobioreactor and an open raceway pond. In terms of economic feasibility and high astaxanthin yields, this combination seems to be the most suitable (Li et al., 2011; Borowitzka, 2013). Data availability was another reason for choosing these cultivation systems, since most large scale systems for microalgae cultivation are either tubular photobioreactors or open raceway ponds (Molina-Grima et al., 1999; Chisti, 2007; Mata et al., 2010). The horizontal tubular PBR was used for the 'green stage' (cell growth and proliferation of *Haematococcus pluvialis*), since controllable environmental and nutritional conditions facilitate optimal growth. The raceway pond was used for the 'red stage' (inhibition of cell proliferation and accumulation of astaxanthin), principally in order to offset high costs generated during the PBR cultivation (see disadvantages of PBRs in section 3.3.3). Furthermore, stress conditions introduced in the 'red stage', which trigger astaxanthin accumulation (see section 3.4), are relatively easy to achieve and the simpler raceway pond is more preferable (Li et al., 2011).

3.5.2 Horizontal Tubular Photobioreactor

A horizontal tubular photobioreactor consists of an array of straight transparent tubes and either a reservoir (i.e. degassing column) with a mechanical pump or an airlift system for agitation, mixing and gas supply (see figures 4A and 4B) (Acién et al., 2001; Chisti, 2007; Eriksen, 2008; Brennan & Owende, 2010). The tubes are usually made of glass, polyethylene or polycarbonate, while their diameter is generally less than 0.1 (m), since the light cannot penetrate too deeply in the dense algal broth that is required for high biomass productivity of the PBR (algal broth is denser than in open ponds, see section 3.3 and table 4) (Chisti, 2007; Iersel et al., 2009). Furthermore, the tubes are oriented is such a way that sunlight capture is maximized (Sánchez-Mirón et al., 1999). The tubes are always oriented from North to South, are placed parallel to each other and flat above the ground, while the array is often covered with white sheets of plastic to increase albedo (Chisti, 2007).

Like in raceway ponds (see section 3.5.3), agitation, mixing of the substrates (mainly CO_2 and nutrients) and prevention of biomass sedimentation in the tubes is succeeded by maintaining continuous turbulent flow. This can be accomplished by using a mechanical pump (see figure 4A) or a gentler airlift system (see figure 4B) (Mazzuca Sobczuk et al., 2006; García-Camacho et al., 2007;

Brennan & Owende, 2010). Mechanical pumps may have an adverse effect on microalgae cells by damaging them, but they are easy to design, install and operate (Mazzuca Sobczuk et al., 2006; García-Camacho et al., 2007). In a horizontal tubular PBR system with a mechanical pump, the removal of produced oxygen (O_2) in the degassing zone is performed by introducing air from below (Chisti, 2007). Airlift systems, on the other hand, allow besides agitation and mixing the exchange of CO_2 and O_2 between the liquid medium and aeration gas as well. This exchange takes place in the degassing zone. They are more sophisticated systems and require a continuous supply of air to operate (Acién et al., 2001; Chisti, 2007; Eriksen, 2008). Generally, the behavior CO_2 and O_2 plays a crucial role in microalgae cultivation in PBRs. More information about CO_2 and O_2 in microalgae cultivation is presented in section 3.6.4.

Oxygen (labeled as 'waste' product, see section 3.6.4) cannot be removed within the tube. This has an impact on the maximum length of a continuous run tube before oxygen removal becomes imperative. Molina-Grima et al. (2001) conducted an abundance of experiments and have concluded that a continuous tube run should not exceed 80 m. Nevertheless, Eriksen (2008) mentions that this number is only an estimate and the exact length depends on the combination of various factors, such as the concentration of the biomass, the light intensity, the flow rate, and the concentration of oxygen at the entrance of tube.

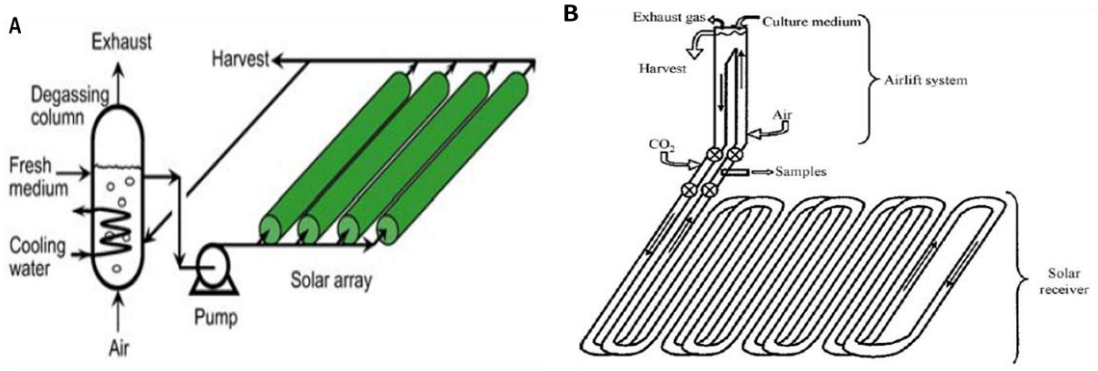

Figure 4: Schematic view of a horizontal tubular photobioreactor with: (A) a mechanical pump (Chisti, 2007)[1]; (B) an airlift system (Brennan & Owende, 2010).

In an attempt to increase the number of tubes that can be accommodated in a given area, horizontal tubular PBRs are often assembled like a fence (see figure 5) (Chisti, 2007). The geometric arrangement of the fence is of particular significance, since the mutual shading of the tubes determines the irradiance levels on the surface of the tubes (Molina-Grima et al., 2001). In this thesis, a 15-stage horizontal tubular PBR fence with an airlift system was used assuming that shading does not play any role on the model, which means that all tubes receive the same amount of irradiance. The reasons behind the selection of this arrangement are presented in detail in sections 6.1, 9.2.1 and Appendix B.

[1] The green color in the tubes represents the 'green stage'.

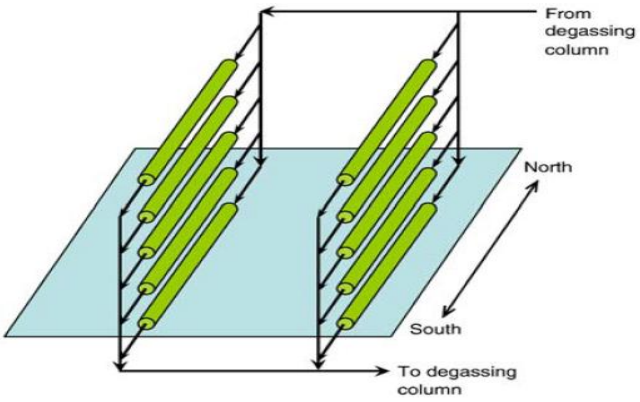

Figure 5: Schematic view of a fence-like horizontal tubular photobioreactor (Chisti, 2007)[1].

Advantages and limitations of tubular PBRs are presented in section 3.3.3.

3.5.3 Raceway Ponds

The raceway pond was chosen as the culture system for the 'red stage' of *Haematococcus pluvialis* cultivation. Since the 1950s, raceway ponds are the most commonly used artificial systems for mass microalgae cultivation (Chisti, 2007; Brennan & Owende, 2010). A raceway pond is typically a closed loop of oval shaped recirculation channels, in which low-energy-consuming paddlewheels circulate the algal broth and mix all the substrates (mainly CO_2 and nutrients) needed during the cultivation phase (see figure 6) (Chisti, 2007; Jorquera et al., 2010; Brennan & Owende, 2010; Costa & de Morais, 2013). In other words, the paddlewheels ensure the homogenization of the culture, resulting in stabilization of algal growth and productivity (Costa & de Morais, 2013). Flow of the broth is guided around bends by baffles placed in the recirculation channels (Chisti, 2007).

Raceway ponds are generally between 0.1-0.5 (m) deep, in order microalgae to receive appropriate solar illumination (Jorquera et al., 2010). The deeper a pond is the more difficult sunlight can reach algae cells, which lie in the deep layers (Mata et al., 2010). Regarding the other dimensions, raceway ponds are usually 10-300 (m) long and 1-20 (m) width. The optimal area covered by a raceway pond is assumed to range from 300 (m^2) to 4000 (m^2) (Ben-Amotz 2008). Different materials for the construction of the raceway pond lining have been used over time. Raceway ponds made of clay, concrete, asphalt, fiberglass, high density polyethylene (HDPT), polypropylene and PVC, have been recorded around the world. From an economic attraction's and durability's point of view, PVC and concrete are the most preferable (Ben-Amotz 2008).

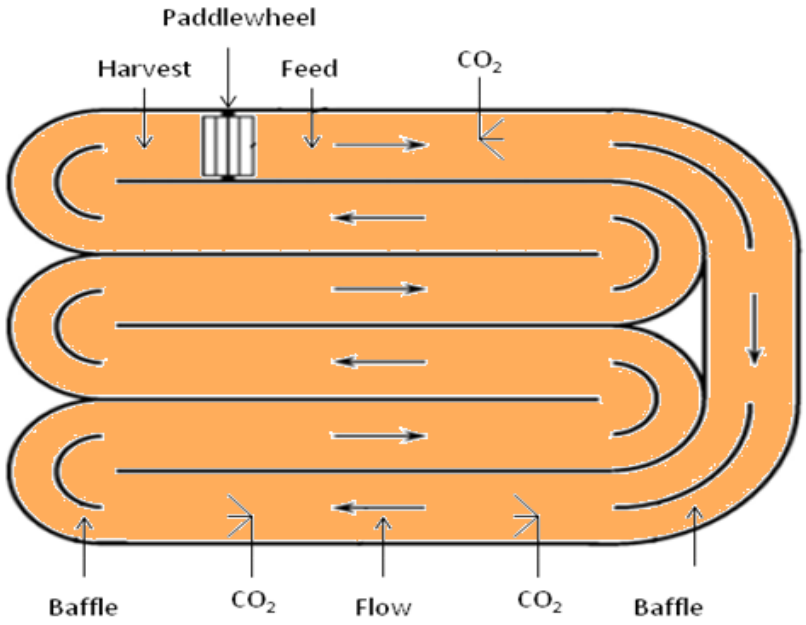

Figure 6: Schematic view of a raceway pond (adjusted by Chisti, 2007; Brennan & Owende, 2010)[2].

In order to prevent biomass sedimentation, the paddlewheel should be in continuous operation (Chisti, 2007). Furthermore, substrates and new algal broth should be fed in front of the paddlewheel (see figure 6), in order to achieve optimal homogenization (Brennan & Owende, 2010). In the same realm, wet algal biomass is harvested behind the paddlewheel, when the circulation loop is completed (Jorquera et al., 2010). Last but not least, CO_2 requirements can be satisfied from the surface air or industrial gas emissions, since raceway ponds, as all open pond systems are open to the atmosphere (see section 3.3.2). Nevertheless in most cases, submerged aerators are installed to enhance CO_2 uptake, since microalgae need high values of CO_2 in order to thrive (Brennan & Owende, 2010) (see section 3.6.4).

Advantages and limitations of raceway ponds are presented in section 3.3.2.

3.6 Parameters affecting microalgae growth

3.6.1 Introduction

As already mentioned in section 3.4, the production of astaxanthin involves two stages. *Haematococcus pluvialis* growth refers to the 'green stage', where microalgal cells grow and continuously divide (cell proliferation), driven by solar energy (in photoautotrophic nutritional mode, which is selected). This process requires mainly the input of light as an energy carrier for photosynthesis, water, CO_2 and the sufficient supply of macro- and micronutrients in a dissolved form, while maintaining the temperature of the broth on sufficient levels (Iersel et al., 2009). On the other side, astaxanthin accumulation takes place in the 'red stage', which is a process driven by adverse environmental conditions. The most important of them are nutrient starvation and high light intensity. This section provides an overview of the basic cultivation inputs for both stages that were used to run the microalgae process model (see section 6).

[2] The orange color in the pond represents the 'red stage'.

3.6.2 Light-Incident solar irradiation uptake efficiencies

Photosynthesis constitutes one of the most important mechanisms of the natural world, since all forms of vegetative life depend directly or indirectly on it as a primary tool for production of energy during their metabolism. Oxygenic photosynthesis in microalgae cultivation can be expressed as a reaction driven by light energy (harvested by chlorophyll molecules), in which carbon dioxide, water and nutrients are converted to algal biomass (mainly carbohydrates) and oxygen (Richmond, 2004). Algal stoichiometry during oxygenic photosynthesis is given by the following equation (Orosz & Forney, 2008):

$$106CO_2 + 16NO_3^- + H_2PO_4^- + 122H_2O + 17H^+ \xrightarrow{\text{Photosynthesis}} \{C_{106}H_{263}O_{110}N_{16}P_1\} + 138O_2$$

This chemical reaction depicts the carbon substrate (C) included in carbon dioxide (CO_2), the macronutrients nitrogen (N) and phosphorus (P) included in nitrate (NO_3^-) and phosphate (PO_4^-), oxygen (O_2) evolution and the approximate chemical formula of algal biomass (~CH_2O).

Sunlight is the ultimate source of energy in photoautotrophic microalgae cultivation. Although the wavelength range of solar irradiation is very broad, microalgae can utilize only a fraction of it, which is called Photosynthetically Active Radiation (PAR) (Richmond, 2004). PAR ranges between 400nm-750nm[3] (see figure 7), which is basically the spectral pattern of visible light and corresponds to approximately 40-45% of the total light spectrum (see figure 8) (Richmond, 2004; Orosz & Forney, 2008; Iersel et al., 2009). Wavelengths outside this range cannot be absorbed by microalgae.

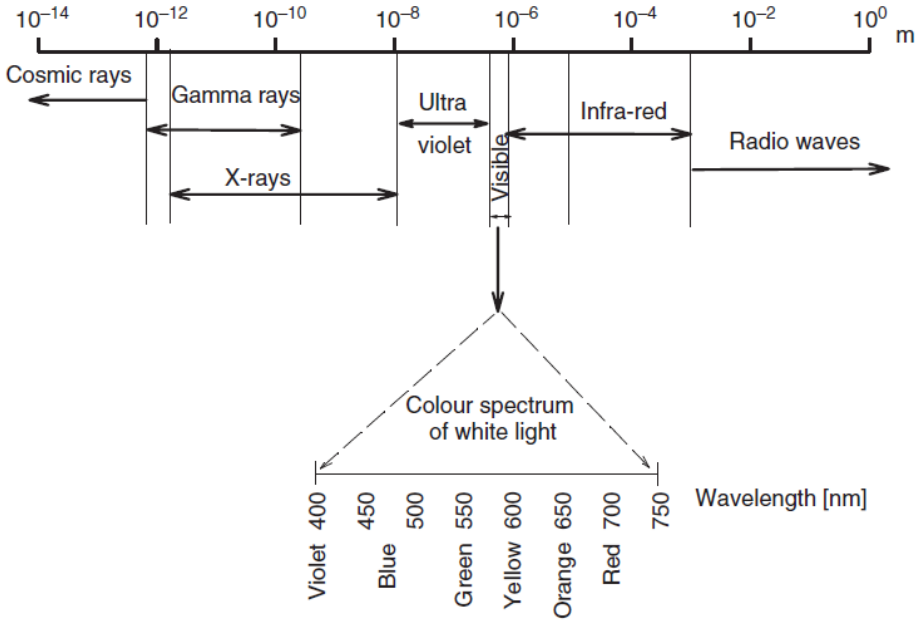

Figure 7: Spectra of electromagnetic radiation and spectral pattern of visible light. Photosynthetically Active Radiation (PAR) ranges from 400 to 750 nm (Richmond, 2004).

[3] 1nm = 10^{-9}m

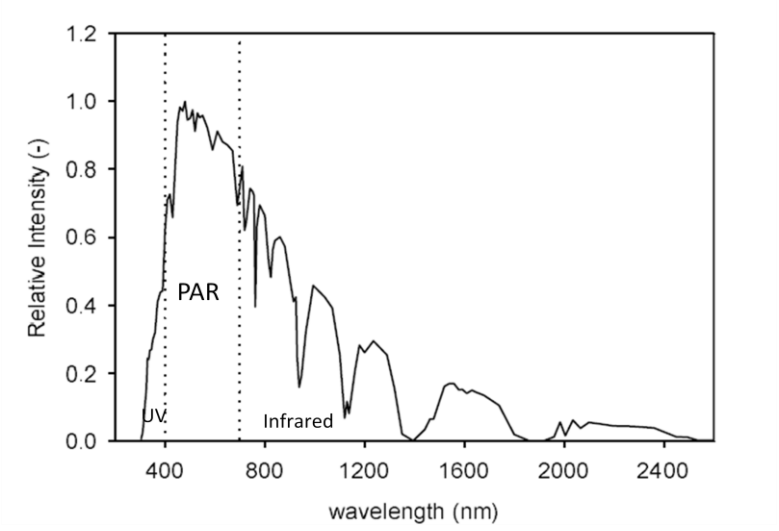

Figure 8: Relative sunlight intensity of solar energy on ground level (Orosz & Forney, 2008).

According to the quantum theory, light energy is delivered in the form of separated packages called *light quanta* or *photons*, which are the tools to drive photosynthesis (Zajonc et al., 2003). Light intensity can be expressed as the number of photons that strike a flat surface per unit of time (μmol m^{-2} s^{-1}). This rhythm is called Photon Flux Density (PFD) (Jannsen, 2002). Scientists prefer to measure light intensity on a surface, in units of power per area, (Wm^{-2} or Jm^{-2} s^{-1}). Nevertheless, as already mentioned photosynthesis is a quantum process (Richmond, 2004). Therefore, a conversion factor between μmol m^{-2} s^{-1} and Wm^{-2} is needed. Integrating Einstein's law ($E = N * h\frac{c}{\lambda}$, where E is the light energy, $N = 6.023 * 10^{23}$ is the Avogadro number, $h = 6.626 * 10^{-34}$ (Ws^2) is Planck's constant, $c = 3 * 10^8$ (m s^{-1}) is the speed of light and λ is the wavelength), this conversion factor, which is dependant and unique for every wavelength, can be determined. It is found that for PAR, the values of the photon flux density conversion factor range from 4.5-5.14 (μmol $m^{-2}s^{-1}$) per (Wm^{-2}) (Jannsen, 2002; Richmond, 2004).

From the total amount of light impinging upon the surface of water, one fraction is reflected as a function of Frenzel's law (Orosz & Forney, 2008). In literature, different averages for the fraction of incident light reflected on clear day can be found. This is happening, because the measurements of each research took place in different locations with different environmental conditions and using different cultivation systems. Thus, the deviation is high (in an extended research throughout the existing papers a range from 5% to 30% was found). In this research, the reflection losses values involved a fraction of 10% for the raceway pond, while in the absence of information for the tubular PBR, a fraction of 12% was assumed (Ben-Amotz 2008; Park et al., 2011)[4].

The rest fraction of solar irradiation enters the water and it can be either absorbed by water and substances dissolved in it or it can enter an algal cell (Orosz & Forney, 2008). As the light enters the deeper layers, its intensity attenuates. This intensity attenuation is a function of the incident irradiation (I_0) on the surface and the exponent of a constant X called attenuation coefficient

[4] The assumed reflection value for the tubular PBR is higher than the one measured for the raceway pond, since the transparent plastic tube filled with broth should have higher reflectivity than the surface of the broth alone, which is the case, regarding ponds.

multiplied by the depth (Z). This function is called the Beer's law expressed in (μmol $m^{-2}s^{-1}$) and is presented below (Orosz & Forney, 2008):

$$I_Z = I_0 * e^{-X*Z} \quad (3)$$

The attenuation coefficient for algae cultivation ranges from 0.15-0.6 (m^{-1}) (Jannsen, 2002; Orosz & Forney, 2008). Last but not least, Sudhakar et al. (2012b) mention that incident light is affected from land efficiency, which amounts to 98% in optimal conditions.

As already mentioned in section 3.4, various stress environmental conditions inhibit cell proliferation (microalgae growth), resulting in accumulation of the desired product to be extracted from the cell. One of these stress conditions refers to the continuously increasing light intensity. However, for optimal cell proliferation (i.e. in 'green stage'), moderate light intensity is required. Algal cells cannot bear a light intensity higher than a certain point, leading to the irreversible damage of the parts in algae cells that are responsible for photosynthesis and consequently to a reduction of the biomass growth rate (Rubio-Camacho et al., 2003). This phenomenon is called photoinhibition. This point is slightly greater than the light level, at which the specific growth rate peaks. More specifically, Giannelli et al. (2015) mention, that saturation intensity for *Haematococcus pluvialis* is 250 (μmol $m^{-2}s^{-1}$) for a temperature of 20°C and 500 (μmol $m^{-2}s^{-1}$) for a temperature of 27°C in the medium (see figure 9), while the typical midday solar light intensity in equatorial regions exceeds 2000 (μmol $m^{-2}s^{1}$) (Chisti 2007). Because of light saturation, the biomass growth rate is much lower, when cultivating microalgae using sunlight as the energy carrier rather than controllable artificial light devices (Chisti 2007).

Figure 9, pictures the Photosynthesis-Intensity (PI) curve of *Haematococcus pluvialis* under different temperature conditions (Giannelli et al., 2015).

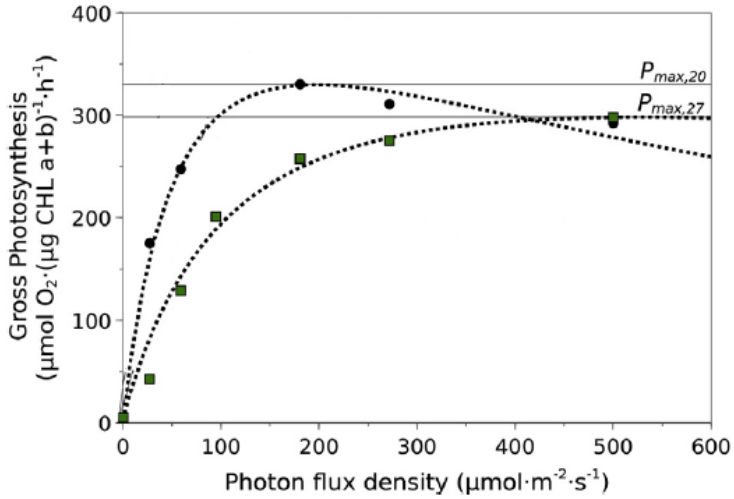

Figure 9: Photosynthesis-intensity (PI) curves of *Haematococcus pluvialis* under different temperature conditions: 20°C (circles) and 27°C (squares) (Giannelli et al., 2015).

Among others, a very significant factor in microalgae growth is the photosynthetic efficiency. The gross photosynthetic efficiency amounts to ~27%. However, various inefficiencies and loss mechanisms (such as respiration and photo-utilization efficiency) decrease this number, resulting in a maximum theoretical efficiency of ~20%[5] for the conversion of sunlight to algal biomass (see formulas 4 and 5) (Orosz & Forney, 2008; Sudhakar et al., 2012b). Other authors have suggested values of 12.4% (Tredici, 2010), 11.7% (Williams & Laurens, 2010) and 11% (Iersel et al., 2009). The existence of these variations depends on the various ways to calculate the maximum theoretical efficiency. For instance, considering the maximum quota of respiratory CO_2 losses, a theoretical efficiency of ~11% can be achieved (see formulas 4 and 5)[5]. On the other side, the simplest way to calculate the maximum theoretical efficiency is to just multiply PAR with gross photosynthetic efficiency (i.e. 43%*27%), which results in an efficiency of 11.6% (Milledge, 2013). In practice, nonetheless, the photosynthetic efficiency varies from 3% to 4% and in some laboratory cases, values of 6.5% can be achieved (Kleinegris et al., 2014). In order to be more analytical and precise when running the microalgae process model the photosynthetic efficiency was calculated using the following formulas (Sudhakar et al., 2012b):

$$\mathrm{PE} = \eta_{\mathrm{Photosynthesis\_Gross}} * \bar{\eta}_{\mathrm{Photo-utilization}} * (1 - \mathrm{R}) \quad (\mathbf{4})$$

- $\mathrm{PE} =$ Maximum photosynthetic efficiency.
- $\eta_{\mathrm{Photosynthesis\_Gross}} = 27\%$.
- $\bar{\eta}_{\mathrm{Photo-utilization}} = \frac{\frac{I_{SAT}}{I_0}\left[\ln\left(\frac{I_0}{I_{SAT}}\right)+1\right]+\frac{I_{SAT}}{I_Z}\left[\ln\left(\frac{I_Z}{I_{SAT}}\right)+1\right]}{2}$ $(\mathbf{5})$, where I_{SAT}= 250 (µmol $m^{-2}s^{-1}$) and 500 (µmol $m^{-2}s^{-1}$) the saturation intensity for the 'green' and 'red stage' respectively, while I_0, I_Z the solar intensities on surface and in depth (Z) respectively (see formula 3). The formula was modified according to the Bushes' equation mentioned in the research of Sudhakar et al. (2012b)
- $\mathrm{R} = 30\%$ the CO_2 respiration losses (Zhu et al., 2008)[6].

As can be noticed, the photosynthetic efficiency calculation is based on how one defines this term. For example, formula 4 does not include PAR, which means that it does not agree with the way of calculation proposed by Milledge (2013). However, this does not pose any issue in the final determination of astaxanthin. The reason lies on the fact that algae biomass calculation is defined as a function of solar irradiation multiplied with all individual parameters proposed by the different authors, which should be used in the photosynthetic efficiency calculation. Detailed information on this statement can be found all through section 6.1.

3.6.3 Temperature

The different strains of microalgae thrive in a vast range of ecosystems with high variations in temperature. Most species of microalgae are photosynthetically active at 10°C, but the optimum temperature for photosynthesis varies from 15°C to 35°C (Arnold, 2013). Regarding the strain *Haematococcus pluvialis*, the growth rates under different temperatures are shown in figure 10A

[5] Using formula 4, a maximum theoretical photosynthetic efficiency of ~20% can be achieved, when $\bar{\eta}_{\mathrm{Photo-utilization}} = 1$ (optimum photo-utilization) and respiratory CO_2 losses amount to 30% (minimum quota). A maximum theoretical photosynthetic efficiency of ~11% can be achieved, when $\bar{\eta}_{\mathrm{Photo-utilization}} = 1$ (optimum photo-utilization) and respiratory CO_2 losses amount to 60% (maximum quota).

[6] Measured ratios of respiratory CO_2 losses as a fraction of photosynthetic uptake for microalgae vary from 30% to 60% (Zhu et al., 2008). This research assumed respiratory CO_2 losses of 30%.

(Giannelli et al., 2015). The culture cultivated at the lowest temperature (20°C) demonstrated the highest growth in terms of cell number. Nevertheless, when the maximum culture dry weight is considered to be a function of temperature, the opposite trend can be noticed (see figure 10B) (Giannelli et al., 2015). Figures 9, 10A, 10B, describe adequately the 'green stage' mentioned in section 3.4, where optimal environmental conditions in terms of cell proliferation involve moderate light intensity and temperature (i.e. 250 (µmol $m^{-2}s^{-1}$) and 20°C).

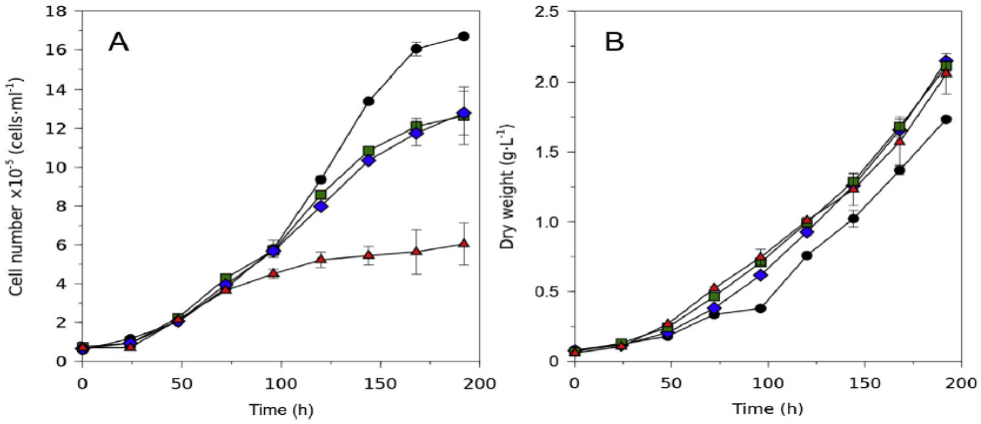

Figure 10: Growth curves of *Haematococcus pluvialis* cultures at 20°C (circles), 23.5 °C (diamonds), 27°C (squares) and 30.5°C (triangles): (A) culture cell number; (B) dry weight (Giannelli et al., 2015).

For the accumulation of astaxanthin ('red stage'), adverse environmental and nutritional conditions are required (see section 3.4). Evens et al. (2008) and Giannelli et al. (2015) have conducted different experimental researches on astaxanthin accumulation in the *Haematococcus pluvialis* and both agree that an increased temperature of 27°C combined with nutrient starvation led to an increased final astaxanthin production. These findings are depicted in figures 11A and 11B.

Figure 11A illustrates astaxanthin accumulation in the *Haematococcus pluvialis* cultivated under different temperatures. Figure 11B portrays a year-round temperature variation in the laboratory (Giannelli et al., 2015).

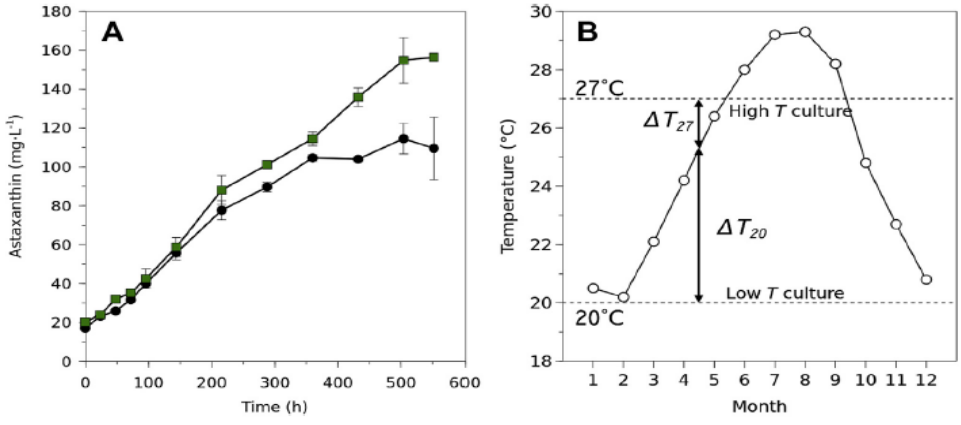

Figure 11: (A) Astaxanthin accumulation in the *Haematococcus pluvialis* cultivated under different temperatures: 20°C (circles), 27°C (squares). (B) Year-round temperature variation in the laboratory. ΔT_i is the difference between the room temperature and the culture temperature i (Giannelli et al., 2015).

As spotlighted in figure 9 (see section 3.6.2), algal growth rate increases with light intensity up to an optimal point (saturation intensity point) and decreases with higher irradiance than this point. Regarding temperature, however, it remains widely debated whether the relationship between the growth rate and temperature is exponential or linear (James & Boriah, 2010). This state can be illustrated in figures 10 and 11 as well, where the curves do not show either a linear or an exponential behavior. The relationship between growth rate and temperature can be expressed as an efficiency factor on solar energy absorbed by the cells (James & Boriah, 2010). In this thesis, the calculation of this factor follows an exponential variation, which is given by the following formulas (James & Boriah, 2010):

$$T_{EFFECT} = e^{-K(T_{WATER}-T_{OPT})^2} \quad (6)$$

- T_{EFFECT} = The effect of non-optimal temperature ($0 \leq T_{EFFECT} \leq 1$).
- T_{WATER} = Medium temperature as calculated by using the formula from Sukenik et al. (1991): $T_{WATER} = F_{TEMP}(T_{AVG} - T_{AMP} * \cos\left(2\pi * \frac{hour}{24}\right))$ (7)
  - $F_{TEMP} = 0.9$, the temperature following factor (Sukenik et al., 1991).
  - T_{AVG} = The average temperature.
  - T_{AMP} = The amplitude temperature.
  - $hour$ = The hour of the day, when the water temperature is determined.
- T_{OPT} = Medium temperature at optimal growth. For the 'green stage' this temperature amounts to 20°C, while for the 'red stage' it amounts to 27°C (see figures 10 and 11).
- K = An empirical constant that was assumed as 0.007, in order to match the growth rate data presented by Montagnes and Franklin (2001).

3.6.4 Carbon Dioxide (CO_2) & Oxygen (O_2)

Like all photosynthetic organisms, microalgae (in photoautotrophic nutritional mode) need CO_2 as a carbon source, which will be converted into chemical energy inside the algal cell (Wang et al., 2008; Iersel et al., 2009). In fact, no microalgae growth can take place in the absence of CO_2 and an insufficient supply of CO_2 constitutes a limiting factor in algal biomass productivity. Microalgae can capture CO_2 mainly from three different sources: 1) Atmospheric CO_2; 2) CO_2 included in gas emissions from industrial processes (e.g. flue gases and flaring gases); 3) fixed CO_2 in the form of soluble carbonates (e.g., $NaHCO_3$ and Na_2CO_3) (Brennan & Owende, 2010).

The introduction of atmospheric CO_2 in microalgae life-cycle is the most basic method to sink carbon and it simply involves the mass transfer from the air to the growth medium (Venkata Subhash et al., 2013). However, there is a significant limitation: Based on the average chemical composition of algal biomass ($C_1H_{1.83}O_{0.48}N_{0.11}$), approximately 1.8 tons of CO_2 are needed in order to harvest 1 ton of algal biomass (Chisti, 2007; Wang et al., 2008; Iersel et al., 2009). The average chemical composition of algal biomass assumes carbon mass fraction of 50% in the cells approximately (see also section 3.7). The concentration of CO_2 in the air corresponds to 0.036% or 360ppm[7] (Stepan et al., 2002), which means that the whole amount of CO_2 included in approximately 37000 (m^3) air is needed for 1 ton of dry algae (Iersel et al., 2009). Capturing CO_2 from such an amount of air requires significant time, resulting in a slow rate of microalgae cell growth and consequently in high operational costs (Wang et al., 2008).

[7] ppm=parts per million.

In contrast, capturing CO_2 included in industrial gas emissions (e.g. flue gases from a power plant that burn fossil fuels) seems to be a better solution for high algal biomass productivity (Bilanovic et al., 2009). This can be attributed to the high concentration of CO_2 existed in these gas emissions. For instance, CO_2 in flue gases ranges from 5% to 15% v/v and it is free or even result in revenues if a financial scheme for the prevention of greenhouse gas emissions exists. The only cost refers to the supply from the source into the culture system (Wang et al., 2008). Nevertheless, there is the limitation that most microalgae strains may not be able to tolerate the toxicity of nitrogen oxides (NO_x) and sulfur dioxide (SO_2) that are present in dense industrial gas emissions as well (Brennan & Owende, 2010). Doucha et al. (2005), on the other side, support that industrial gases can be used to cultivate microalgae without any harmful effects. In fact, they support that dissolved NO_x and SO_x in low concentrations could be used as nitrogen and sulfur source, which serve the role of fertilizer in the growth medium (Doucha et al., 2005).

The concentration of dissolved CO_2 in the culture system follows the similar relationship between microalgae growth rate and sunlight intensity (see section 3.6.2). In order to avoid reduced fixation and/or loss to the atmosphere, the concentration should be neither less nor higher than required for maximum growth for a particular microalgae strain (Sung et al., 1999; Cheng et al., 2006). Several studies propose different amounts of CO_2 that should be introduced in the culture system.

No information was found on the capture of CO_2 by the strain *Haematococcus pluvialis*. Jonker & Faaij (2013) recommend in general that for high biomass productivity, a CO_2 concentration that exceeds 2.2 (mg/l) is required.

The photosynthetic equation in section 3.6.2 shows that the uptake of CO_2 results in the production of molecular oxygen (O_2), which doesn't facilitate microalgae growth. In fact, dissolved oxygen is labeled as a 'waste' product, which at higher concentrations than air saturation values can obstruct the capture of CO_2 and produce photo-oxidative damage to algal cells, affecting consequently algal growth (Molina-Grima et al., 2001). This is a significant issue for microalgae cultivation in PBRs, where algal broth is isolated in the closed system and oxygen cannot escape. Even with frequent gas exchange, concentrations of oxygen in PBRs may reach 100 (mg/liter), something that renders an extremely toxic cultivation environment (Weissman et al., 1988). In an open pond, dissolved oxygen rises much more slowly, as a consequence of the much greater volume per unit surface area and the outgassing of oxygen to the atmosphere. The molecular oxygen (O_2) limit, above which microalgae suffer, ranges from 25-40 (mg/liter of water) (Weissman et al., 1988; Jonker & Faaij, 2013).

In this thesis, it was assumed that CO_2 needs were facilitated by supplying the hybrid system with flue gases. Although, CO_2 demand was calculated by using the general rule mentioned before, which is based on the average chemical composition of algal biomass (i.e. 1.8 tons CO_2 needed for the production on 1 ton of microalgal biomass; for detailed calculation see section 8.2 and Appendix C2), the selection of a flue gases supply has a binary goal: First, to calculate a realistic O_2 mass flow having CO_2 as a benchmark[8]; and second, to subject our system into a sustainable development regime,

[8] If only air was pumped into the hybrid system, the volume of oxygen (21% v/v of air) entering the system would be tremendous. This would happen, because without the forced supply, CO_2 intake only from the atmosphere corresponds to only 360ppm or 360 (mg/l) and thus, a very high volume of air (i.e. 37000 m^3) would have to be pumped into the system in order to satisfy the general rule (1.8 tons of CO_2 per 1 ton of algae biomass). Since oxygen is labeled as a 'waste' product, the removal of the excess would be practically inevitable.

which uses a waste product (i.e. industrial CO_2) as a valuable substrate for microalgae growth, mitigating that way GHG emissions. Regarding concentrations, the average values of CO_2 and O_2 existing in flue gas were taken into account; namely, 10% v/v for CO_2 (range is 5%-15%) and 3% v/v for O_2 (range is 2.5-3.5%) (Wang et al., 2008; Beychok, 2012).

In section 6.1, more information on the impact of CO_2 and O_2 on the model is discussed, while in section 8.2 the mass balances of CO_2 and O_2 during cultivation phase can be found.

3.6.5 Nutrients

In photoautotrophic cultivation, besides the capture of light as the energy carrier and CO_2 as the carbon source, the supply of nutrients is essential for successful microalgae growth. The combination of nutrients and light leads to the production of chlorophyll through photosynthesis and consequently to the proliferation of microalgal cells (Iersel et al., 2009) (see photosynthetic equation in section 3.6.2). In other words, these nutrients serve the role of fertilizers. They are divided into two main categories: 1) Macronutrients and 2) micronutrients. The demand and the kind of nutrients depend on the microalgae species and cultivation conditions. Regarding the strain *Haematococcus pluvialis* nutrient demand (in grams and %) was derived from the elementary composition of the initial medium recipe or the stoichiometry of growth presented by Li et al. (2011) (see section 3.7). In general, the macronutrients, considered essential for normal microalgae growth, involve mainly carbon (if CO_2 supply is inadequate), nitrogen, phosphorus, hydrogen, oxygen, sulfur, calcium, magnesium, potassium and chlorine. On the other hand, the micronutrients constitute trace quantities of micro-, nano- or even picograms per liter and involve mainly iron, boron, manganese, copper, zinc, molybdenum, vanadium, cobalt, nickel, silicon and selenium (Suh & Lee, 2003). These groups for macro- and micronutrients are a general guide of the fertilizers introduced in the growth medium. In section 3.7, where the composition of the initial medium recipe is presented, some of the macronutrients are used in trace quantities, constituting that way part of the micronutrients. Furthermore, not every element from the abovementioned categories is used.

During the 'green stage', the vegetative cells are produced under controlled conditions of nutrient concentration. After a sufficient volume of vegetative cell suspension is produced, the culture is subjected under complete nutrient starvation, along with increased temperature, light intensity and acidity (Garcia-Malea et al., 2005) (see also section 8.1).

More information about nutrients' role in the microalgae process model is delineated in section 6.1, while in section 8.1 the mass balances of the macro- and micronutrients are portrayed.

3.6.6 Acidity (pH levels)

Acidity in the growth medium plays a crucial role during the different phases of cultivation. Different values of pH influence algae growth as well as the accumulation of the desirable metabolites to be extracted. There is an abundance of studies proposing different pH values during 'green' and 'red stage', resulting in a pH range that varies from 6.0-9.0 (Sarada et al., 2002; Garcia-Malea et al., 2005; Aflalo et al., 2007; Li et al., 2011). In a hybrid system comprising by a tubular PBR and a raceway pond, Li et al. (2011) propose for the tubular PBR ('green stage') an acidity level of 7.5, while for the raceway pond ('red stage') an increased acidity level of 8.0 maintained by controlled addition of CO_2. More information on the influence of acidity levels in the microalgae process model is presented in section 6.1.

3.6.7 Energy stored in Biomass

The three primary compositions of microalgae are lipids, carbohydrates and proteins (Mata et al., 2010). Indisputably, lipids are the dominant among them and their concentration ranges from 20-80% of the total dry weight of microalgae (Spolaore et al., 2006).

In photoautotrophic cultivation, the energy absorbed by the algal cells is derived from a source of light. When sun is the source of light, algal cells do not absorb the whole amount of solar energy, but only a fraction of it. This happens because sunlight is subjected to different inefficiencies and loss mechanisms that weaken light's intensity (see section 3.6.2). The amount of sunlight absorbed is the energy stored in the biomass (Orosz & Forney, 2008). In order to calculate biomass productivity, when solar energy uptake is known, the higher heating value (HHV) or heat of combustion can be used (Sudhakar et al., 2012b). The HHV is the amount of energy (i.e. heat) released during the combustion of a specified amount of a substance. In case of microalgae biomass, the HHV could be considered as the solar energy metabolized by the primary compositions (lipids, carbohydrates and proteins), translated into heat, which is released when one unit of biomass (usually kg) is burned in a device, such as a combustion boiler. In other words, dividing solar energy uptake (in MJ) with the HHV (in MJ/kg), the biomass productivity can be calculated (see formula 10 in section 6.1).

Depending on the concentration of the primary compositions, HHV can be calculated (Sudhakar et al., 2012b). This thesis assumed a chemical composition with 40% lipids, 40% carbohydrates and 20% proteins. Each fraction has a specific calorific value called lower heating value (Sudhakar et al., 2012b), which are presented in table 5. Using the LHV of each composition as well as their fraction in the microalgae cell, HHV can be calculated using the following formula:

$$\mathrm{HHV} = \mathrm{f_L} * \mathrm{LHV_L} + \mathrm{f_C} * \mathrm{LHV_C} + \mathrm{f_P} * \mathrm{LHV_P} \quad (\mathbf{8})$$

- $\mathrm{HHV} =$ Higher heating value (MJ/kg).
- $\mathrm{f_L}, \mathrm{f_C}, \mathrm{f_P} =$ Content (%) of lipids, carbohydrates and proteins respectively.
- $\mathrm{LHV_L}, \mathrm{LHV_C}, \mathrm{LHV_P} =$ Lower heating value of lipids, carbohydrates and proteins respectively.

Table 5 illustrates the biomass fractions assumed in this study, the net calorific values derived by Sudhakar et al. (2012b) as well as the HHV calculated using formula 8.

Composition	Fraction	LHV (MJ/kg)	HHV (MJ/kg)
Lipids	40%	38.3	**23.6**
Carbohydrates	40%	13	
Proteins	20%	15.5	

Table 5: HHV calculation using assumed biomass fractions and net calorific values derived by literature.

3.7 Growth medium and microalgae composition

Each strain for cultivation needs specific environmental conditions in order to thrive. As mentioned in section 3.6.5, besides light absorption and CO_2 supply, the growth medium needs a sufficient supply of macro- and micronutrients, which will serve the role of fertilizers. These fertilizers are inoculated in the culture system in the form of chemical compounds, synthesizing the so called 'initial medium recipe' (Garcia-Malea et al., 2005). This recipe varies among the different reports, which study astaxanthin accumulation using *Haematococcus pluvialis* (Marker et al., 1996; Zhang et al., 1999; Sarada et al., 2002; Garcia-Malea et al., 2005; Aflalo et al., 2007; Li et al., 2011). The reason behind

these variations lies on the fact that, except few companies, astaxanthin production using microalgae is still on laboratory scale (less than 1% of the commercialized astaxanthin is derived by microalgae, see section 1.2.2.2). Since the hybrid system, presented in section 3.5, consists of a tubular PBR and a raceway pond, this section presents the composition of the initial recipe derived by Li et al. (2011), who used in their study the same hybrid system for cultivation. A weight analysis of the chemical elements was made (in grams/liter as well as % of the whole recipe), using the initial medium recipe (in the form of chemical compounds). Table 6 depicts the composition of the initial recipe and the weight percentages of the chemical elements that exist in it, while in Appendix A the weight analysis is presented.

Element	Weight (grams/liter)	Weight (%)
Oxygen (O)	0.745	48.32
Potassium (K)	0.39	25.29
Nitrogen (N)	0.141	9.14
Sodium (Na)	0.138	8.95
Phosphorus (P)	0.062	4.02
Carbon (C)	0.03	1.95
Sulfur (S)	0.016	1.04
Magnesium (Mg)	0.012	0.78
Hydrogen (H)	0.005	0.32
Chlorine (Cl)	0.0013	0.08
Manganese (Mn)	0.00066	0.04
Boron (B)	0.00055	0.04
Iron (Fe)	0.00028	0.02
Vanadium (V)	0.000077	0.00
Zinc (Zn)	0.000052	0.00
Copper (Cu)	0.000025	0.00
Cobalt (Co)	0.000012	0.00

Table 6: Composition of the initial recipe (before entering the tubular PBR).

The chemical elements depicted in table 6 are inoculated in the tubular PBR in order to facilitate the 'green stage'. Regarding the 'red stage', which takes place in the raceway pond, microalgal cells are stressed under nutrient starvation and under increased solar intensity, temperature and acidity (see sections 3.6.2-3.6.6). As CO_2 is induced in the growth medium all through the two stages, carbon concentration in the algal cells increases dramatically, while oxygen levels decrease, since oxygen is characterized as waste product during cultivation and should be removed (see section 3.6.4). Nutrient deprivation leaded to decreased weight percentages of intracellular nutrients as well. Table 7 highlights the general elemental microalgae composition after completing the 'green stage', as well as after subjecting *Haematococcus pluvialis* under adverse environmental conditions during the 'red stage'. The weight percentages presented in table 7 are derived from different sources and do not represent an accurate final composition following the initial recipe illustrated in table 6, since this information was not reported in total by Li et al. (2011). The goal is to mark general variations in nutrients' concentration before and after cultivation and to have a basis for calculating the mass balances (see section 8).

Element	'Green Stage' Weight (%)	'Red Stage' Weight (%)
Carbon (C)	45.00	49.50
Oxygen (O)	27.00	29.00
Potassium (K)	11.00	9.32
Hydrogen (H)	7.38	7.23
Nitrogen (N)	5.80	2.44
Sodium (Na)	1.35	0.8
Phosphorus (P)	1.20	0.7
Sulfur (S)	0.65	0.40
Magnesium (Mg)	0.60	0.60
Chlorine (Cl)	0.01	0.005
Iron (Fe)	0.01	0.005
Manganese (Mn)	0.00	0.00
Boron (B)	0.00	0.00
Vanadium (V)	0.00	0.00
Zinc (Zn)	0.00	0.00
Copper (Cu)	0.00	0.00
Cobalt (Co)	0.00	0.00

Table 7: General elemental microalgae composition after 'green' and 'red stage' respectively (combined information from Richmond 2004; Del Rio et al., 2005; Garcia-Malea et al. 2005; Li et al. 2011).

4 Harvesting phase

4.1 Introduction

The harvesting of biomass constitutes a critical part within the production line, since it usually represents 20-30% of the total production costs (Molina-Grima et al., 2003; Brennan & Owende, 2010; Mata et al., 2010; Christenson & Sims, 2011; Rawat et al., 2011; Salim et al., 2011; Barros et al., 2014). Fractions as high as 50% of the total production costs have been reported as well (Greenwell et al., 2010). High harvesting costs are due to various algal features that make the recovery of algal biomass difficult. These features are: 1) Low microalgae cell densities in the broth (typically mass concentrations are in the range of 0.3-5 g/l); 2) the small size of most algal cells (typically in the range of 2-40 μm); 3) the negatively charged algal cell surface that results in a stable dispersed state of the algal suspension; and 4) the fast growth rates of microalgae, which require frequent harvesting compared to terrestrial plants (Li et al., 2008; Danquah et al., 2009; Brennan & Owende, 2010; Milledge, 2013; Barros et al., 2014). The harvesting phase constitutes one of the most challenging issues in the scientific community and a limiting factor for commercial dry algal biomass production. There is hardly a harvesting method that is economically viable and energy efficient simultaneously (Milledge, 2013; Barros et al., 2014).

There are two methodologies to follow in the harvesting process: 1) A two-step approach, where the algal suspension is primarily thickened to slurry consisting of 2-7% of the total suspended solids (TSS). The concentration factor of this operation ranges between 100 and 800. Afterwards, the slurry is further dewatered to a cake comprising of 15-25% TSS (the concentration factor ranges between 2 and 10) (Brennan & Owende, 2010; Barros et al., 2014); 2) a single step approach, where thickening and dewatering processes are merged (Uduman et al., 2010). There is an abundance of methods to harvest microalgae biomass. Microalgae harvesting currently involves mechanical, chemical, biological and, to a lesser extent, electrical based methods. As most bio-refineries adopt the two-step approach for microalgae harvesting, two or more of these methods can be combined in order to reduce operational costs (Barros et al., 2014). The selection of the appropriate methods depends on the end product and a number of factors that have to be taken into account, such as moisture and salinity levels and species properties (Chen et al., 2011; Milledge, 2013). But the most important aspect regarding microalgae harvesting is that algal biomass must be further processed in the extraction phase and, thus, the selected method should not be toxic or contaminate the algal cells (Barros et al., 2014). Figure 12 delineates a schematic overview of the harvesting phase in the production line.

In this study, the harvesting phase refers to the selection of the most appropriate techniques to recover the ‘red’ biomass, after the accumulation of astaxanthin in the *Haematococcus pluvialis* cells was achieved. The suspended solids at the ‘red stage’ were calculated 0.035% or 0.35 g/l (see detailed calculation in section 8.3), while the size of the ‘red’ algal cells amounts to 20 μm (Gu et al., 2013).

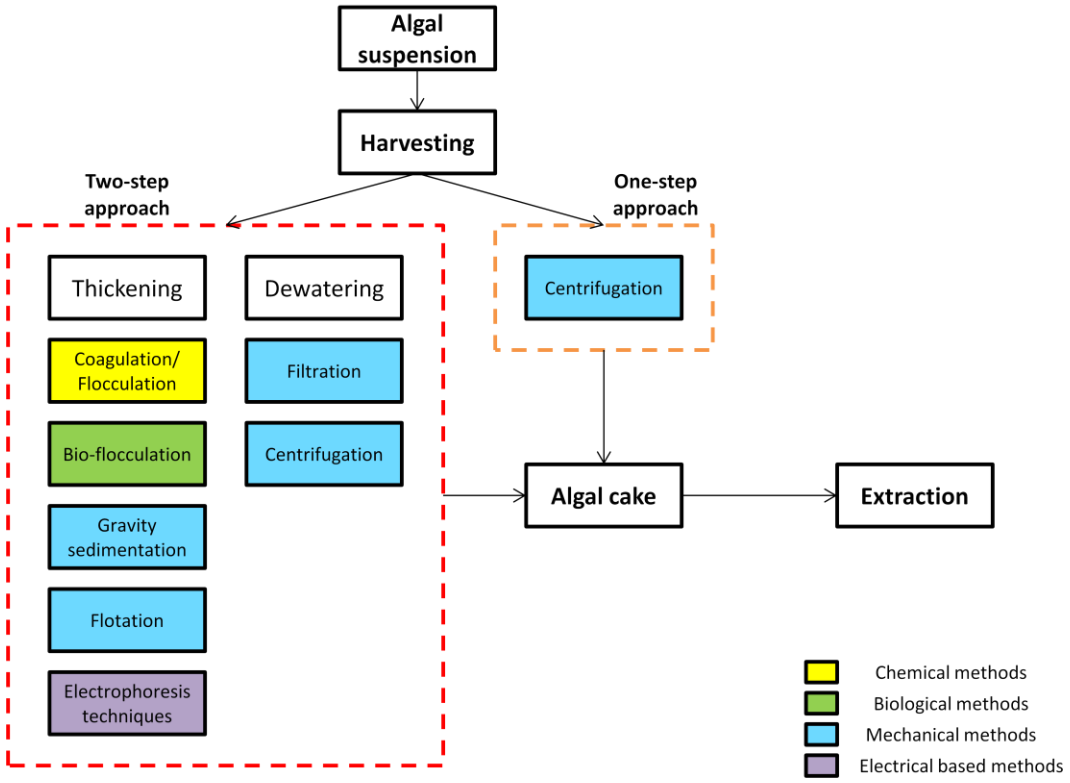

Figure 12: Flow chart of the harvesting phase.

An overview and comparison analysis on the different harvesting methods is presented in the following sections. The ultimate goal of the comparison analysis was to select the appropriate method/combination of methods that would facilitate cost-efficient astaxanthin extraction in the last phase (i.e. extraction phase, see section 5).

4.2 Thickening methods

4.2.1 Chemical coagulation/flocculation

Chemical coagulation/flocculation involves the inoculation of chemicals into the broth, which concentrate the suspension 20-100 times (Vandamme et al., 2013). These chemicals are labeled as coagulants and basically they stimulate finely divided particles (algal cells) to aggregate forming larger clumps of cells that are called 'flocs' (Milledge, 2013). Finely divided particles float in the broth since they are not heavy enough to settle in the bottom of the vessel by gravity. This is due to the fact that microalgae cells carry a negative charge that prevents aggregation of cells in suspension (Molina-Grima et al., 2003). On the other side, 'flocs' have the mass to accumulate in the bottom of vessel, forming thickened slurry and leaving a clear supernatant (i.e. layer) of water in the surface (Barros et al., 2014). There is a variety of chemical coagulants, and according to their chemical composition they are divided in organic and inorganic. Chemical coagulation/flocculation is characterized as the most attractive method towards economical optimization, since it can handle fast large quantities of algal suspension, while it is applicable to a wide range of algae strains (Uduman et al., 2010). Furthermore, it does not require any energy needs, reducing consequently operational costs (Barros et al., 2014). Nonetheless, coagulants are still 'expensive' and can be toxic to algae biomass, which besides deteriorating the quality of the biomass it leads to limited recycling of the culture medium as well (Chen et al., 2011; Milledge, 2013; Barros et al., 2014). Cell harvest

efficiency of chemical coagulation/flocculation exceeds 95%, while the concentration of TSS ranges between 3-8% (Molina-Grima et al., 2003; Uduman et al., 2010; Milledge, 2013).

4.2.2 Bio-flocculation

The concept of bio-flocculation is the same as of chemical coagulation/flocculation. The difference lies on the coagulant used. In bio-flocculation, bacteria, fungi and flocculating microalgae constitute the flocculants, which are mixed with the algal suspension. Bio-flocculation represents an inexpensive and non-toxic alternative, while the absence of chemicals in the suspension enables total broth reuse (Molina-Grima et al., 2003). A great advantage of this method is that bacteria grown in wastewater could be used as coagulants, using wastewater as the main environment to cultivate algae (Milledge, 2013). This application has a binary objective: 1) the cleaning of wastewater could be achieved stimulating sustainable development; and 2) the fossil fuel input can be reduced, since no extra energy is needed for mixing; the bacteria are already mixed in wastewater. Furthermore, energy within the bacterial biomass could be recovered along with that of the micro-algae, increasing that way the levels of the extracted bio-energy (Milledge, 2013). Van den Hende et al. (2011) mention that bio-flocculation in sewage waters supplemented by flue gas from a coal power plant led to a 97.5% removal of the biomass within 30 minutes producing 2% bacterial/algal dry biomass (TSS) as well. Nonetheless there are two drawbacks that impede this method from being selected at industrial scale: 1) It causes changes in cell composition, since biological flocculants react with the existing algae cells and 2) microbial organisms may cause microbiological contamination, exacerbating the quality of the metabolites that are destined for food and feed applications, which are currently the only cost-efficient ones (Vandamme et al., 2013).

4.2.3 Gravity sedimentation

In gravity sedimentation, gravitational forces separate liquids or solid particles from others of different density. It is a method based on Stoke's Law, which assumes that the settling velocity is proportional to the density difference and the radius of the algal cells (Schenk et al., 2008; Milledge, 2013). Gravity sedimentation is a highly energy efficient method and therefore, it is selected when the end product is of low value, such as biofuels, or biomass from wastewater treatment (Nurdogan & Oswald, 1996; Molina-Grima et al., 2003; Rawat et al., 2011). When density difference or/and cell size is small (<70 μm), this process can be extremely slow (Brennan & Owende, 2010; Milledge, 2013). Thus, in order to fasten algal settling rates, coagulation/flocculation is often implemented prior to gravity sedimentation (Barros et al., 2014). Further drawbacks involve deterioration of microalgae biomass quality and low biomass recovery efficiency (30-65%) as well as concentration of TSS (0.5-1.5% using a lamella-type separator and 3% using a sedimentation tank) existed in the algal slurry (Uduman et al., 2010; Milledge, 2013; Barros et al., 2014).

4.2.4 Flotation

Flotation is often labeled as 'inverted' sedimentation, since dispersed gas or micro-air bubbles, supplied into the algal suspension, adhere to the solid particles and carry them to the liquid surface (Chen et al., 2011; Barros et al., 2014). The minimum size of aggregates should not be less than 10 μm, requiring in most cases a pre-coagulation/flocculation step using chemical as coagulants (Rubio et al., 2002; Milledge, 2013). Generally, flotation is characterized as a more effective and fast technique in harvesting microalgae than sedimentation (Milledge, 2013). The major advantage of flotation is that it has been implemented and proven at large scale (Hanotu et al., 2012). Further advantages include low space requirements and relatively short operational times (Barros et al.,

2014). Nevertheless, flotation involves high capital and operational costs, while in high salinity environments, due to high ionic strength, gas bubbles tend to rupture more easily, decreasing biomass recovery efficiency (Liu et al., 1999). Currently, there are four main flotation techniques: 1) Dissolved air flotation (DAF-bubble diameter <100μm); 2) dispersed air flotation (DiAF-bubble diameter 100-1000μm); 3) electrolytic flotation (see section 4.2.5); and 4) ozonation dispersed flotation (ODF) (Chen et al., 2011; Rawat et al., 2011; Barros et al., 2014). DAF is the most efficient and widely applied flotation technique, leading to a recovery efficiency of 80-90% and to a TSS concentration of 1-6% in the algal slurry (Uduman et al., 2010; Chen et al., 2011).

4.2.5 Electrophoresis techniques

Another potential solution to harvest microalgae refers to electrophoresis techniques. Microalgae are able to behave as hydrocolloid particles (i.e. dispersed hydrophilic polymers that are suspended throughout water), which can be separated from the water-based medium solution by activating an electric field using sacrificial or non-sacrificial electrodes (Aragon et al. 1992; Uduman et al., 2010; Barros et al., 2014). The most common electrophoresis techniques refer to electrolytic coagulation, electrolytic flotation and electrolytic flocculation (Uduman et al., 2010).

Electrolytic coagulation involves the use of active metal electrodes (sacrificial) as flocculant agents, such as aluminum or iron. These electrodes create positively charged metal ions that aggregate with algal cells forming 'flocs', which in turn precipitate in the bottom of the vessel (Mollah et al., 2004). Aragon et al. (1992) conducted several experiments on electrolytic coagulation and ended up with the deduction that this method is superior to chemical coagulation/flocculation. Electrolytic coagulation was more cost-efficient (the cost of energy was lower than the cost of coagulants), while the time of precipitation was shorter. Recovery efficiency for aluminum and iron electrodes corresponds to >95% and 78.9% respectively, rendering aluminum electrodes more desirable to ferric ones (Danquah et al., 2009; Uduman et al., 2010; Barros et al., 2014).

Electrolytic flotation follows the same principles as flotation. The only difference lies on the way the bubbles are created. Instead of supplying the suspension with gas or micro-air bubbles (flotation), in electrolytic flotation mechanism an electrode from inactive metal (i.e. sacrificial electrochemically non-depositing) is used, generating hydrogen bubbles from water electrolysis (Uduman et al., 2010). Like flotation the bubbles adhere to algal cells carrying them to the liquid surface (Azarian et al., 2007). The disadvantages of electrolytic flotation include scaling of the electrode and the high cost of power rectifiers. On top of that, at high shear forces, the bubbles trapped in the 'flocs' can disperse, destructing the algal 'flocs' (Uduman et al., 2010). The concentration of TSS that can be achieved employing electrolytic flotation ranges from 3-5% (Uduman et al., 2010).

Last but not least, electrolytic flocculation does not involve the exploitation of sacrificial electrodes but the use of non-sacrificial ones. This means that no flocculants are required (Barros et al., 2014). Contrariwise, the principle of this method is based on the movement of the negatively charged algal cells towards the electrode. When reaching the electrode, the cells lose their charge enabling them to form aggregates that are carried to the surface by bubbles, which were created from water electrolysis (Uduman et al., 2010). Recovery efficiency of electrolytic flocculation amounts to 80-95%. Besides the absence of flocculants, minimum energy is consumed rendering this method one of the most energy efficient thickening options (Uduman et al., 2010). On the other side, in electrolytic flocculation the electrodes are very prone to fouling (Barros et al., 2014).

Electrophoresis techniques seem to be very attractive when harvesting microalgae. They constitute environmental friendly methods, since they do not require the addition of chemicals, which may contaminate the broth. By the same token, electrochemical processes introduce energy efficiency compared to other methods, cost effectiveness and applicability to a wide variety of microalgae strains. Nonetheless, they are not largely disseminated rendering them grave to large scale production lines (Uduman et al., 2010; Zenouzi et al., 2013; Barros et al., 2014).

4.3 Dewatering methods

4.3.1 Filtration

The principle of filtration involves the utilization of a permeable medium (i.e. membrane), through which algal broth is pumped. By maintaining a pressure drop, microalgae solids deposit irreversibly on the permeable medium, forming over time a thick algal 'wall' that increases resistance and decreases filtration flux. This leads to a greater capture of solids (Molina-Grima et al., 2003; Show et al., 2013; Barros et al., 2014). This process is called fouling/clogging, but it also constitutes one of the major problems associated with filtration. Surpassing a critical point of resistance, the dense algal 'wall' inhibits the broth pass through the membrane, which separates the solids from the liquid (Milledge, 2013; Barros et al., 2014). Thus, regular backwashes are needed in order to ensure sanitation and reusability, increasing operational costs (Uduman et al., 2010; Christenson & Sims, 2011). Furthermore, although this dewatering method is suitable for very low density suspensions, it is not commonly applied on a large scale (Molina-Grima et al., 2003). This is due to high costs of the membranes and pumping (Barros et al., 2014). This method is cost-effective only for small volumes and only for harvesting large size algal cells (Uduman et al., 2010). Namely, for strain cells that exceed 70μm (Brennan & Owende, 2010).

Filtration can be divided in four different categories by classifying the membranes in terms of pore size: 1) macro-filtration (>10 μm); 2) micro-filtration (0.1-10 μm); 3) ultra-filtration (0.02-0.2 μm); and 4) reverse osmosis (<0.001 μm) (Milledge, 2013). These categories can be further classified to two new categories: 1) Dead-end filtration, which includes macro-filtration; and 2) tangential flow filtration (TFF), which includes micro-, ultra-filtration and reverse osmosis (Barros et al., 2014). Taking into account the minimum algal size for cost-effective harvesting (i.e. 70 μm), it can be inferred that only dead-end filtration is an attractive dewatering option. This can be attributed to the fact that the pressure to force algal broth pass through the membrane is inversely proportional to the membrane pores size. The smaller the membrane pores the higher the pressure and consequently the higher energy is needed, which results in higher operational costs (Milledge, 2013). However, the majority of algal species do not exceed 70μm in size. Therefore, in most cases, coagulation/flocculation is applied prior to filtration (Barros et al., 2014). Various experiments implementing pressure dead-end filtration on large size microalgae species, have shown that a slurry/cake with 2-27% TSS can be produced (Molina-Grima et al., 2003; Semerjian & Ayoub, 2003; Brennan & Owende, 2010; Milledge, 2013). On the other side, although TFF allows the separation of shear sensitive species, it results to an algal biomass recovery of 70-89%, while the concentration of the TSS ranges from 1-4% (Uduman et al., 2010; Milledge, 2013; Barros et al., 2014).

4.3.2 Centrifugation

Centrifugation is a dewatering process, where centrifugal forces replace gravity in order to drive separation (Molina-Grima et al., 2003; Uduman et al., 2010; Christenson & Sims, 2011; Rawat et al.,

2011; Milledge, 2013). It constitutes the fastest harvesting method, but also the most energy intensive. The latter attribute results in the highest operational costs among the different methods (Molina-Grima et al., 2003; Uduman et al., 2010; Barros et al., 2014). This limits its applicability only for the recovery of high-value products, such as highly unsaturated fatty acids, pigments for pharmaceuticals and cosmetics and high-value nutritional metabolites (Barros et al., 2014). Besides the rapid times of harvesting, centrifugation can be applied to the majority of microalgae strains, while it is the only method that can be highly efficient as a one-step process (Rawat et al., 2011; Show et al., 2013). There are plenty designs of centrifuges, but they can be roughly classified into three groups: 1) Disk-stack; 2) Simple bowl; and 3) Scroll conveyor bowl (decanter) (Milledge, 2013). Disk-stack centrifuge constitutes the most common option of harvesting in large scale production lines for high-value algal products. It is implemented mainly as a one-step process and its construction involves a bowl and a stack of closely spaced metal cones (disks) that rotate with the bowl (Molina-Grima et al., 2003; Milledge, 2013). The broth is fed to the center of the disk-stack and under high centrifugal forces, the denser algal solids move outwards towards the rotating bowl wall, while the less dense fluids moves towards the centre. After separation, a centrifugal pump creates a pressure to discharge the clear liquid from the centrifuge and the concentrated slurry is extracted through nozzles for further processing (see figure 13) (Milledge, 2013). The centrifugal forces applied inside the bowl range from 1300 to 14000 times the gravitational force (g) (Heasman et al., 2000; Molina-Grima et al., 2003; Milledge, 2013). Biomass recovery efficiency depends on the level of chosen centrifugal force. Heasman et al. (2000) investigated the extent of biomass recovery experimenting on different centrifugal forces. They found that at 13000g, 6000g and 1300g, the recovery efficiency was >95%, 60% and 40% respectively. Nevertheless, exposure to high gravitational and shear forces may result in cell structure damage (Barros et al., 2014). TSS concentration, when applying disk-task centrifugation, is measured 12% and can reach up to 22% employing other centrifugal options (the upper limit is achieved in a decanter bowl) (Molina-Grima et al., 2003; Uduman et al., 2010). Li et al. (2011), who cultivated *Haematococcus pluvialis* in a hybrid system similar to this study, measured a fraction of 13.5% TSS in the algal cake, applying centrifugation. Disk-stack centrifugation is ideally implemented for algal strains with a size between 3-30 μm and concentration between 0.02-0.05% (Milledge, 2013).

Figure 13 presents overview of the technical parts that build the disk-stack centrifuge (GEA Westfalia Separator Group, 2015).

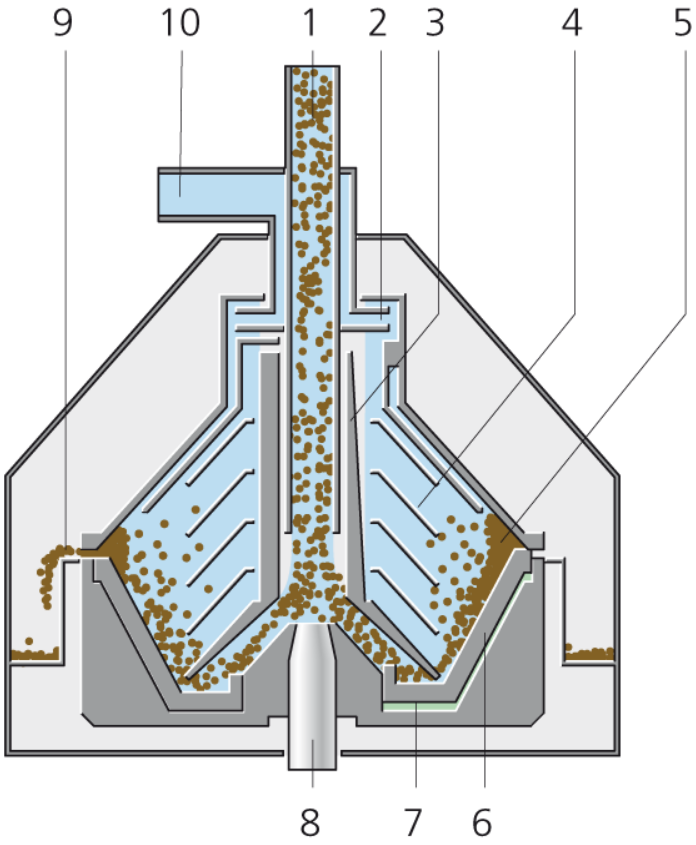

Figure 13: Technical drawing of a disk-stack centrifuge: 1) Product feed; 2) centripetal pump; 3) distributor; 4) disk-stack; 5) solids holding space; 6) sliding piston (nozzle); 7) closing chamber; 8) spindle, drive; 9) solids ejection port; 10) discharge, clarified phase (GEA Westfalia Separator Group, 2015).

4.4 Comparison of the different harvesting methods

An abundance of studies have been conducted on the harvesting techniques of algal solids existed in a diluted suspension. Due to the large number of microalgae species and to differences in their biology, it is hard to choose a method as the most appropriate. In general, the criteria to choose a method can be divided into two main categories: 1) Desired microalgae features and 2) desired harvesting process. Desired algal features that facilitate the harvesting process involve large cell size, high specific gravity compared to the medium and reliable flocculation (Uduman et al., 2010). An ideal harvesting process should be applicable to the majority of microalgae species and should result in high TSS concentration, while requiring minimum capital and operational costs, energy and maintenance (Barros et al., 2014). Chemical coagulation/flocculation and bio-flocculation are very attractive harvesting options, since they do not require any energy, while they are fast. Furthermore, they are characterized by high biomass recovery efficiency as well as by decent TSS concentration in the algal slurry. However, they are involved in toxicity and contamination issues, which lead to algal quality deterioration. Since astaxanthin is a pigment that is destined to the food market as the most powerful antioxidant, quality plays the most important role. Thus, these options cannot be selected. Likewise, although gravity sedimentation is considered as the most energy efficient method, it is extremely time consuming for strains with size smaller than 70μm, such as 'red' *Haematococcus pluvialis* cells (20 μm). Furthermore, gravity sedimentation involves the poorest recovery efficiencies as well as TSS concentration among all other options. Electrophoresis techniques are environmental friendly, cost-efficient processes that are applicable to a wide range of strains. However, they are not vastly disseminated rendering them risky for large scale production lines. Filtration is a cost-effective

option only for small volumes and only for algal species, whose cell size exceeds 70 μm. Thus, it cannot be considered as an attractive option for our system. Consequently, taking into account *Haematococcus pluvialis* properties as well as the end-product (i.e. astaxanthin), flotation and centrifugation are the most compatible options. Flotation is a less expensive method than centrifugation, relatively fast and has been implemented and proven at large scale. However, it is usually applied in conjunction with chemical coagulation/flocculation, posing risks in terms of contamination. On the other side, although centrifugation is the most energy intensive and expensive method, its operational times are rapid, it can be applied to the majority of algal strains and it is the only method highly effective as a one-step process. Furthermore, disk-stack centrifugation constitutes an ideal method for species with size between 3-30 μm and suspended solids in the broth between 0.02-0.05%. Considering the size of *Haematococcus pluvialis* (i.e. 20μm) as well as the calculated concentration of suspended solids in the 'red stage' (i.e. 0.035%, see section 8.3) in association with the high TSS concentration of disk-stack centrifugation (12%), this option at 13000g was selected for harvesting. Implementing disk-stack centrifugation at 13000g, a biomass recovery efficiency that exceeds 95% can be achieved. In this thesis, a recovery efficiency of 98% was assumed. The high operational costs should not pose any issues, since they are offset by the high value of astaxanthin.

Table 8 presents a summary of the performance of the different harvesting techniques.

Harvesting technique	Recovery efficiency	TSS	Reliability[9]	Advantages	Limitations
Chemical coagulation/ flocculation	>95%	3-8%	Very good	No energy requirements; fast; applicable to wide range of species; cost-efficient	high cost of coagulants; toxic to algae biomass; limited recycle of the growth medium
Bio-flocculation	97.5%	2%	Good to very good	inexpensive; non-toxic to algae biomass; total growth medium recycle; applied in wastewater treatment	changes in cellular composition; possible microbiological contamination
Gravity sedimentation	30-65%	0.5-3%	Poor	Highly energy efficient; simple and inexpensive	time consuming; possible deterioration in biomass quality; poor TSS concentration
Dissolved air flotation	80-90%	1-6%	Good to very good	Proven method at large scale; low space requirements; relatively fast	High capital-operational costs; rupture of gas bubbles in high salinity environments; suitable only to specific species; generally coagulation is needed prior to DAF
Electrolytic coagulation	78.9% for Fe >95% for Al	N/A	Very good	Superior to chemical coagulation/flocculation; no chemicals required; environmental friendly; cost-effective; applicable to wide range of species	Poorly disseminated; electrodes to be replaced periodically
Electrolytic flotation	N/A	3-5%	Very good	Environmental friendly; applicable to wide range of species; relatively fast	Poorly disseminated; scaling of the electrodes and thus to be replaced periodically; high cost of power rectifiers; at high shear forces bubbles can separate from flocs
Electrolytic flocculation	80-95%	N/A	Very good	Environmental friendly; one of the most energy efficient methods; applicable to wide range of species	Poorly disseminated; electrodes prone to fouling and thus to be replaced periodically
Dead-end filtration	N/A	2-27%	Very good	Suitable for very low density suspensions; high TSS concentration	Not commonly applied at large scale; high costs of the membranes and pumping; fouling/clogging; regular backwashes needed increase costs; suited to large algal cells
Tangential flow filtration	70-89%	1-4%	Good	Allows the separation of shear sensitive species; suitable for very low density suspensions	Not an attractive method yet
Disk-stack centrifugation	>95% at 13000g	12%	Very good	Fastest method; applicable to the majority of microalgae strains; highly efficient as a one-step process; high recover efficiencies and TSS concentration	Most energy intensive method; highest operational costs among all methods; suitable only for the recovery of high-value products; high shear forces may damage algal cells

Table 8: Summary of the performance of the different harvesting techniques.

[9] In terms of biomass quality.

5 Extraction phase

5.1 Introduction

After implementing disk-stack centrifugation, an algal cake of 12% TSS is produced. One of the main obstacles to fully taking advantage of astaxanthin and channel it into the market refers to the ability to successfully and efficiently extract the pigment from the cake. Extraction phase can be divided into three main processes: 1) Cell disruption; 2) dehydration; and 3) recovery of the desired metabolite (Olaizola, 2003)

An abundance of literature is available on the topic of efficient cell disruption and recovery techniques. Depending on the algal cell wall and on the nature of the product to be obtained, these techniques are based either on mechanical forces (expeller pressing, homogenization, bead milling, ultrasonic-assisted extraction and autoclave) or on bio-chemical reactions (solvent extraction, supercritical fluid extraction, enzymatic treatment and osmotic shock) (Brennan & Owende, 2010; Mata et al., 2010; Mercer & Armenta, 2011; Mohan et al., 2014). These processes of cell disruption and recovery can be facilitated by implementing one or a combination of the abovementioned techniques. In other words, the techniques to disrupt the algal cells may be implemented also for the recovery of the desired metabolite and vise versa (Olaizola, 2003; Mercer & Armenta, 2011). There is not a specific route to follow all through the extraction phase for all metabolites existed in the algal cells. Regarding dehydration, the final product determines if this technique will be employed or not. In commercial astaxanthin production, dehydration is an imperative step, since it ensures the quality of the pigment and leads to the final form of the product, which is powder (Mata et al., 2010; Li et al., 2011).

For astaxanthin extraction, literature provides different combinations of techniques to follow (Olaizola, 2003; Thana et al., 2008; Mata et al., 2010; Razon & Tan, 2011). In this chapter these procedures for cell disruption, dehydration and recovery of astaxanthin are analyzed and compared, resulting in the most appropriate combination to be used. Figure 14 presents the most prevailing techniques for cell disruption, dehydration and recovery associated with the astaxanthin as part of the production line.

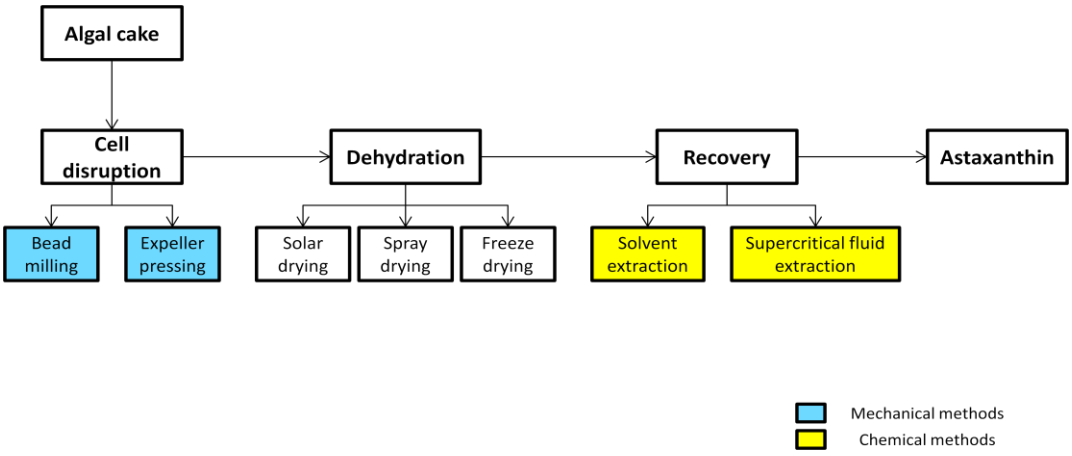

Figure 14: Flow chart of the extraction phase.

5.2 Cell disruption

5.2.1 Introduction

The major component of the tough outer (exine) walls of plant spores and pollen grains is called sporopollenin. *Haematococcus pluvialis* cells are characterized by a thick sporopollenin wall, which impedes astaxanthin extraction from the intracellular part (Mendes-Pinto et al., 2001). Thus, different techniques have been developed in order to disrupt the algal cell and recover the intracellular metabolites. The algal cell disruption, which takes place prior to dehydration and recovery, is of particular significance, since the selection of the appropriate technique constitutes a key factor for enhancing the desired metabolite recovery efficiency (Olaizola, 2003; Lee et al., 2010). Most of the methods reported for cell disruption have been adjusted from applications on intracellular non-photosynthetic bio-products (Brennan & Owende, 2010). The most appropriate cell disruption methods to enhance recovery of astaxanthin from *Haematococcus pluvialis* at a commercial scale involve mechanical processes and more specifically expeller pressing and bead milling (Lorenz & Cysewski, 2000; Olaizola, 2003; Mercer & Armenta, 2011; Mohan et al., 2014).

5.2.2 Expeller pressing

Expeller pressing (or pulverizer) is a mechanical method, where microalgae cells are squeezed under high pressure in order to rupture the thick sporopollenin wall (Mohan et al., 2014). It is a method that follows the same principle as a pressing device to squeeze seeds in order to extract vegetative oil and constitutes the easiest and simplest method to use in the microalgae industry. Besides simplicity, its main advantage refers to the minimization of contamination from external sources. Nevertheless, expeller pressing is a slow process and requires a large amount of biomass in order to be efficient (Mercer & Armenta, 2011). This disruption method can be implemented as a recovery method as well, when the desired product to be recovered refers to algal oil for the production of biofuels. An algal oil recovery efficiency of 75% can be achieved in a single step expeller pressing (Mohan et al., 2014).

5.2.3 Bead milling

Bead milling involves the usage of vessels filled with tiny glass, ceramic or steel beads that are agitated at high speeds. The dried biomass is fed in these vessels, where continuous exposure of biomass to the grinding media (beads) leads to cell-wall rupture, which results in the release on intracellular metabolites (Lee et al., 2010; Mercer & Armenta, 2011). The degree of disruption depends on the size, shape and composition of the beads as well as the resistance and strength of the strain's cell walls (Doucha & Lívanský, 2008). Similar to expeller pressing, this method can be employed as a single step process to recover algal oil for the production of biofuels (Mohan et al., 2014). This method is most effective and energy wise, when biomass concentration after harvesting in the algal cake is between 100-200 g/l (Greenwell et al., 2010). An operational overview of a bead mill is illustrated in figure 15.

5.2.4 Comparison of cell disruption methods

Both methods are reliable for the *Haematococcus pluvialis* cells disruption at a commercial scale. Nevertheless, the main criterion to prefer one method to the other lies on the energy needs of each technique. Regarding expeller pressing, the power consumption ranges between 3.2-3.6 (kWh/kg), while for bead milling it is reported that power of 2.8-10 (kWh/kg) is required (Li et al., 2011; Razon & Tan, 2011). Calculating the mean values for each range, it can be inferred that expeller pressing is

more energy efficient option. However, the constraint of large biomass that is needed for efficient expeller pressing may not be satisfied during the cold months, when 'red' biomass productivity especially for Amsterdam is very low. Thus, bead milling was chosen as a cell disruption method. This decision is also enhanced by biomass concentration in the algal cake after harvesting. After a single step disk-stack centrifugation which was the selected method for harvesting, an algal cake of 12% TSS was produced for the selected locations. This means can be translated into 120 g/l for both cities. This value is within the range for an efficient and energy-wise bead milling mentioned before. Like expeller pressing, bead milling is usually combined with some kind of solvent or supercritical fluid extraction when targeting to astaxanthin (Olaizola, 2003; Mata et al., 2010; Mercer & Armenta, 2011). As already mentioned these mechanical methods are efficient for simultaneous cell disruption and recovery, only when algal oil is the desired product. A more detailed approach on solvent or supercritical fluid extraction is presented in the section 5.4. Regarding biomass recovery efficiency associated with bead milling, no values have been found in the literature. Thus, it was assumed that 100% of the biomass subjected into bead milling, was recovered.

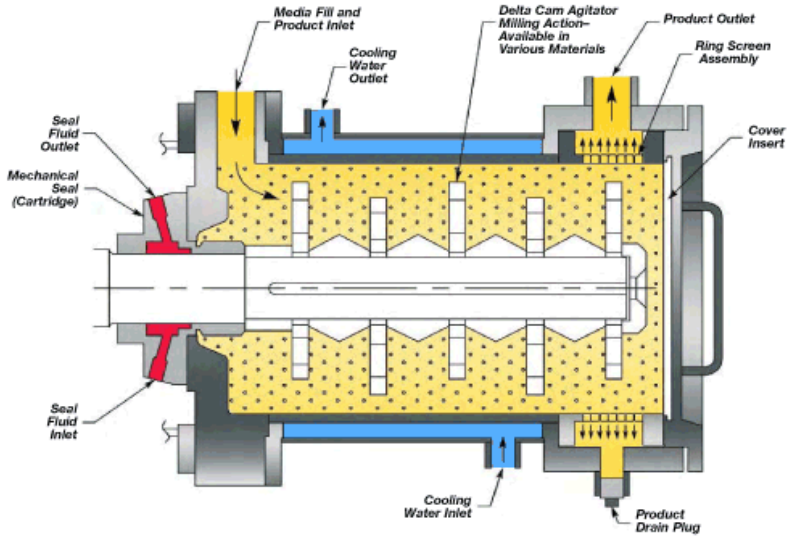

Figure 15: Operational overview of a bead mill (Kadirjo, 2011).

5.3 Dehydration

After algal cell walls have been disrupted, biomass must be further processed rapidly, or it can be spoiled within few hours. Thus, dehydration is a process applied prior to recovery of the desired metabolite, in order to extend the shelf-life of the algal biomass (Molina-Grima et al., 2003; Mata et al., 2010). Dehydration poses a significant economic constraint in the production line, since it may constitute 70-75% of the total extraction phase costs (both capital investment and energy requirements) (Show et al., 2013). The selection of the appropriate dehydration technique depends strongly on the scale of operation as well as on the desired product to be recovered (Brennan & Owende, 2010; Show et al., 2013). The most known dehydration techniques that have been employed on microalgae refer to solar drying, spray drying and freeze drying (Molina-Grima et al., 2003; Brennan & Owende, 2010; Milledge, 2013; Show et al., 2013).

In remote areas with limited access on electricity solar drying constitutes the only option of dehydration (Show et al., 2013). Among the three methods, solar drying is the simplest and most

cost-efficient (Milledge, 2013). Nonetheless, it poses an abundance of drawbacks, which render this method inappropriate; especially when recovering high-value metabolites, such as astaxanthin. In order to achieve a successful solar dehydration, large areas are required. More specifically, 1 m^2 is required to produce 100 grams of dry biomass (Milledge, 2013). Furthermore, this technique is dependent on the local weather conditions, while usually long drying times are required (Brennan & Owende, 2010). Last but not least, under high solar radiation algal chlorophyll disintegrates altering the texture and color of the final product (Molina-Grima et al., 2003; Show et al., 2013).

Spray drying has been labeled as the most appropriate method to dry high-value microlagal products (Brennan & Owende, 2010; Milledge, 2013). This method involves liquid atomization, gas/droplet mixing and drying from liquid droplets. Using an atomizer or spray nozzle, the atomized slurry droplets are sprayed downward into a vertical chamber, through which hot gases are supplied. Hot gases dry the liquid rapidly, leaving the dry biomass on the bottom, while the gas stream is exhausted through a cyclonic dust separator (Show et al., 2013). Figure 16 portrays a schematic view of the different operations associated with a spray dryer (Bahnasawy et al., 2010).The main drawbacks of spray drying refer to the high operational costs and the deterioration of some microalgae pigments (Molina-Grima et al., 2003).

Freeze drying, also known as lyophilisation or cryodesiccation, involves the freezing of algal cake and then the reduction of the surrounding pressure, to allow the frozen water in the material to sublimate directly from the solid phase to the gas phase (Molina-Grima et al., 2003). It is a technique that causes less damage to organic materials than spray drying, but it is even more expensive, especially on a commercial scale (Milledge, 2013).

For the recovery of most carotenoids spray drying is selected (Leach et al., 1998; Li et al., 2011). The dry biomass (in powder) recovery efficiency of this method exceeds 95% and in some occasions it may also reach 100% (Leach et al., 1998). Thus, in this study, spray drying was selected for dehydration assuming a recovery efficiency of 98%. After spray drying, the moisture content in 'red' biomass corresponds to 5% (Pérez-López et al., 2014).

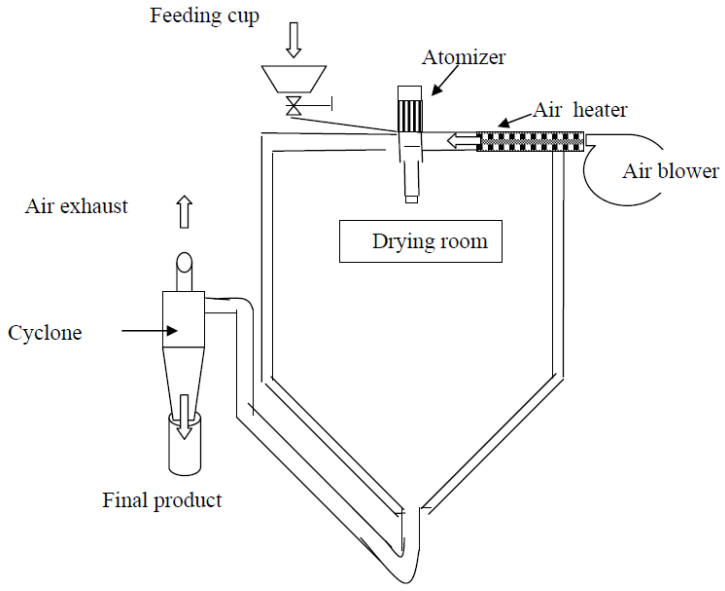

Figure 16: Schematic view of the different operations associated with a spray dryer (Bahnasawy et al., 2010).

5.4 Recovery of astaxanthin

5.4.1 Introduction

By the time the cell wall is disrupted and the biomass is fully dried, the intracellular content is protected only by the thin cell membrane and the recovery of the desired product is possible. There is an abundance of recovery methods to be applied, but solvent extraction and supercritical fluid extraction are considered as the most efficient and compatible methods, when astaxanthin is targeted (Olaizola, 2003; Brennan & Owende, 2010; Mata et al., 2010; Cuellar-Bermudez et al., 2014).

5.4.2 Solvent extraction

Solvent extraction is a widely implemented method in order to recover fatty acids and high value metabolites, such as astaxantin and β-carotene (Molina-Grima et al., 2003; Brennan & Owende, 2010). This technique involves the usage of organic solvents, such as benzene, cyclohexane, hexane, acetone, methanol, hydrochloric acid, dodecane and chloroform in order to cause alterations to the algal cell membrane, enhancing the movement of intracellular globules towards the outer part of the cell. Intracellular products that are characterized by high solubility in the selected organic solvents can be then recovered easily (Brennan & Owende, 2010; Mercer & Armenta, 2011; Cuellar-Bermudez et al., 2014). Thus, an ideal solvent should be insoluble in water but solubilize the desired product, have a low boiling point and a considerable different density than water to enable its removal after recovery, and be inexpensive and reusable. But above all, an ideal solvent should fully penetrate the cell membrane and match with the polarity of the desired product (Mercer & Armenta, 2011). Solvent extraction is a technique that can be implemented as a one-step extraction method, without a prior mechanical cell wall disruption. A one-step extraction method can be employed only when solvents can easily penetrate both the cell wall and membrane (Mohan et al., 2014). In case of algal strains that are distinguished by a thick cell wall, such as *Haematococcus pluvialis*, the solvent may not manage to break the cell wall and contact the cell membrane, hindering that way the recovery (Molina-Grima et al., 2003; Brennan & Owende, 2010; Lee et al., 2010). This is the reason, why this study included a mechanical cell wall disruption step prior to recovery of astaxanthin. Among the different solvents, a two-stage solvent process using a combination of hydrochloric acid followed by acetone and a combination of dodecane and methanol resulted in a recovery astaxanthin efficiency of 87% and 85% respectively (Cuellar-Bermudez et al., 2014).

Solvent extraction includes several drawbacks. The main disadvantage of solvent extraction involves the degradation of the intracellular content, since most organic solvents are highly flammable and/or toxic. Furthermore, this technique is energy intensive leading to high operational costs, while albeit solvents are relatively inexpensive, a high volume per unit of biomass is required (Mercer & Armenta, 2011). In like manner, solvent recovery requires extra unit operations, which results in higher cost and lower recoveries. Last but not least, solvents are characterized by poor selectivity. This means that during solvent extraction, polar substances form polymers which lead to discoloration of the desired product (Sahena et al., 2009).

5.4.3 Supercritical fluid extraction

Supercritical fluid extraction (SFE) is a modern and a widely accepted method to recover high value metabolites from microalgae that are destined for the pharmaceutical and food processing sector (Thana et al., 2008; Mercer & Armenta, 2011). This can be attributed to the fact that unlike solvent extraction, SFE results in highly purified extracts that are free from the potential harmful effects of solvents (flammability and toxicity), while it is a simple and fast technique (Mendes et al., 2003; Sahena et al., 2009). The main principle behind this method is the utilization of supercritical fluid, whose physicochemical properties are between those of a liquid and a gas (Mohan et al., 2014). Carbon dioxide is considered as an ideal compound for this process. Carbon dioxide usually behaves as a gas in the air, when subjected to standard temperature and pressure (STP), or as a solid (labeled as 'dry ice') when frozen (Mendiola et al., 2007). When both temperature and pressure are increased to or above a critical point (31.1°C and 7.4 MPa or 73 atm), CO_2 enters a phase between gas and liquid and can behave as a supercritical fluid, which means that it can expand like a gas while its density is like that of a liquid (Mohan et al., 2014). Figure 17 presents the phase diagram of CO_2 (UCSB ScienceLine, 2015). Supercritical fluids are characterized by special properties such as high diffusivity, low viscosity, and low surface tension, which increase solvating efficiency and enable the recovery of the desired product (Thana et al., 2008). The way of the supercritical CO_2 to enter the intracellular environment is the same as the one when employing solvent extraction presented above (Cuellar-Bermudez et al., 2014). After the supercritical fluid has diffused through the natural solid matrix, pressure and temperature are reduced below critical point leading to the loss of the special properties of the fluid. The targeted extract that exists in high concentrations, can then be easily recovered, while the fluid can be recycled (Thana et al., 2008; Mercer & Armenta, 2011; Cuellar-Bermudez et al., 2014).

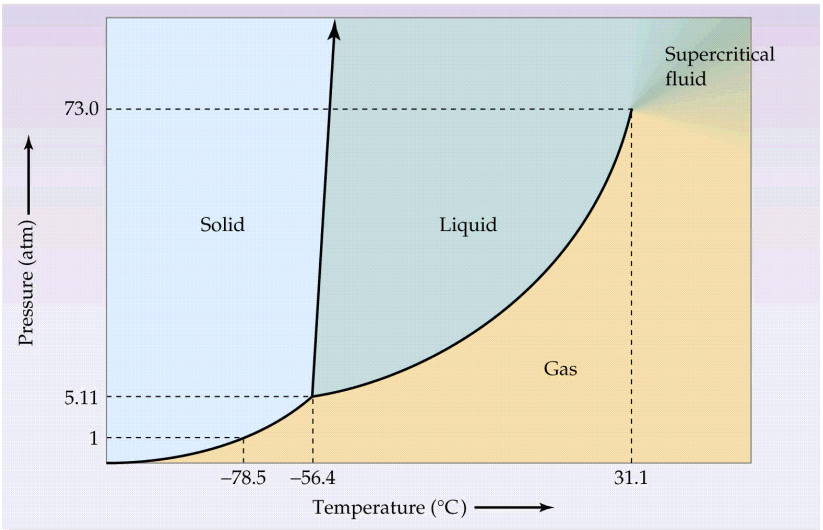

Figure 17: Phase diagram of CO_2 (UCSB ScienceLine, 2015).

CO_2 is the most favorable among the existing supercritical fluids, since its critical temperature and pressure are relatively low compared to others, while due to its gaseous behavior in room temperature it can be easily removed after recovery. This renders this compound safe for nutritional metabolites. Furthermore, like in cultivation phase, CO_2 can be supplied using flue gases as well as safely recycled, enhancing the sustainable profile of the production line (Cooney et al., 2009; Sahena et al., 2009; Mercer & Armenta, 2011). By the same token, CO_2 is a highly selective compound, which unlike organic solvents minimizes the possibility of polymerization of polar substances. Last but not

least, no extra unit operations are required, resulting in high yields (Sahena et al., 2009). The main drawback of this method is the high power consumption, often higher than solvent extraction (Mercer & Armenta, 2011; Mohan et al., 2014). Nevertheless, when ethanol is used as a co-solvent, solvating power of CO_2 is enhanced, which leads to lower temperature and pressure requirements and consequently to reduced operational costs (Nobre et al., 2006; Mendiola et al., 2007; Mercer & Armenta, 2011). Another restriction of supercritical CO_2 extraction revolves around moisture levels in the sample, which affects the efficiency of this method. High level of moisture acts as a barrier against diffusion of CO_2 in the sample. Thus, drying prior to implementation of this method is usually required (Sahena et al., 2009).

Several studies have reported experiments on supercritical CO_2 extraction for the recovery of astaxanthin from *Haematococcus pluvialis.* Thana et al. (2008) have subjected *Haematococcus pluvialis* cells into supercritical CO_2 extraction varying the temperature and pressure above the critical point. They found out that the optimal conditions for highly purified astaxanthin recovery correspond to 70°C and 50 MPa for the temperature and pressure respectively. The recovery efficiency was determined at 84%. On the other hand, Valderrama et al. (2003) modified temperature and pressure at 60°C and 30 MPa respectively, while using ethanol (9.4%) as a co-solvent. This process resulted in an astaxanthin recovery efficiency of 97%. Nobre et al. (2006) conducted the same experiment as Valderrama et al. (2003) using the same values for temperature and pressure and altering slightly the concentration of ethanol (10%). They ended up with a recovery efficiency of 92%.

5.4.4 Comparison of recovery methods

Although supercritical CO_2 extraction is a more energy intensive method than solvent extraction, it is more preferable technique for astaxanthin recovery due to various reasons. It is a simple and fast method that results in excellent quality products compared to solvent extraction, where the risk of contamination exists. Supercritical CO_2 extraction enhances sustainable development, when CO_2 from flue gases is used, while higher recovery efficiencies than solvent extraction have been reported. Furthermore, CO_2 is a highly selective compound compared to solvents, while in supercritical CO_2 extraction no extra unit operations are required, something that does not go for solvent extraction. The drawback of moisture level dependence, involved in supercritical CO_2 extraction, is eliminated for this study, since spray drying has been already taken into account in the production line prior to pigment's recovery (see section 5.3). Considering astaxanthin quality as the most important criterion as well, supercritical CO_2 extraction is the most favorable option and, thus, it was chosen for this thesis. Regarding astaxanthin recovery efficiency, the one determined from Valderrama et al. (2003) (i.e. 97%) was selected.

6 Microalgae process model

6.1 Schematic view of the model

A simulation of *Haematococcus pluvialis* life-cycle was achieved, by developing a mathematical model, which included all three phases (cultivation, harvesting and extraction) presented in sections 3, 4 and 5[10]. Cultivation constitutes the most important part of the model, since algae growth is the most complex process to be modeled. Thus, the goal of the process model is binary: 1) To illustrate seasonal fluctuation of the annual 'wet' biomass productivity after cultivation; and 2) to determine the annual astaxanthin yield after employing harvesting and extraction for the two locations selected. 'Wet' biomass productivity is the dry biomass prior to harvesting and extraction. It constitutes in reality, the amount of dry biomass existed in the broth during cultivation phase.

Since cultivation is the most significant part of the production line, algae growth parameters play the most important role. For photoautotrophic cultivation illumination and temperature are of utmost important among them. Thus, the main model input referred to solar irradiation and temperature data for Livadeia and Amsterdam throughout 2014. Besides solar irradiation and temperature data, the model takes into account an abundance of other parameters that are crucial for algae growth (see figure 18). These parameters are assumed as constant values and are based on the information presented all through section 3 (see also table 11 in section 6.2). The central idea behind the creation of the model is to translate incident solar irradiation into biomass productivity using HHV (see also section 3.6.7). However, incident solar irradiation is subjected to various inefficiencies and loss mechanisms that reduce the final uptake of solar energy by the algal cells. These inefficiencies and loss mechanisms refer to reflection (REFL), PAR, photosynthetic efficiency (PE), land efficiency (L_{EFF}) and distribution ($\eta_{DISTRIBUTION}$) of light during the day and are presented in detail all through sections 3.6.2 and 6.2. Furthermore, temperature impact on the system was translated into an efficiency factor (T_{EFFECT}), which acts on solar irradiation, by using temperature data for the selected locations (see formulas 6 and 7 in section 3.6.3).

The general formula to calculate the 'wet' biomass productivity after cultivation phase, which was found in literature, is presented below (Sukenik et al., 1991; James & Boriah, 2010; Sudhakar et al., 2012b):

$$\mathrm{PROD_{WET}} = \frac{\eta_{\mathrm{DISTRIBUTION}} * \mathrm{REFL} * \mathrm{PAR} * \mathrm{PE} * \mathrm{L_{EFF}} * \mathrm{T_{EFFECT}} * \mathrm{SUN}}{\mathrm{HHV}} \quad (9)$$

Nevertheless, the proposed formula for calculating the 'wet' biomass productivity does not take into account the impact of CO_2, O_2, pH, nutrients and mixing. Involved data of these parameters, such as concentrations and flow rates, are not considered in studies that try to simulate algae growth on the desktop without conducting an experiment. This happens, because CO_2, O_2, pH, nutrients and mixing do not play any direct role on the amount of solar energy absorbed by the algal cells, but they facilitate other parts of cultivation. Therefore, they cannot fit in the biomass productivity formula that exists in the literature. On the other side, if these parameters wouldn't play any role in biomass productivity calculation, it could be considered as invalidity, since they are of great significance during cultivation (see sections 3.5 and 3.6.4-3.6.6). The only way to include these parameters into

[10] The biggest part of the model was based on previous attempts to simulate algae growth and mostly on the researches of Sukenik et al. (1991), James & Boriah (2010), Sudhakar et al. (2012b) and Jonker & Faaij (2013).

biomass productivity determination is to conduct experimental/empirical research. This issue was tackled by translating the impact of these parameters into an efficiency factor (F_{SUB}), which was assumed at will.

Furthermore, since the cultivation of *Haematococcus pluvialis* is divided into two stages, one very important parameter to be taken into account is that the amount of broth (in liters) existed in the 'green stage' (i.e. in the tubular PBR) should be equal to the one existed in the 'red stage' (i.e. in the raceway pond). More specifically, after cultivating *Haematococcus pluvialis* cells in the tubular PBR to a level that they can be subjected into adverse environmental conditions, the whole broth transferred to the raceway pond should fill the pond completely if needed. Although the volume of broth did not play any direct role in algae growth, this predication of equalizing the volumes of the two culture systems enhances validity of the mass and energy flows as functions of biomass productivity as well as economic performance (see sections 8, 9 and 10). Assuming that the raceway pond covers the whole area selected, while the distance between the tubes at tubular PBR fence is 0.05 (m), and taking into account the depths of the pond and the tubes (0.3m and 0.05m respectively, see table 11), the ratio to equalize the volume of broth between an one-stage horizontal tubular PBR and a raceway pond amounts to 15:1. In other words, for the same area, a fence comprised by 15 stages of tubes is needed in order the broth existed in the tubular PBR fence to fill the raceway pond completely if needed. This ratio was translated into an equalizing factor (F_{EQ}). Since the model created in this study is a general tool for any culture system, when having a hybrid system the equalizing factor should be taken into account. For single-stage cultivation this factor can be excluded. Detailed calculation of this ratio can be found in Appendix B.

The formula to calculate 'wet' biomass productivity, reformed to the needs of this study, is the following:

$$\mathrm{PROD_{WET}} = \frac{\eta_{\mathrm{DISTRIBUTION}} * \mathrm{REFL} * \mathrm{PAR} * \mathrm{PE} * \mathrm{L_{EFF}} * \mathrm{T_{EFFECT}} * \mathrm{F_{SUB}} * \mathrm{F_{EQ}} * \mathrm{SUN}}{\mathrm{HHV}} \quad (\mathbf{10})$$

The 'wet' biomass productivity is the one achieved after cultivation phase and prior to harvesting and extraction phases. During harvesting phase, the 'wet' biomass is dewatered applying disk-stack centrifugation, while all through extraction phase the algal cake is subjected into bead milling, spray drying and supercritical CO_2 extraction for the processes of cell disruption, dehydration and recovery of astaxanthin respectively (see sections 4 and 5). All of these processes are accompanied with recovery efficiencies (RE). In order to calculate the astaxanthin yield, the 'wet' biomass calculated using formula 10 has to be multiplied with these efficiencies of the harvesting and extraction phases. Last but not least, the concentration of astaxanthin in the 'red' biomass varies from 1-4% of the final dry biomass weight (Lorenz & Cysewski, 2000; Zhekisheva et al., 2005; Zhang et al., 2009; Li et al., 2011; Markou & Nerantzis, 2013). This variation in astaxanthin concentration, among the different studies that conducted laboratory experiments, can be attributed to the different culture systems used for *Haematococcus pluvialis* cultivation, as well as to the different parameters taken into account during the two stages, such as irradiance levels, selected temperature in the medium and substrate supply. In this thesis the average concentration of astaxanthin (i.e. 2.5%) was assumed. Consequently, astaxanthin yield for the selected locations can be determined using the following formula:

$$\text{Dried Astaxanthin} = \text{PROD}_{\text{WET}} * \text{RE}_{\text{CENTR}} * \text{RE}_{\text{BEAD}} * \text{RE}_{\text{SPRAY}} * \text{RE}_{\text{CO2}} * \%\text{C}_{\text{ASTAX}} \quad (\mathbf{11})$$

The description of each abbreviation depicted in formula 11 can be found in table 11 in section 6.2. In figure 18, the different parts of the formulas 10 and 11 and the way for their calculation, when needed (e.g. calculation of PE and T_{EFFECT}), are elucidated individually. Diamonds are fixed input values, blocks are calculated values and small round shapes are formulas. Model input and formulas, which lead to biomass productivity calculation, are depicted in tables 11 and 12 in section 6.2.

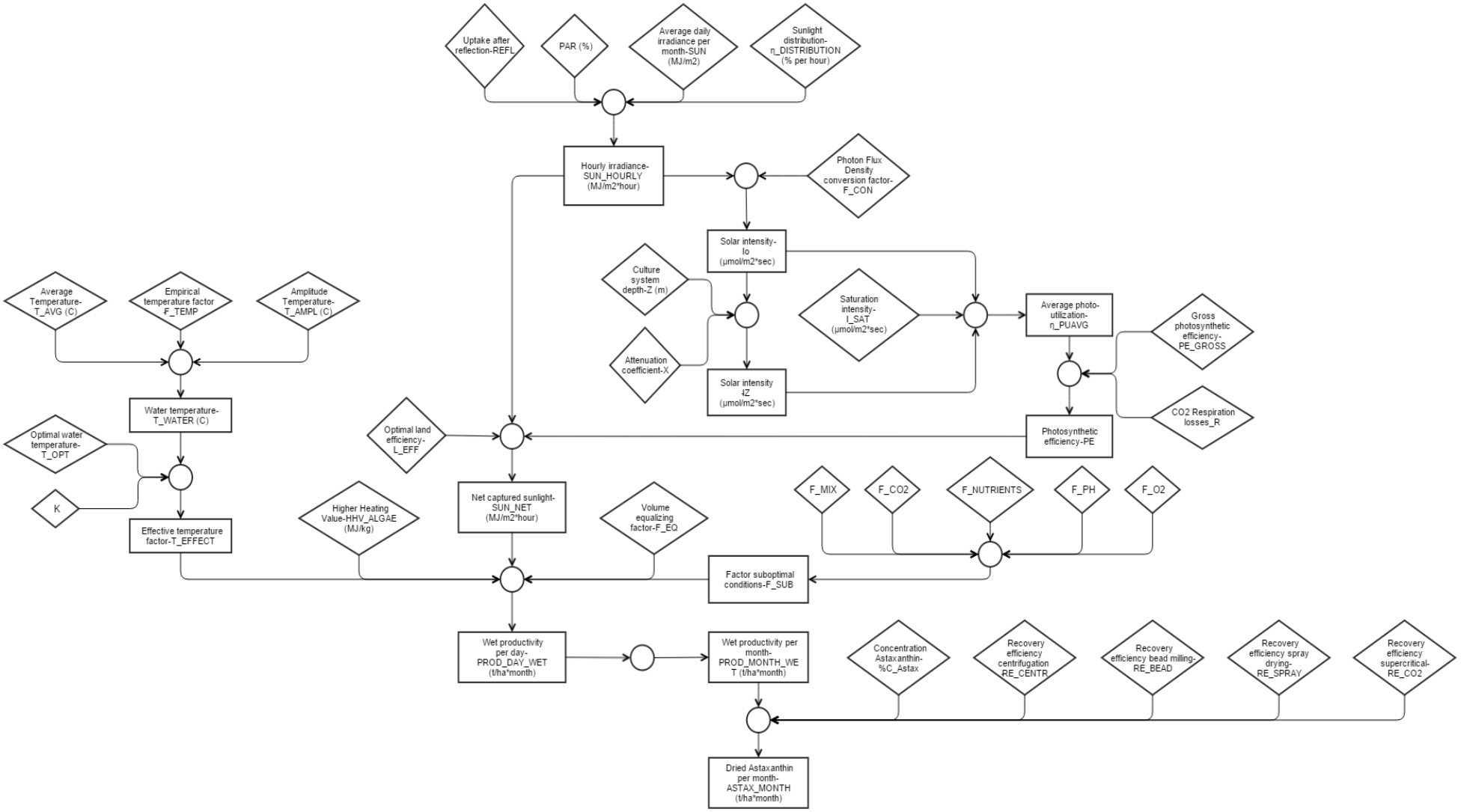

Figure 18: Flow chart of the microalgae process model.

6.2 Model input

As mentioned in section 6.1, the main input for the model involves solar irradiation and temperature data for the two cities all through 2014. Data represent an average day per month for both cities and they are depicted in table 9.

Solar irradiation data for Livadeia have been provided by ETHER, a Greek company focused on photovoltaic parks (Panetas, 2015). Average and amplitude temperature data for Livadeia were found in the official website of the national observatory of Athens, which holds all climate data for all cities in Greece (NOA, 2015). Regarding Amsterdam, solar irradiation as well as average and amplitude temperature data were derived by the official website of Royal Netherlands Meteorological Institute (in Dutch Koninklijk Nederlands Meteorologisch Instituut-KNMI) (KNMI, 2015). Solar energy is expressed in (MJ/m^2/day), while temperature is expressed in (°C).

Year:2014	**Livadeia**			**Amsterdam**		
Month	**Irradiance**	**Temperature**		**Irradiance**	**Temperature**	
		Average	Amplitude		Average	Amplitude
	(MJ/m^2/day)	(°C)		(MJ/m^2/day)	(°C)	
January	6.91	9	5	2.74	3	2
February	9.11	10	5	5.18	4	4
March	12.89	12	6	9.32	6	3
April	17.5	15	7	14.72	8	4
May	20.77	19	8	19.87	13	5
June	25.27	24	8	20.05	15	4
July	24.77	26	8	19.58	17	4
August	22.21	26	8	16.81	17	4
September	17.1	22	7	10.66	15	3
October	11.27	16	6	5.83	12	3
November	7.13	13	4	2.98	7	2
December	5.58	10	5	1.94	5	2
Total	**180.51**			**129.68**		

Table 9: Main model input of the microalgae process model.

Nevertheless, irradiance values fluctuate during the day, since the distribution of light between sunrise and sunset varies as well. Calculating biomass productivity using hourly irradiance data enhances validity of the results, since a more detailed approach is followed. By the same token, Sudhakar et al. (2012b) mention in their research that hourly light distribution during day is imperative, when modeling algae growth. Therefore, in this thesis, the hourly solar irradiation uptake by the *Haematococcus pluvialis* cells was calculated (see figure 18 and table 12). In order to accomplish this task the average distribution of sunlight per hour for every month is needed. This process could be avoided if hourly irradiance data for each location would have been provided. Nonetheless, hourly irradiance data are not easily accessible and in most cases they even cost significant amount of money, since their detailed collection constitutes a demanding challenge. ETHER was willing to provide confidentially hourly solar irradiation data all through 2014 for Livadeia. However, regarding Amsterdam, it was impossible to access the respective data. Thus, using the data from ETHER, the average distribution of sunlight per hour for every month in Livadeia was calculated and this research assumed that the same distribution goes for Amsterdam as well. Table 10 illustrates this distribution expressed in quota per total daily solar irradiation.

Month	Hour															
	<6:00	7:00	8:00	9:00	10:00	11:00	12:00	13:00	14:00	15:00	16:00	17:00	18:00	19:00	20:00	>21:00
January	0.00	0.00	0.00	0.06	0.11	0.14	0.16	0.17	0.15	0.12	0.08	0.02	0.00	0.00	0.00	0.00
February	0.00	0.00	0.02	0.07	0.11	0.13	0.15	0.15	0.14	0.12	0.08	0.04	0.00	0.00	0.00	0.00
March	0.00	0.00	0.03	0.07	0.10	0.13	0.14	0.14	0.13	0.11	0.08	0.05	0.01	0.00	0.00	0.00
April	0.00	0.00	0.02	0.06	0.10	0.13	0.14	0.13	0.07	0.16	0.07	0.10	0.01	0.00	0.00	0.00
May	0.00	0.00	0.03	0.07	0.07	0.10	0.12	0.12	0.13	0.10	0.09	0.09	0.05	0.02	0.00	0.00
June	0.00	0.01	0.03	0.04	0.10	0.12	0.09	0.12	0.10	0.06	0.13	0.10	0.07	0.04	0.01	0.00
July	0.00	0.01	0.02	0.06	0.09	0.10	0.10	0.10	0.12	0.12	0.09	0.08	0.06	0.03	0.01	0.00
August	0.00	0.00	0.02	0.05	0.08	0.10	0.12	0.13	0.13	0.11	0.10	0.08	0.06	0.02	0.00	0.00
September	0.00	0.00	0.00	0.03	0.03	0.10	0.12	0.09	0.28	0.16	0.09	0.06	0.03	0.00	0.00	0.00
October	0.00	0.00	0.00	0.05	0.10	0.14	0.16	0.17	0.12	0.15	0.08	0.02	0.01	0.00	0.00	0.00
November	0.00	0.00	0.01	0.05	0.11	0.16	0.28	0.14	0.14	0.08	0.03	0.00	0.00	0.00	0.00	0.00
December	0.00	0.00	0.00	0.06	0.12	0.15	0.31	0.15	0.08	0.08	0.04	0.00	0.00	0.00	0.00	0.00

Table 10: Average distribution of sunlight over a day per month.

In section 6.1 the layout of the microalgae process model as well as the relationship between the different compartments for 'wet' biomass and astaxanthin yield calculation are discussed. The main model input referred to solar irradiation and temperature data, while all other parameters involved in the production line were assumed as constants and derived by the literature. An important part of the model is the determination of photosynthetic efficiency, which occupies a whole node in the schematic view of the model. For its calculation, formulas 3, 4 and 5 as well as the conversion factor between (MJ/m^2s) and ($\mu mol/m^2\ s$) were used (see section 3.6.2). In this thesis, the general formula to determine 'wet' biomass productivity after cultivation found in literature (see formula 9) was modified by adding the impact of CO_2, O_2, pH, nutrients and mixing in the form of efficiencies (determined at will) as well as the a factor to equalize the broth in the two different cultivation systems of the hybrid system. The 'wet' biomass was then subjected to the different recovery efficiencies during harvesting and extraction phase in order to result in dried astaxanthin powder.

Table 11 presents all parameters introduced in the microalgae process model, while table 12 depicts an overview of the mathematical formulas used to build the model.

Definition	Abbreviation	Value		Source
		Horizontal tubular PBR ('green stage')	Raceway Pond ('red stage')	
Average daily irradiance per month	SUN	See table 9		(Panetas, 2015; KNMI, 2015)
Distribution of sunlight over the day	$\eta_{DISTRIBUTION}$	See table 10		(Panetas, 2015)
Photon Flux Density conversion factor[11]	F_{CON}	$4.82*10^6$ (µmol/m^2 s/ MJ/m^2s)		(Jannsen, 2002; Richmond, 2004)
Uptake after reflection	REFL	88%	90%	(Ben-Amotz 2008; Park et al., 2011)
Percentage PAR	PAR	43%		(Orosz & Forney, 2008)
Culture system depth[12]	Z	0.05 (m)	0.3 (m)	(Chisti, 2007; Jorquera et al., 2010)
Attenuation coefficient[13]	X	0.38 (m^{-1})		(Jannsen, 2002; Orosz & Forney, 2008)
Saturation intensity[14]	I_{SAT}	250(µmol/m^2s)	500(µmol/m^2s)	(Giannelli et al., 2015)
Gross photosynthetic efficiency	PE_{GROSS}	27%		(Orosz & Forney, 2008)
CO_2 Respiration losses	R	30%		(Zhu et al., 2008)
Average temperature	T_{AVG}	See table 9		(NOA, 2015; KNMI, 2015)
Temperature amplitude	T_{AMPL}	See table 9		(NOA, 2015; KNMI, 2015)
Empirical temperature factor	F_{TEMP}	0.9		(Sudenik 1991)
Optimal water temperature	T_{OPT}	20°C	27°C	(Giannelli et al., 2015)
Empirical factor in formula 6	K	0.007		(Montagnes & Franklin, 2001)
Factor mixing	F_{MIX}	0.93	0.91	[-]
Factor CO_2	F_{CO2}	0.97	0.92	[-]
Factor nutrients	$F_{NUTRIENTS}$	0.99	0.95	[-]
Factor pH	F_{PH}	0.98	0.92	[-]
Factor Oxygen	F_{OXYGEN}	0.95	1.00	[-]
Factor to equalize the volume of the broth when having a two-stage cultivation	F_{EQ}	15	1	[-]
Higher Heating Value algae biomass	HHV_{ALGAE}	23.6 (MJ/kg)		(see table 5)
Optimal land efficiency	L_{EFF}	98%		(Sudhakar et al., 2012b)
Biomass recovery efficiency disk-stack centrifugation	RE_{CENTR}	[-]	98%	(Heasman et al., 2000)
Biomass recovery efficiency bead milling	RE_{BEAD}	[-]	100%	[-]
Biomass recovery efficiency spray drying	RE_{SPRAY}	[-]	98%	(Leach et al., 1998)
Astaxanthin recovery efficiency supercritical CO_2 extraction	RE_{CO2}	[-]	97%	(Valderrama et al., 2003)
Astaxanthin concentration in biomass	$\%C_{ASTAX}$	[-]	2.5%	[-]

Table 11: Model input for the horizontal tubular PBR and the raceway pond.

[11] The conversion factor ranges from 4.5 (µmol $m^{-2}s^{-1}$) to 5.14 (µmol $m^{-2}s^{-1}$) per (Wm^{-2} or Jm^{-2} s^{-1}) (Jannsen, 2002; Richmond, 2004). In this research the mean value of the range was selected.

[12] In this research an average value of the proposed range of depth (0.1-0.5 (m) for raceway ponds and <0.1 (m) for tubular PBRs (Chisti, 2007; Jorquera et al., 2010)) was chosen.

[13] The attenuation coefficient factor ranges from 0.15 (m^{-1}) to 0.6 (m^{-1}) (Jannsen, 2002; Orosz & Forney, 2008). In this research the mean value of the range was selected.

[14] The saturation intensity differs for the two stages. Figure 9 (see section 3.6.2) shows the different saturation intensities for *Haematococcus pluvialis* growth under different temperature conditions. In figure 9 these temperature conditions refer to 20°C and 27°C. Since in this thesis these particular temperatures were selected as optimal (T_{OPT}) for the 'green' and 'red stage' respectively (see formula 5), the saturation intensity values were determined from the curves in figure 9 (see also sections 3.6.2 and 3.6.3).

Definition	Abbreviation	Formula	Source
Hourly irradiance	SUN_{HOURLY}	$=REFL*SUN*\eta_{DISTRIBUTION}*PAR$	[-]
Solar intensity on pond/reactor top-surface (µmol/m^2 s)	I_0	$=(SUN_{HOURLY}/3600)*F_{CON}$	[-]
Solar intensity on pond/reactor in depth Z (µmol/m^2 s)	I_Z	$=I_0*e^{-X*Z}$	(Orosz & Forney, 2008)
Photo-utilization efficiency on surface	η_{PUS}	$=(I_{SAT}/ I_0)*[(\ln(I_0/ I_{SAT})+1)]$	adjusted by Sudhakar et al. (2012b)
Photo-utilization efficiency in depth Z	η_{PUZ}	$=(I_{SAT}/ I_Z)*[(\ln(I_Z/ I_{SAT})+1)]$	adjusted by Sudhakar et al. (2012b)
Average photo-utilization efficiency	η_{PUAVG}	$= (\eta_{PUS}+ \eta_{PUZ})/2$	[-]
Photosynthetic efficiency	PE	$= PE_{GROSS}*\eta_{PUAVG}*(1-R)$	(Sukenik et al., 1991; Sudhakar et al., 2012b)
Net captured sunlight per hour	SUN_{NET}	$= SUN_{HOURLY}*PE*L_{EFF}$	adjusted by Sudhakar et al. (2012b)
Water temperature	T_{WATER}	$= F_{TEMP}*[T_{AVG}- T_{AMPL}* \cos(2\pi*hour/24)]$	(Sudenik 1991)
Effective non-optimal temperature factor	T_{EFFECT}	$=e^{[-K*(T_{WATER} -T_{OPT})^2]}$	(James & Boriah, 2010)
Factor suboptimal conditions	F_{SUB}	$= F_{MIX}* F_{CO2}* F_{NUTRIENTS}* F_{PH}* F_{OXYGEN}$	(Jonker & Faaij, 2013)
Wet Productivity (g/m^2/day)	$PROD_{DAY\_WET}$	$=1000*\Sigma[(T_{EFFECT}* F_{SUB}*F_{EQ}* SUN_{NET})/ HHV_{ALGAE}$	[-]
Wet Productivity (t/ha/month)	$PROD_{MONTH\_WET}$	$=0.3*PROD_{DAY}$	[-]
Dried Astaxanthin	$ASTAX_{MONTH}$	$= PROD_{MONTH\_WET}* RE_{CENTR}* RE_{BEAD}* RE_{SPRAY}* RE_{CO2}*\%C_{ASTAX}$	[-]

Table 12: Formulas used throughout the model

6.3 Results

6.3.1 Introduction

Although the ultimate goal of this study is to calculate the astaxanthin yield for the selected locations, the seasonal fluctuation of the biomass during the two stages of cultivation phase was delineated. This analysis is of particular importance, since microalgae growth constitutes the biggest and more complex process of the model. Thus, the model ran two times first, one for the 'green stage' and one for the 'red stage', without taking into account the harvesting and extraction phase. The main difference between the two stages during cultivation phase is saturation intensity. As portrayed in table 11, the saturation intensities for the 'green' and 'red stage' are 250 (µmol $m^{-2}s^{-1}$) and 500 (µmol $m^{-2}s^{-1}$) respectively. For optimal growth in the 'green stage' (i.e. algal cell proliferation), solar intensity on surface and in depth Z should be below saturation point, since exceeding this point results in the irreversible damage of the parts in algae cells that are responsible for photosynthesis and consequently to decreased growth (see figure 9 in section 3.6.2). Therefore, all through 'green stage', solar intensities above 250 (µmol $m^{-2}s^{-1}$) were not taken into account in 'green' biomass production calculation for the selected locations. This decision goes in line with various studies such as the one from Domínguez-Bocanegra et al. (2004), who state that maximum growth of *Haematococcus pluvialis* has been obtained under continuous illumination of 177 (µmol $m^{-2}s^{-1}$). Other studies, such as the one from Evens et al. (2008) and from Zhekisheva et al. (2005) mention for the 'green stage' a light intensity of 80 (µmol $m^{-2}s^{-1}$) and 75 (µmol $m^{-2}s^{-1}$) respectively.

On the other hand, in the 'red stage', the adverse condition of high solar intensities is needed in order to inhibit cell proliferation and induce astaxanthin accumulation. The values of solar intensity on surface and in depth Z, which induce astaxanthin accumulation, usually exceed the saturation point (i.e. 500 (μmol $m^{-2}s^{-1}$) in 'red stage). Exceeding saturation point, cell proliferation is inhibited and chlorophyll levels do not fluctuate, resulting in a continuous increase of astaxanthin content and cellular dry weight (see section 3.4). This statement agrees with several studies, such as the one from Dragos et al. (2010) and from Garcia-Malea et al. (2005), who stressed *Haematococcus pluvialis* cells under 630 (μmol $m^{-2}s^{-1}$) and 350-2500 (μmol $m^{-2}s^{-1}$) respectively. Therefore, all through 'red stage', solar intensities for the two locations under 500 (μmol $m^{-2}s^{-1}$) were not taken into account in 'red' biomass production calculation. For both stages, the chosen solar intensities (i.e. either lower than 250 (μmol $m^{-2}s^{-1}$) or higher than 500 (μmol $m^{-2}s^{-1}$) are labeled in this thesis as 'valid' values of solar intensity.

Further reasons for running the model twice during cultivation phase involve the different parameters for cultivation in each stage, such as culture system, optimal water temperature and substrate needs (see sections 3.5 and 3.6.3-3.6.6).

6.3.2 Biomass Productivity after cultivation ('green'-'red stage')

Two different biomass productivities during cultivation (labeled as 'wet' biomass productivities, see section 6.1) were calculated for the selected locations; one for the 'green' and one for the 'red stage'. The biomass productivity for the 'green stage' doesn't play any direct role on the determination of astaxanthin yield, since astaxanthin is accumulated during the 'red stage'. In other words, since in this thesis *Haematococcus pluvialis* growth is simulated mathematically, running the model only for the 'red stage' would be sufficient in order to calculate the astaxanthin yield. However, it is imperative that 'wet' biomass productivity for the 'green stage' be included in this study, in order to be able to determine adequately the mass and energy flows of the whole cultivation phase, while providing a valid economic performance analysis, without excluding any part from the production line. The same goes for determination of the tubes needed to construct the fence (see section 6.1 and Appendix B). Although the amount of series of tubes does not play any role on the determination of astaxanthin yield (since it is accumulated in the raceway pond), a more detailed approach on the mass and energy flows as well as economic performance was achieved. Last but not least, algae biomass production can be either continuous or in batches (Garcia-Malea et al., 2005; Aflalo et al., 2007; He et al., 2007; Li et al., 2011). This thesis assumed a continuous biomass production for the two stages during 2014. This means that every single day, an individual biomass production took place for both stages.

Figure 19 depict the 'wet' biomass (which is in fact the dry biomass existed in the broth) productivity during 'green stage' for Livadeia and Amsterdam all through 2014 (in t/ha/month).

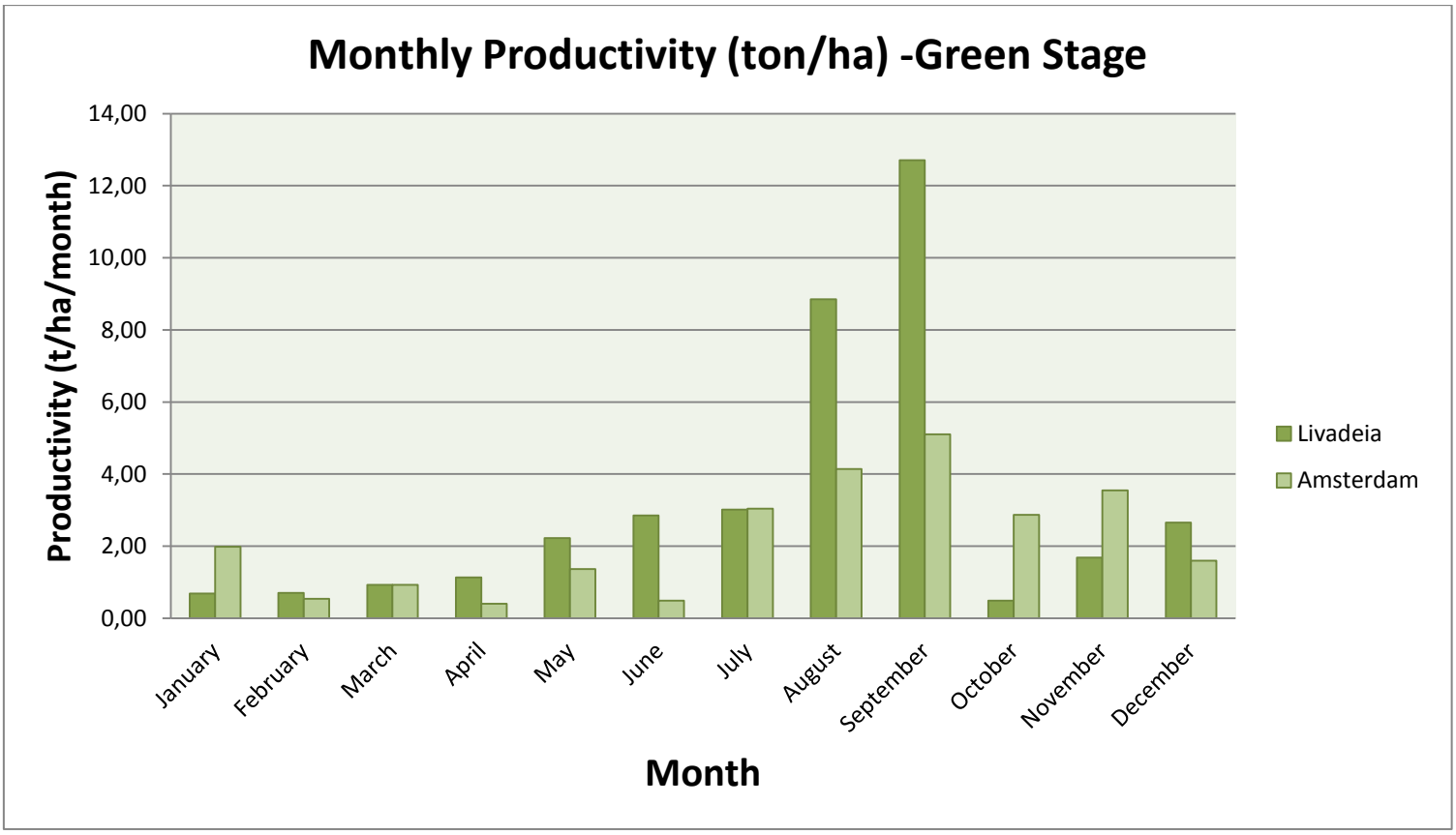

Figure 19: Monthly 'wet' biomass productivity (t/ha) during the 'green stage'.

The annual 'wet' biomass productivities for Livadeia and Amsterdam, during the 'green stage', amount to 37.94 (t/ha/year) and 26.00 (t/ha/year) respectively. It can be claimed that the annual algal biomass productivities during these stage do not vary significantly among the two locations (besides August and September) as it would be expected due to the high difference in climate conditions (see table 9 in section 6.2). This can be attributed to the solar intensities selected as well as the temperature. As mentioned in section 6.3.1, solar intensities that exceeded the saturation point (i.e. 250 (μmol $m^{-2}s^{-1}$)) during 'green stage' were not taken into account, in order to simulate optimal growth. For Livadeia, most solar intensities exceeded by far the saturation point, leading to suffering of microalgae cells and consequently to a productivity that does not differ significantly in total from the much 'colder' Amsterdam. By way of contrast, 'green' biomass productivity in Amsterdam was more stable all through 2014, since solar radiation impinging Amsterdam exceeded saturation point to a lesser extent. Nevertheless, the annual 'green' biomass productivity in the Dutch city is still less than the one from Livadeia. This happens, because 'wet' biomass productivity calculation (see formula 10 and table 12) is a function of solar intensity and temperature, and the higher the 'valid' values of solar intensity (but lower than the saturation point) and the closer to optimal (i.e. 20°C) the temperature of a location is, the higher the productivity. It is proven that the total count of the 'valid' values of solar intensity in Livadeia all through 2014 is slightly higher than the one of Amsterdam, while the temperature in Livadeia was closer to the optimal temperature all through 2014 than the one of Amsterdam. The highest biomass productivity for both cities was observed in September, which stands in the cusp of summer and winter and is characterized by milder environmental conditions.

During August and September a big variation in productivity can be noticed between the two cities. This is due to the fact, that during these months solar intensities and temperature for Livadeia were close but slightly lower to the saturation point and optimal temperature respectively, resulting in peak productivity. For Amsterdam this was not the case and thus a big difference in productivities occurred. Regarding colder months (October, November and January), productivity in Amsterdam exceeds by far the one from Livadeia. This happens, because Livadeia is characterized by high solar intensities during winter, which exceeded saturation intensity to a greater extent than Amsterdam, leading to lower 'wet' biomass values.

An interesting point to mention is the low productivity during June in Amsterdam. One would expect similar productivities during the mild summer period that Amsterdam is characterized. However, the productivity during June was 6-10 times lower than the ones during July-September. This peculiar result can be attributed to the fact that, due to high solar intensities, June of 2014 was the hottest June in more than 130 years of recorded weather history in the Netherlands (Erdman, 2014). This had a significant impact on 'green' algae biomass production in Amsterdam for that month.

Figure 20 portray the 'wet' biomass productivity during 'red stage' for Livadeia and Amsterdam all through 2014 (in t/ha/month).

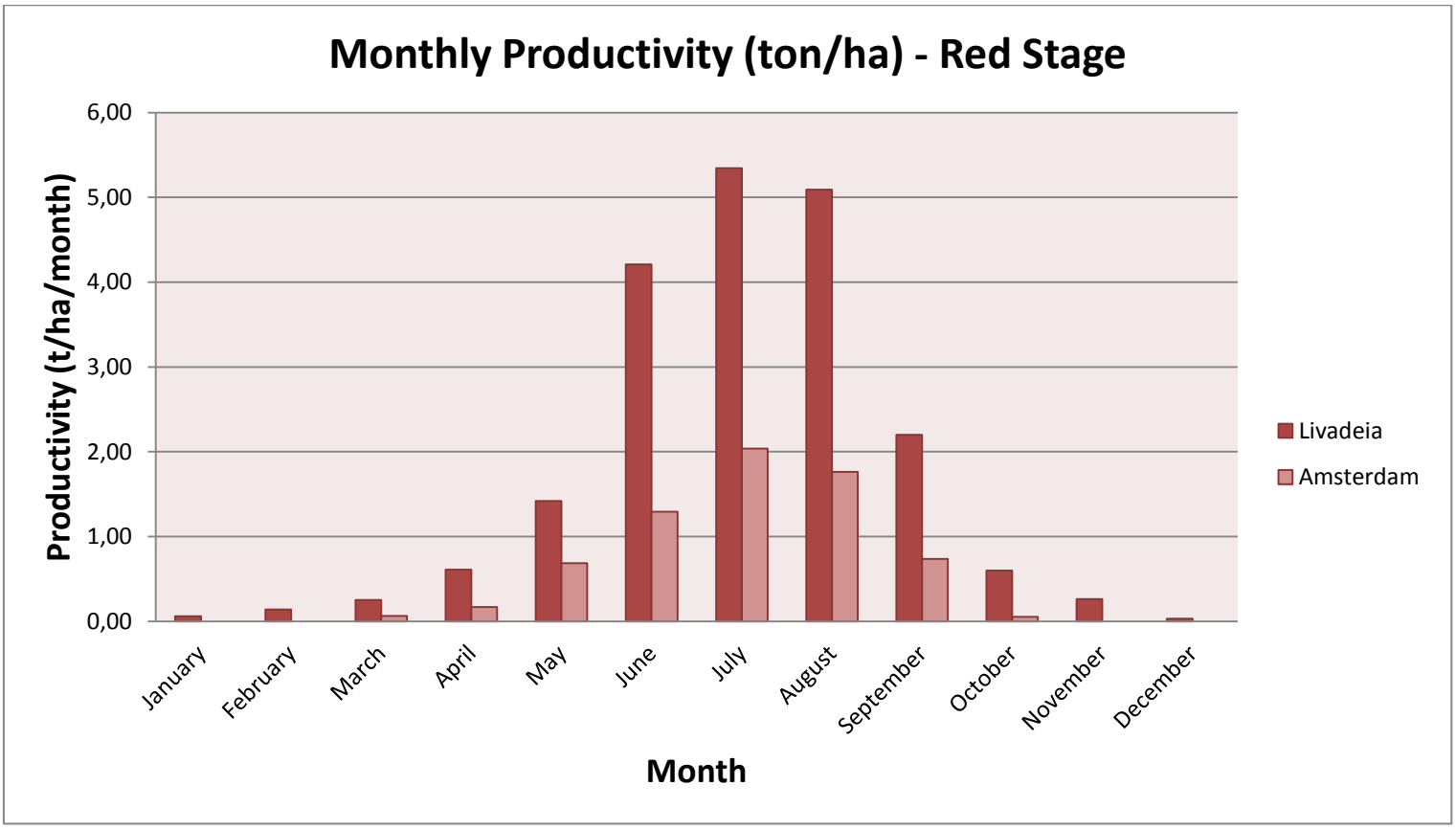

Figure 20: Monthly 'wet' biomass productivity (t/ha) during the 'red stage'.

A total different regime can be noticed during the 'red stage' for the selected locations. As mentioned in section 6.3.1, solar intensity values for the two cities under the saturation point of 500 ($\mu mol\ m^{-2}s^{-1}$) were not taken into account in the microalgae process model, for this stage. The reason was to simulate adverse environmental conditions by increasing the solar intensity, which leads to

inhibition of algae growth and to simultaneous astaxanthin accumulation (see section 3.4). By introducing this conjecture to the model and taking into account that inhibition of algae growth leads to the death and sedimentation of a significant amount of cells (He et al., 2007; Li et al., 2011), a noteworthy decrease of 'red' biomass productivity can be noticed for both cities compared to the 'green' biomass produced in the first stage. In fact, the 'red' biomass productivity for Livadeia amounted to 20.22 (t/ha/year), while the one for Amsterdam reached 6.80 (t/ha/year). This signifies that the respective 'green' biomass productivities for the two cities, determined earlier, are approximately twofold and four-fold higher. Highest monthly differences in 'red' biomass productivity can be observed during summer, when biomass productivities in Livadeia are more than twice as much as these in Amsterdam. This is logical, if we take into account the big differences in temperature and solar intensities for these months between the two cities (see table 9). However, the same difference in values stood for the 'green stage' as well, but the 'green' biomass productivities for the two cities did not differ significantly. The most important factor that affects productivity and signifies the difference between two locations is the amount of 'valid' values of solar radiation for each stage. More specifically, besides the higher values of solar intensity experienced in Livadeia, another reason behind the considerable difference between 'red' biomass productivities is explained by the fact that for Livadeia more 'valid' values of solar intensity (i.e. higher than the saturation point) were taken into account in the model, compared to Amsterdam. This can be clearly justified by noticing the 'red' biomass productivity in Amsterdam during the 'cold' months, i.e. January-April and October-December. As a matter of fact, 'red' biomass productivity in Amsterdam during these months is under 0.5 (t/ha), which means that very few or even not any solar intensity value exceeded the saturation point.

6.3.3 Astaxanthin yield

In order to calculate the astaxanthin yield the recovery efficiencies during harvesting and extraction phase presented all through section 4 and 5, have to be considered. In the previous sections the 'wet' biomass productivity during cultivation phase is analyzed (i.e. the model calculated the amount of dry algal biomass that exists in the hybrid system without considering harvesting and extraction phase). The 'wet' biomass after 'red stage' was calculated 20.22 (t/ha/year) and 6.80 (t/ha/year) for Livadeia and Amsterdam respectively (see section 6.3.2). Applying the recovery efficiencies of the selected dewatering (i.e. 98% for disk-stack centrifugation), cell disruption (i.e. 100% for bead milling), dehydration (i.e. 98% for spray drying) and astaxanthin recovery (i.e. 97% for supercritical CO_2 extraction) methods to the abovementioned values and taking into account the intracellular astaxanthin concentration (i.e. 2.5%), the amount of astaxanthin, can be calculated (see formula 11 in section 6.1).

Figure 21 shows the astaxanthin yield for Livadeia and Amsterdam all through 2014 (in t/ha/month).

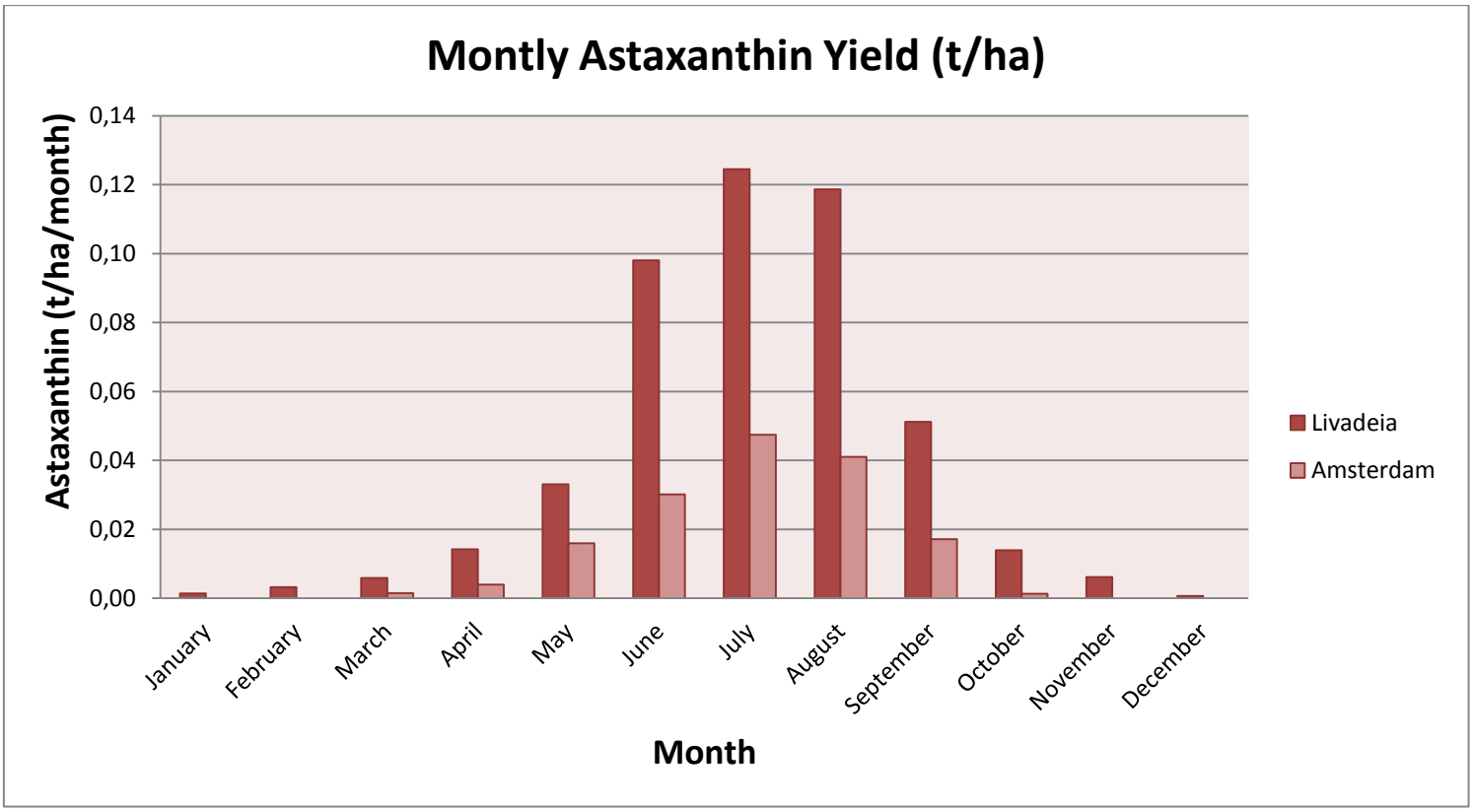

Figure 21: Monthly astaxanthin yield (t/ha).

The pattern of figure 21 is similar to the pattern of figure 20 in section 6.3.2, since the astaxanthin yield constitutes the same quota (2.5%) of the 'red' biomass productivity multiplied with the different recovery efficiencies during harvesting and extraction phase, which are the same for the selected locations. Consequently, the analysis of the environmental impact for the selected locations that led to the results in figure 21, are the same as for figure 20. Therefore, no further analysis was made.

The annual astaxanthin yields for Livadeia and Amsterdam were calculated 471 (kg/ha) and 158 (kg/ha) respectively. Li et al. (2011) conducted a biennial production of astaxanthin on a pilot scale, cultivating *Haematococcus pluvialis* in a hybrid system consisted of a tubular PBR and a raceway pond for the 'green' and the 'red stage' respectively; the same hybrid system as was selected in this thesis. Furthermore, they used disk-stack centrifugation for harvesting and spray drying for dehydration. The recovery of astaxanthin in their pilot scale facility was accomplished using a bed airflow pulverizer without using solvent extraction or SFE. This is the only difference in the production line between this thesis and their experiment. The pilot facility was established in Shenzhen, China, a city located at 22°32'00'' N/114°8'00'' E, with an annual average temperature of 22°C, approximately 2200 (h/year) sunshine time and about 5000 (MJ/m^2) annual solar radiation (Li et al., 2011; Greenstream Publishing, 2015). Based on the estimated process parameters, Li et al. (2011) scaled up the pilot operation and estimated that an astaxanthin production of 450 (kg/ha) at 2.5% of the total dry biomass weight could be achieved. Livadeia is located at 38°43'33'' N/22°86'67'' E, with an annual average temperature of 17°C (see table 9), approximately 2500 (h/year) sunshine time and about 5400 (MJ/ m^2) annual solar radiation (Theoharis, 2014; Panetas, 2015). Based on annual sunshine time and annual incident solar radiation and taking into account the latitude of the

two cities, it can be considered that meteorological conditions do not differ significantly. In this thesis, the astaxanthin yield at 2.5% of the total dry biomass weight has been calculated 471 (kg/ha) for Livadeia. Since Shenzhen and Livadeia experience similar climate conditions, and considering the fact that the production line of this thesis coincides with the pilot scale program to a great extent, it can be noticed that there is a remarkable resemblance between the two astaxanthin yields. Although Shenzhen experience higher average temperatures than Livadeia and one would expect a higher astaxanthin production in the Chinese city, the opposite is portrayed. This may attributed to the fact that the compartments of the factor of suboptimal conditions (F_{SUB}) used in the model were assumed at will, something that may not be patterned precisely after the reality. Nevertheless, the microalgae process model harmonizes in great detail with a real production line, providing an indication of validity.

7 Energy recovery from microalgae residues

7.1 Introduction

In this thesis, the potential to meet the energy needs all through the production line using the biomass residues after extracting astaxanthin is investigated. Due to the fact that the majority of energy needs refer to electricity consumption (see section 9), conversion technologies that lead to electricity production are analyzed. There are different technically viable options to convert microalgae biomass into energy carriers (in liquid or gaseous form), which may be channeled into the market as fuels or constitute a feedstock for the production of electricity and heat. The conversion technologies are based mainly on the ones used for terrestrial biomass (1st and 2nd generation biomass energy carriers) and can be divided into two categories: 1) Thermochemical conversion technologies and 2) biochemical conversion technologies (Brennan & Owende, 2010). The main factors that determine the selection of the most appropriate conversion technology revolve around the type and quantity of the biomass, the desired form of energy to be produced as well as economic efficiency (McKendry, 2002; Brennan & Owende, 2010). Figure 22 delineates an overview of the different energy conversion processes using microalgae biomass as feedstock.

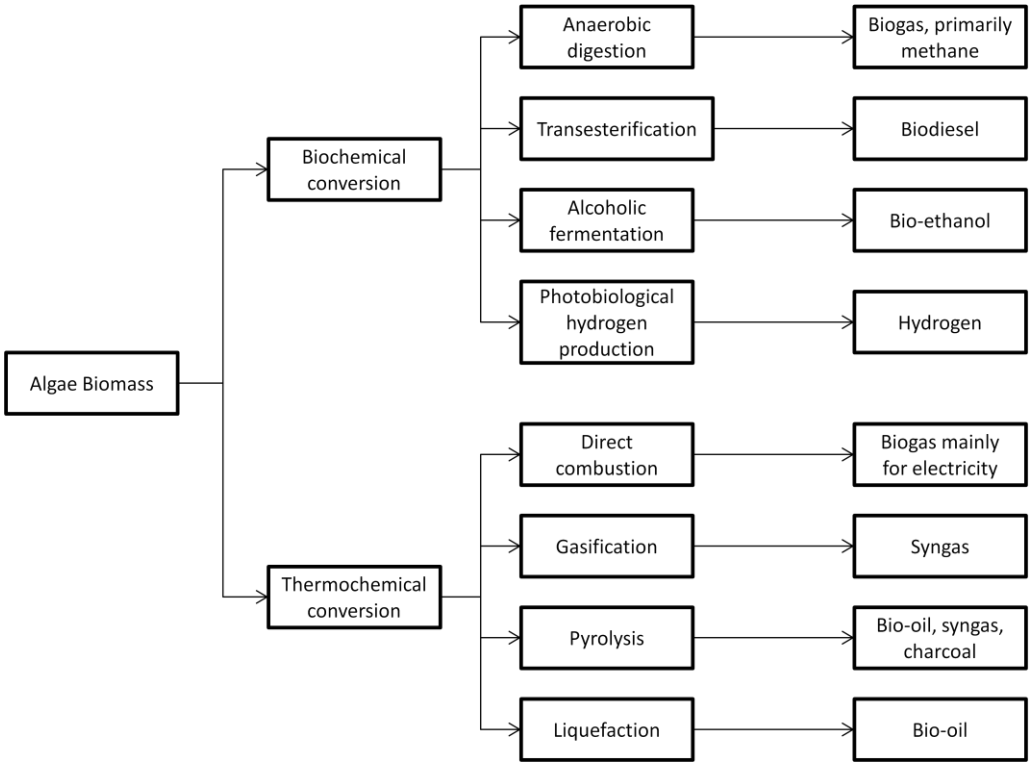

Figure 22: Overview of the different energy conversion technologies using biomass as feedstock (adjusted by Brennan & Owende, 2010; Milledge, 2013)

From the options presented in figure 22, four technologies may result in electricity as an end product: Direct combustion, gasification, pyrolysis and anaerobic digestion. However, only direct combustion and gasification, are investigated in deep in this study. The reason lies on the fact that although in anaerobic digestion the waste (mainly nutrients) of the process can be recycled into a new algal growth medium, while having a higher net energy return and much lower GHG emissions than the others, the methane production rates are low and ultimately it is a method appropriate mainly for 'wet' biomass (Brennan & Owende, 2010; Singh & Olsen, 2011; Delrue et al., 2012;

Milledge, 2013). The production line of this thesis, nevertheless, has included a dehydration phase, resulting in dry biomass powder. Regarding pyrolysis, it is a method that can end to bio-oil, syngas or charcoal (Goyal et al., 2008). It is reported that bio-oil is a more attractive product than the other two and most studies do not investigate the potential of syngas derived by pyrolysis and which would be the feedstock for electricity production (Milledge, 2013). Thus, only direct combustion and gasification, are presented in the following sections.

The annual astaxanthin yields for Livadeia and Amsterdam were calculated 471 (kg/ha) and 158 (kg/ha) respectively (see section 6). These yields are fractions of the dehydrated biomass, which amount to 19.42 (t/ha) and 6.53 (t/ha) for Livadeia and Amsterdam respectively[15]. Subtracting the astaxanthin yields from these values, the residual algal biomass in an annual basis can be calculated. This amounts to 18.95 (t/ha) and 6.37 (t/ha) for Livadeia and Amsterdam respectively.

7.2 Direct combustion

Direct combustion constitutes historically the main method to convert biomass from different sources into energy and it practically involves the usage of furnaces, boilers or steam turbines in order to burn the biomass in the presence of air and at temperatures exceeding 800°C (Milledge, 2013). The solar energy metabolized into chemical energy inside the algal cell is then converted and stored into hot gases, which must be used immediately, since storage is not a viable option (Brennan & Owende, 2010). These hot gases can provide heat or steam for household and industrial uses or can be supplied into a gas turbine in order to produce electricity. 'Wet' biomass cannot be a possible feedstock, since it reduces the amount of heat generated by 20% compared to dry biomass (Milledge, 2013). Thus, the moisture content in algal biomass should not exceed 50%. This means that this option is efficient only if pre-treatment processes such as drying and pulverizing are employed (Brennan & Owende, 2010). These pre-treatment processes have been part of the production line in this study. Therefore, direct combustion is considered as an appropriate option for electricity generation. In section 3.6.7 the amount of energy (i.e. HHV) released during the combustion of a kg of algal biomass is calculated. This value amounts to 23.6 (MJ/kg). Multiplying the HHV with the residual algal biomass mentioned earlier the annual energy in the form of heat can be determined. This amounts to 447220 (MJ/year) and 150332 (MJ/year) for Livadeia and Amsterdam respectively. The efficiency of algal biomass direct combustion for the generation of electrical energy is range from 20-40 % (Demirbas, 2001). Assuming an average value (i.e. 30%), the amount of annual electricity implementing direct combustion on the residual biomass was calculated 134166 (MJ/year) or 37.3 (MWh/year) and 45100 (MJ/year) or 12.5 (MWh/year) for Livadeia and Amsterdam respectively.

7.3 Gasification

There are two different types of algae biomass gasification: 1) Conventional gasification, where the biomass, like in direct combustion, has to be dry before entering the plant (Guan et al., 2012); and 2) supercritical water gasification (SCWG), which is suitable for high moisture biomass (Milledge et al., 2014). Since the residual algal biomass after astaxanthin extraction, are dry due to spray drying, conventional gasification is analyzed. The main principle of conventional gasification is the partial

[15] The 'red' biomass after cultivation amounts to 20.22 (kg/ha) and 6.80 (kg/ha) for Livadeia and Amsterdam. Applying biomass recovery efficiencies during disk-stack centrifugation (98%), bead milling (100%) and spray drying (98%) the amount of the dehydrated biomass can be calculated. The recovery efficiency employing supercritical CO_2 extraction (97%) refers only to astaxanthin recovery and not to biomass.

oxidation of organic matter using controlled amount of oxygen and/or water (in the form of steam) at high temperatures (800-1000°C) (Saidur et al., 2011; Milledge, 2013). It is a method that unlike direct combustion the biomass is not burned, but it reacts with the oxygen and water in order to generate syngas. Syngas is a combustible gas mixture comprising mainly by hydrogen (H, 30-40%), carbon monoxide (CO, 20-30%), methane (CH_4, 10-15%), ethylene (C_2H_4, 1%), nitrogen (N), water vapor and sometimes carbon dioxide (CO_2) (Demirbas, 2001; Brennan & Owende, 2010; Saidur et al., 2011). Syngas can be burnt directly to produce heat, can be used to produce methanol and hydrogen as fuel for gas engines or can be supplied into a gas turbine to generate electricity (Milledge, 2013). The calorific value of syngas derived by conventional gasification of algal biomass ranges from 15.3-22.1 (MJ/kg) and depends on the oil fraction inside the algal cell. This range corresponds proportionally to oil fractions between 0-40 wt% (Azadi et al., 2014). In section 3.6.7 it is mentioned that the oil fraction in *Haematococcus pluvialis* was assumed 40%. This means that the heating value of syngas for this thesis amounts to 22.1 (MJ/kg). Multiplying this value with the residual algal biomass for the selected cities, the amount of energy stored in syngas can be calculated. This corresponds to 418795 (MJ/year) and 140777 (MJ/year) for Livadeia and Amsterdam respectively. The conversion efficiency between energy stored in syngas and electricity generation using syngas corresponds to 50% (Milledge, 2013). Consequently, the annual amount of electricity generated employing conventional gasification was calculated 209398 (MJ/year) or 58.2 (MWh/year) and 70388 (MJ/year) or 19.6 (MWh/year) for Livadeia and Amsterdam respectively.

Taking into account the fact that biogas generated for direct combustion cannot be stored and should be exploited immediately, while conventional gasification results in higher electricity generation, conventional gasification was selected as the method to meet the energy needs of the bio-refinery.

8 Mass Balances

8.1 Macro- and Micronutrients

In Appendix A, a weight analysis of the fertilizers inoculated in the growth medium is presented. These fertilizers have the form of chemical compounds and are divided into two categories: macro- and micronutrients (more information in sections 3.6.5 and 3.7). The analysis led to a detailed depiction of the concentrations of the different chemical elements that compose these fertilizers and consequently the 'initial medium recipe' (see table 6 in section 3.7). The concentrations of the chemical elements that exist in the microalgae cells after cultivation for the 'green' and 'red stage' are delineated as well (see table 7 in section 3.7).

The demand for the macronutrients (KNO_3, Na_2HPO_4, $NaHCO_3$, $MgSO_4$) was calculated for 2014. Furthermore, a variety of micronutrients, 10^{-3} smaller in amount, complete the 'initial medium recipe'. Their volume is so small that the concentrations of some chemical elements that compound these micronutrients amount to 0.00%. To determine all mass requirements and costs of these elements is time consuming and beyond the scope of this research, since they represent traces in the whole process. Therefore, the demand of the micronutrients was calculated at a whole.

The requirement to calculate the demand of the fertilizers refers mainly to the volume of the cultivation system. In Appendix B a detailed calculation of the cultivation systems' volume is presented. Another factor that plays an important role while determining the demand of fertilizers is the daily medium renewal rate. Li et al. (2011) implemented a daily medium renewal rate of 25% all through 'green stage' in Shenzhen, China. The daily medium renewal rate depends highly on the environmental conditions (especially solar intensity) that prevail in a location, since nutrients are directly involved in photosynthesis process (see also in section 3.6.2) (Jonker & Faaij, 2013). Since the compartments of the hybrid system used in the microalgae process model match with these of the study of Li et al. (2011) and taking into account that Livadeia and Shenzhen (the city, where Li et al. (2011) conducted their pilot scale experiments, see section 6.3.3) experience similar climate conditions in terms of annual solar intensity, the same daily medium renewal rate of 25% was assumed for the Greek city. This assumption cannot be made for Amsterdam, which is subjected to a colder climate characterized by significantly lower annual solar intensity and temperature values. Therefore, a daily medium renewal rate of 18% during 'green stage' was calculated (see Appendix C1). On the other hand, for both cities a zero daily medium renewal rate was assumed for the 'red stage', in order to simulate complete nutrient starvation, which triggers astaxanthin accumulation besides high solar intensities. This implies that neither macro- nor micronutrients were inoculated all through 'red stage'. Ultimately, this assumption goes in line with the studies of Fábregas et al. (2001) and Imamoglu et al. (2009), who chose a complete nutrient starvation for their experiments[16]. Furthermore, this assumption agrees with the outcomes presented in table 7 as well; namely, the

[16] Complete nutrient starvation is not followed by all studies. For instance, Zhang et al. (2014) and Garcia-Malea et al. (2005) conducted experiments by subjecting *Haematococcus pluvialis* into different nutrient concentrations conditions.

concentrations of the chemical elements considered as the main fertilizers are diminished in 'red stage' compared to the respective values in the 'green stage'[17].

This study assumed that flue gases constitute the CO_2 carrier. Flue gases, nonetheless, contain, besides CO_2 and O_2 (10% v/v and 3% v/v in average respectively), about 79% v/v gaseous nitrogen (N_2), water vapors (H_2O) and some small amounts of nitrogen oxides (NO_x) and sulfur dioxide (SO_2) (Wang et al., 2008; Beychok, 2012). These molecules could serve the role of fertilizers in the growth medium, affecting consequently nutrients' mass balances. However, in this thesis, the amount of each individual chemical compound labeled as macronutrient as well as the amount of micronutrients as a whole existing in the medium recipe was calculated for the selected locations. Thus, it was assumed that nutrients existing in flue gases do not play any role during cultivation and consequently they were excluded from nutrients' mass balances calculation.

Last but not least, considering that PBRs facilitate better control over culture conditions (see section 3.3) and growth parameters than open ponds, a utilization efficiency of nutrients should be introduced as well. Regarding raceway ponds, the utilization efficiency of nutrients amounts to 75%, while for the horizontal tubular PBR the respective value equals to 90% (Xin et al., 2010; Zaimes & Khanna, 2013). Since all through 'red stage' complete nutrient starvation takes place, the nutrient utilization efficiency of the raceway pond does not play any role in the fertilizer demand calculation. In Appendix C1 a detailed way for calculating the mass balances of the fertilizers is presented.

8.2 Carbon Dioxide-Oxygen

In section 3.6.4 a detailed overview around CO_2 role during microalgae cultivation can be found. CO_2 constitutes the most important substrate all through cultivation, since no algae growth can occur in the absence of CO_2. Taking into account the concentration of carbon in the algae cells in both stages (almost 50% of the total mass, see table 7) it is easy to conceive the importance of CO_2 and its sufficient supply into the system. Based on the average chemical composition of algal biomass (i.e. $C_1H_{1.83}O_{0.48}N_{0.11}$; algal cells have a carbon mass fraction of approximately 50%), approximately 1.8 tons of CO_2 are needed in order to harvest 1 ton of algal biomass (see section 3.6.4). Nevertheless, an important parameter to be taken into account refers to the utilization efficiency of CO_2 of the different cultivation systems due to degassing. Weissman et al., (1989) mention that generally for open pond systems the overall CO_2 utilization efficiency amounts to 60%. On the contrary, Slade & Bauen (2013) state that CO_2 utilization efficiency in raceway ponds may be in practice less than 10%. In this study the average value of the CO_2 utilization efficiency range (i.e. 10%-60%) found in literature was selected; this amounts to 35%. Undoubtedly, the rest 65% is degassed. As a consequence, an increased supply of CO_2 (from flue gases, see section 3.6.4) to be injected in the raceway pond, is needed. For closed systems, such as photobioreactors that are more controlled systems, utilization efficiency increases to 75% (Acién et al., 2012; Slade & Bauen, 2013); 25% is degassed.

Another inflow of CO_2 during the production line refers to the supply of CO_2 in order to employ supercritical CO_2 extraction, which leads to the recovery of astaxanthin as the final product. In this study, supercritical CO_2 extraction at 60°C and 30 MPa enhanced with ethanol as co-solvent at 9.4%

[17] Certain elements of the macronutrients (KNO_3, Na_2HPO_4, $NaHCO_3$, $MgSO_4$) serve the role of the fertilizer in algal growth, although the whole chemical compound is considered as a fertilizer. These elements for *Haematococcus pluvialis* growth are: Nitrogen (N), phosphorus (P), potassium (K), sulfur (S) and sodium (Na).

was implemented (CO_2 is derived from flue gases, see section 5.4.3). Using data from Valderrama et al. (2003), who experimented on astaxanthin recovery applying supercritical CO_2 extraction, a trend-line was created in order to calculate the amount of solvent per kg of feed (i.e. dried 'red' biomass) at 2.5% astaxanthin content.

In section 8.1 it was mentioned that the impact of the chemical compounds existing in flue gases would not be taken into account during cultivation. This limitation refers to these compounds that in the right concentrations could be labeled as nutrients; namely, N_2, NO_x, SO_2. Regarding molecular oxygen (O_2), it exists in flue gases as well as in the medium recipe. Since O_2 is labeled as a 'waste' product that inhibits algal cell proliferation and - its mass balance is of particular significance - a more detailed approach was followed with respect to molecular oxygen, including all sources that inoculate this compound in the growth medium as well as the amount of O_2 to be extracted using the suffering limit of microalgae (see section 3.6.4). An aspect that was not taken into account regarding O_2 mass balance refers to de-oxygenation due to respiration in dark conditions. At night no O_2 is produced by photosynthesis but it is consumed through respiration (Milledge, 2013). In other words, respiration and photosynthesis are opposite concepts. Respiration uses oxygen and produces carbon dioxide, while photosynthesis uses carbon dioxide and produces oxygen. The uptake of oxygen during night is called de-oxygenation (Milledge, 2013). Delving deeply into the changes in algal composition during light/dark cycles is out of the scope of this study and thus, de-oxygenation impact was not taken into account. Regarding degassing of O_2, in PBRs this process is accomplished using an exhaust, while in raceway ponds it happens naturally since raceways are open to the atmosphere.

A detailed methodology on how to calculate CO_2 and O_2 mass balances for both stages can be found in Appendix C2.

8.3 Water

Algae require considerable amounts of water in order to grow and thrive. The organisms themselves are 80-85% water (cellular water) (Murphy & Allen, 2011). Besides water incorporated in the algal cell, most algae grow in aqueous suspension. Nevertheless, the suspended solids are proven to be marginal. Typically miroalgal biomass varies from 0.02-0.05% in raceway ponds and between 0.1% and 0.5% in tubular PBRs (Iersel et al., 2009; Zamalloa et al., 2011). These low concentrations of algae existed in the broth insinuate a significant amount of water to be exploited during cultivation phase. In this thesis the average values of these ranges were assumed: 0.035% Algal biomass in the raceway pond and 0.3% in the tubular PBR. Furthermore, a critical parameter for the determination of water demand is the amount of water lost due to evapotranspiration from the raceway pond. Regarding the horizontal tubular PBR it is assumed that no significant amount of water can be evaporated, since it is a closed system. Evapotranspiration is preferred to single evaporation as a parameter that affects water demand, because microalgae are plants that utilize water for their growth and dismiss fractions of it in the form of vapors that are emitted from their cells (this mechanism is called transpiration). Evaporation rate, on the other hand, is a function of solar radiation, temperature, wind velocity over the raceway pond surface, and current velocity of the broth in the raceway pond (Sazdanoff 2006). Calculating evapotranspiration rate requires a significant amount of data including seasonal fluctuation. This process is out of the scope of this study. Thus, annual fixed evapotranspiration data for the selected locations during 2014 were incorporated to the needs of the raceway pond resulting in an additive factor that was used in the water demand formula.

Furthermore, disk-stack centrifugation and spray drying were implemented for harvesting and dehydration respectively. Suspended solids after disk-stack centrifugation amount to 12% in the cake, while the moisture content in 'red' biomass after spray drying corresponds to 5% (see sections 4.3.2 and 5.3). A detailed presentation on the way to calculate water mass balances throughout cultivation, harvesting and extraction phase can be found in Appendix C3.

8.4 Results

All information presented in sections 8.1-8.3 as well as in Appendix C can be represented concisely by a mass balance factsheet. Figure 23 represents the mass balances all through production process. Additionally, table 13 contains the values of the annual mass balances involved in the production line for the selected locations expressed in tons per hectare.

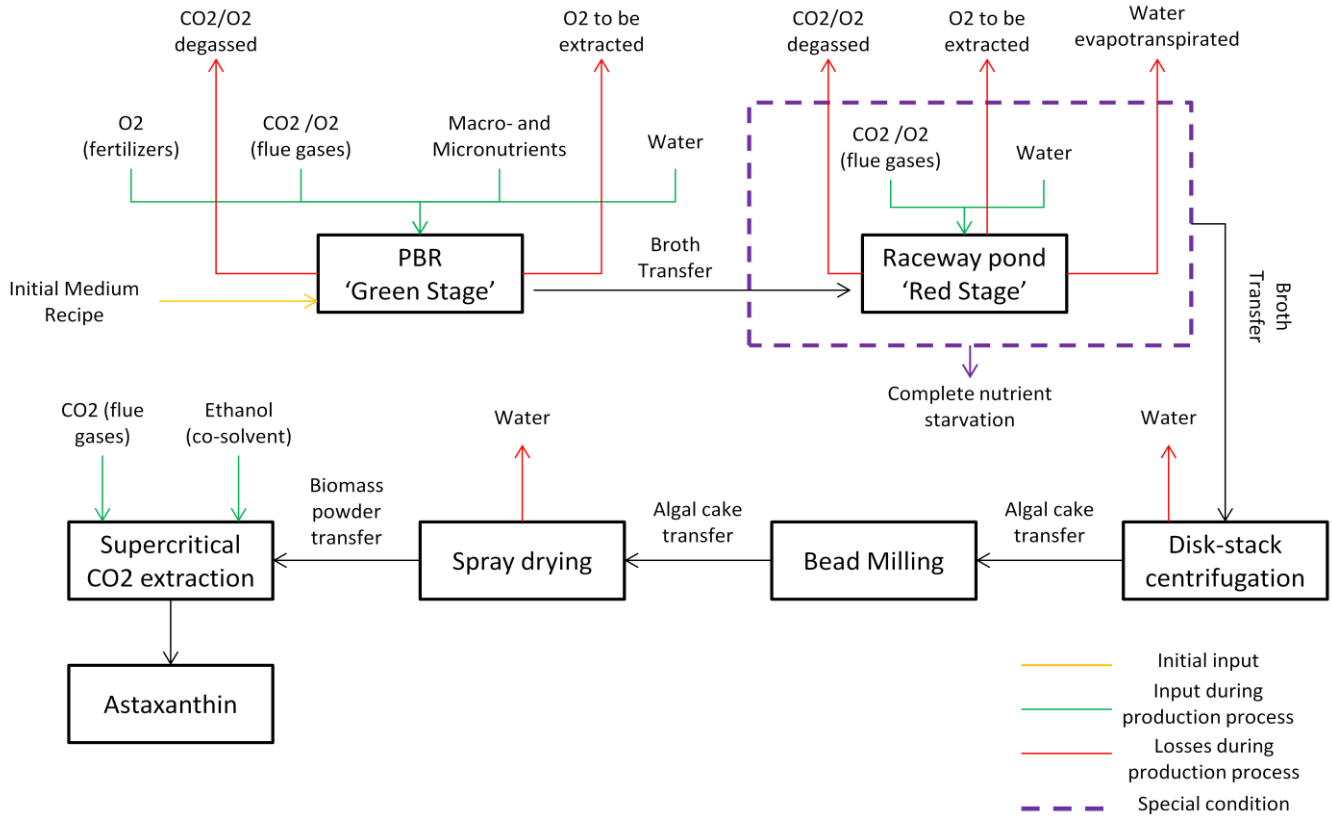

Figure 23: Flow chart of the mass in- and outflows during cultivation phase.

Mass Balances				
(t/ha/year)	**Livadeia**		**Amsterdam**	
	Horizontal Tubular PBR ('green stage')	Raceway Pond ('red stage')	Horizontal Tubular PBR ('green stage')	Raceway Pond ('red stage')
	Cultivation phase			
'Wet' biomass productivity	37.94	20.22	26.00	6.80
KNO_3	303	0	218.2	0
Na_2HPO_4	85.2	0	61.3	0
$NaHCO_3$	50.4	0	36.3	0
$MgSO_4$	18	0	13	0
Micronutrients	6.2	0	4.4	0
CO_2 demand (from flue gases)	46.9	104	30.6	35
CO_2 degassed	11.7	67.6	7.7	22.8
O_2 inoculated (from flue gases)	10.2	22.6	6.6	7.6
O_2 degassed	2.6	14.7	1.7	4.9
O_2 inoculated (from fertilizers)	111.8	0	80.4	0
O_2 in the algal cells	5.1	2.9	3.5	1.0
O_2 suffering limit in the growth medium	0.4	2.2	0.3	0.8
O_2 to be extracted	113.9	2.8	81.5	0.9
Broth	12633	69087	8657	25657
Water	12595	69067	8631	25650
Water evapotranspirated	0	11316	0	6228
	Harvesting phase			
Biomass in algal cake	0	19.82	0	6.66
Water in cake after centrifugation	0	145	0	49
Water removal employing centrifugation	0	68922	0	25601
	Extraction phase			
Dry biomass	0	19.42	0	6.53
Water in the powder after spray drying	0	1	0	0.3
Water removal after spray drying	0	144	0	48.7
CO_2 demand supercritical CO_2 extraction	0	354	0	119
Ethanol (9.4%) as co-solvent supercritical CO_2 extraction	0	36.7	0	12.4

Table 13: Annual mass balances during the production line (in t/ha)

9 Energy requirements and Energy Balance Ratio (EBR)

9.1 Introduction

The three phases of the production process as well as the gasification plant consist of various stages discussed in sections 3-5 and 7, which consume power in order to operate. An investigation on the energy life-cycle all through the production of astaxanthin and gasification of the residual biomass was conducted. The energy needs analysis resulted in the creation of the energy balance ratio during the production line (EBR). The energy balance ratio is defined as the ratio of total energy inputs to the total energy outputs inside the boundaries selected for a system (see formula 1 in section 2.4) (Shirvani et al., 2011; Khoo et al., 2013). The total energy output in this thesis refers to electricity generated by syngas that was produced through conventional gasification of the residual biomass, after astaxanthin is extracted (see section 7.3). In this study, the EBR is calculated for the different processes separately, in order to portray the potential of residual bio-energy on offsetting the energy needs of each process. In the following sections the energy needs of the different processes are analyzed.

9.2 Energy requirements during cultivation phase

Cultivation phase is divided into two stages: the 'green' and the 'red stage'. Since each stage takes place in a different culture system (see section 3.5), they are associated with different energy needs. Literature energy values were adjusted to the boundaries of the hybrid system and taking into account the biomass productivity calculated by the process model as well as mass balances associated with the cultivation phase (see sections 6.3.2 and 8.4), the annual energy requirements of the two stages per hectare of cultivation are determined. The following sections provide an analysis to this realm.

9.2.1 Mixing/Circulation

The tubular PBR fence ('green stage') and the raceway pond ('red stage') use a different system for continuous turbulent flow (24h) in order to ensure homogenization of the culture. Regarding the tubular PBR fence, either a mechanical pump or a more sophisticated airlift system can be selected for mixing/circulation (see section 3.5.2). Although the mechanical pump is a simpler device, it is associated according to the literature with higher energy requirements than the airlift system. In fact, the mechanical pump in continuous operation has an annual power consumption of 144 (MWh/ha) for both cities. This value was adjusted by the data (500W over $300m^2$) of a small facility in the Netherlands mentioned in the study of Jonker & Faaij (2013). On the other hand, the mixing/circulation in the airlift system is associated with a power consumption of 170 (W/m_{BROTH}^3) (Acién et al., 2001). Multiplying this value with the annual broth for the 'green stage' for the two locations selected (see table 13 in section 8.4), the annual power consumption per hectare can be calculated: 51.5 (MWh/ha) for Livadeia and 35.3 (MWh/ha) for Amsterdam. In this study, the airlift system was selected for mixing/circulation during the 'green stage'.

For the raceway pond, a paddlewheel serves the role of the mixing/circulation device (see section 3.5.3). Different authors propose different ranges and ways to express energy requirements for the paddlewheel. For instance, Jonker & Faaij (2013) mention a range of 18-54 (kWh/ha/day). Assuming an average value of 36 (kWh/ha/day), a power consumption of 13 (MWh/ha) for Livadeia and 8.6

(MWh/ha) for Amsterdam[18]. In this realm, Tredici (2012) and Rogers et al. (2013) have calculated a value of 2 (kW/ha). Annually and adjusted to the boundaries of our system this value can be translated as 17.3 (MWh/ha) for Livadeia and 11.5 (MWh/ha) for Amsterdam[18]. On the other hand, Lohrey & Kochergin (2012) state a value of 0.1 (kWh/kg). Multiplying this value by the algal biomass existing in the broth after cultivation, the annual energy needs for the paddlewheel for the two locations can be calculated: 2 (MWh/ha) for Livadeia and 0.68 (MWh/ha) for Amsterdam. The first two sets of results resemble relatively one another unlike the third one. Thus, the first set (i.e. 13 (MWh/ha) for Livadeia and 8.6 (MWh/ha) for Amsterdam) was selected for this thesis.

9.2.2 Flue gases supply- O_2 removal

In section 3.6.4 it is mentioned that CO_2 needs were facilitated by supplying the hybrid system with flue gases. Carbon dioxide is assumed to correspond to 10% v/v of the total flue gases and under this basis, the mass balances of CO_2 and O_2 were determined (see sections 8.2, 8.4 and Appendix C2). The energy needs to introduce flue gases in the hybrid system can be expressed as the energy requirements of CO_2 capture and compression from flue gases (Lohrey & Kochergin, 2012). These processes are accomplished using the airlift system and submerged aerators that enhance CO_2 uptake for the tubular PBR fence and raceway pond respectively (see section 3.6.4). The energy needs of CO_2 capture and compression from flue gases at 13% v/v amounts to 0.2 (KWh/kg_{CO2}). In this study, this reference value was assumed for both the airlift system and the submerged aerators. Consequently, multiplying the reference value with the CO_2 demand for the two stages for the selected locations the energy needs for the flue gases supply can be calculated. For Livadeia, the energy needs amount to 9.4 (MWh/ha) and 20.8 (MWh/ha) for the tubular PBR fence and the raceway pond respectively. The respective values for Amsterdam were calculated at 6.1 (MWh/ha) and 7 (MWh/ha).

The inoculation of flue gases into the hybrid system introduces besides CO_2 other gases in the growth medium, which can hamper microalgae growth. The most important of them is O_2, which labeled as a waste product and has to be removed, when surpassing a critical point (see sections 3.6.4, 8.2, 8.4 and Appendix C2). In the raceway pond, O_2 is removed naturally, since the pond is open to the atmosphere (see section 3.6.4). On the other hand, in tubular PBRs that are closed systems, a degassing zone inside the airlift system is built, where oxygen is separated from liquid and blown off through an exhaust (Acién et al., 2001). The annual power consumption for the degassing zone in a tubular PBR with an airlift system has been calculated from Jonker & Faaij (2013) as 47 (MWh/ha).

9.2.3 Water pumping

The medium renewal rate is assumed on a daily basis. In other words, fresh culture medium is pumped daily to the tubular PBR fence, where the 'green stage' takes place, and when *Haematococcus pluvialis* cells have grown optimally, the broth is further pumped to the raceway pond for astaxanthin accumulation. Furthermore, due to evapotranspiration losses during 'red stage', the raceway pond must be oftenly replenished with water (see section 8.1, 8.3, 8.4 and Appendix C3). Therefore, water pumps are employed in order to fill and maintain the water levels in

[18] The different values between the selected locations are due to the days of operation. Regarding Amsterdam, for January-February and November-December, *Haematococcus pluvialis* could not grow suffiently, as the model calculated (see section 6.3.2). As a matter of fact, the 'red' biomass was zero for these months. Thus, these months were excluded from the days of operation, which means that instead of 360 days that a year consists of and were applied for Livadeia, for Amsterdam only 240 days were assumed operational.

the hybrid system all through cultivation phase. In this thesis, it is assumed that the pumps to introduce water into the hybrid system or transport the broth are of the same energy intensity (Sazdanoff 2006): 0.09 (kWh/m^3). The process of water/broth pumping can be divided into two categories: 1) Pumping water into the tubular PBR fence and transport of broth into the raceway pond; and 2) Adding water into the raceway pond due to evapotranspiration and for optimal cultivation and transport of broth to the harvesting device. Considering the mass balances for water during cultivation (see section 8.4), the energy requirements can be calculated. For the abovementioned categories the results for Livadeia and Amsterdam are presented respectively: 1) 2.3 (MWh/ha) and 1.6 (MWh/ha); 2) 11.3 (MWh/ha) and 3.8 (MWh/ha).

9.3 Energy requirements during harvesting phase

For the harvesting phase the disk-stack centrifugation was selected. Disk-stack centrifugation is considered as the most energy intensive among the harvesting options, but it is a rapid method with high recovery efficiencies, which results in high TSS concentration in the algal cake as well. In this thesis a disk-stack centrifuge at 13000g that led to 12% TSS in the algal cake, was selected for harvesting (see section 4.3.2). Molina-Grima et al. (2003) has reported a one step power consumption of 1 (kWh/m_{BROTH}^3) using a Westfalia self-cleaning disk stack centrifuge on the strain *Scenedesmus*, which led to an algal cake with 12% TSS. Besides the strain used, the process matches perfectly with the one followed in this thesis, and thus, this value was assumed as a reference value to calculate the energy requirements during harvesting for the selected locations. Taking into account the broth pumped from the raceway pond after cultivation, the energy needs of harvesting phase for Livadeia and Amsterdam amount to 69.1 (MWh/ha) and 25.7 (MWh/ha) respectively.

9.4 Energy requirements during extraction phase

For the extraction phase of astaxanthin production, in section 5, three processes were selected: 1) Bead-milling for cell disruption; 2) Spray drying for dehydration; and 3) Supercritical CO_2 extraction enhanced with ethanol at 9.4% as co-selvent. In the following sections the energy requirements of each process using reference values from the literature adjusted to the boundaries of this study are analyzed.

9.4.1 Bead milling

Bead milling is a process to disrupt the thick algal wall of *Haematococcus pluvialis*, preparing the biomass for the recovery of the desired intracellular metabolite. Razon & Tan (2011) have reported a power consumption range between 2.8 and 10 (kWh/kg). Assuming the mean value of this range, this is 6.4 (kWh/kg) and calculating the biomass in the algal cake after centrifugation (i.e. 19.82 t/ha and 6.66 t/ha for Livadeia and Amsterdam respectively), the annual energy requirements for bead milling for the two cities can be calculated[19]. These needs amount to 126.8 (MWh/ha) and 42.6 (MWh/ha) for Livadeia and Amsterdam respectively.

[19] The amount of biomass in the algal cake can be calculated by multiplying the 'red' biomass existed in the broth prior to disk-stack centrifugation (i.e. 20.22 t/ha and 6.8t/ha for Livadeia and Amsterdam respectively) with the biomass recovery efficiency (i.e. 98%) of the harvesting method.

9.4.2 Spray drying

Spray drying has been labeled as the most appropriate method to dry microalgae biomass when targeting to high-value products. Regarding energy requirements during spray drying, Pérez-López et al. (2014) have calculated a value of 82.7 (kWh) per 0.8 kg of astaxanthin as the end product. The astaxanthin yield calculated in section 6.3.3 is used for the determination of the energy requirements during spray drying. This was calculated 471 (kg/ha) and 158 (kg/ha) for Livadeia and Amsterdam respectively. Using the power consumption of spray drying mentioned by Pérez-López et al. (2014) as a functional unit, the annual energy requirements for this process can be calculated: 48.7 (MWh/ha) and 16.3 (MWh/ha) for Livadeia and Amsterdam respectively.

9.4.3 Supercritical CO_2 extraction

The same methodology as followed in section 9.4.2 was implemented in order to calculate the energy requirements during supercritical CO_2 extraction enhanced with ethanol at 9.4% as co-solvent. Pérez-López et al. (2014) have calculated a value of 158.25 (kWh) per 0.8 kg of astaxanthin existing in the dried 'red' biomass after supercritical CO_2 extraction. Considering the astaxanthin yield calculated by the process model, the respective annual energy needs during supercritical CO_2 extraction correspond to 93.2 (MWh/ha) and 31.3 (MWh/ha).

9.5 Energy requirements of the gasification plant

Gasification exploiting 1st and 2nd generation biomass (such as rice husk, wood chips, saw dust, and crop stalks) constitutes a widespread method for power generation. However, there is little information in the literature on the gasification of algal biomass (3d generation) and especially on the energy balances associated with this process (Milledge et al., 2014). In this study, the energy needs during gasification were calculated by adjusting the net electric efficiency reported for 1st and 2nd generation biomass gasification to the boundaries of our system. The net electric efficiency of the gasifier (NEEG) corresponds to the ratio between the power input (PI) and the net electric power produced (i.e. NEP = gross electric power-electricity losses): $\mathrm{NEEG} = \mathrm{PI}/\mathrm{NEP}$. This ratio has been calculated at 3% using data from DEA & Energinet (2012). The net electric power produced through algal residues gasification was calculated 58.2 (MWh/ha) and 19.6 (MWh/ha) for Livadeia and Amsterdam respectively. Consequently, adjusting the NEEG to the abovementioned values, the power input for the operation of the gasification plant corresponds to 1.7 (MWh/ha) and 0.6 (MWh/ha) for Livadeia and Amsterdam respectively.

9.6 Energy Balance Ratios (EBR)

Table 14 presents concisely the findings of the investigation on the energy requirements all through the production of astaxanthin and gasification of the residual biomass. These values constitute the basis of the EBR calculation.

Energy requirements				
Annual power consumption (MWh/ha)	**Livadeia**		**Amsterdam**	
	Horizontal Tubular PBR (‘green stage’)	Raceway Pond (‘red stage’)	Horizontal Tubular PBR (‘green stage’)	Raceway Pond (‘red stage’)
	Cultivation phase			
Mixing/Circulation	51.5	13	35.3	8.6
Flue gases supply	9.4	20.8	6.1	7
O_2 removal	47	0	47	0
Water/broth pumping	2.3	11.3	1.6	3.8
Total cultivation phase	**155.3**		**109.4**	
	Harvesting phase			
Disk-stack centrifugation	**69.1**		**25.7**	
	Extraction phase			
Bead milling	126.8		42.6	
Spray drying	48.7		16.3	
Supercritical CO_2 extraction	93.2		31.3	
Total extraction phase	**268.7**		**90.2**	
Grand total energy needs production line	**493.1**		**225.3**	
	Energy recovery phase			
Conventional gasification	**1.7**		**0.6**	
Grand total energy requirements of the system	**494.8**		**225.9**	

Table 14: Energy requirements of the system.

In figure 24 the energy requirements of the three phases of the production process excluding the energy recovery phase are presented for the selected locations. They are expressed in numerical values as well as fractions of the total energy needs of the production process. In order to assess the results and provide a second proof of model’s validity (the first is discussed in section 6.3.3), a comparison with literature values is essential. Very few studies have been found that report in detail the energy needs all through production line of astaxanthin. Most studies that investigate astaxanthin from *Haematococcus pluvialis* focus mainly on technological breakthroughs to cultivate the strain and/or extract the pigment, excluding the power consumption part. From the few reports, only the one from Pérez-López et al. (2014) provides detailed data on the energy requirements all through astaxanthin production line. Using a two-stage photoautotrophic process with stirred-tank PBRs, they have calculated the energy needs of the three phases of the production line. Nevertheless, the photoautotrophic cultivation was accomplished by employing artificial illumination. Consequently, a power consumption comparison during cultivation phase between two production lines that use different sources of illumination for autotrophic microalgae growth would

not be valid. This is due to the fact that artificial illumination is associated with an increased power consumption, which does not apply to the system of this thesis.

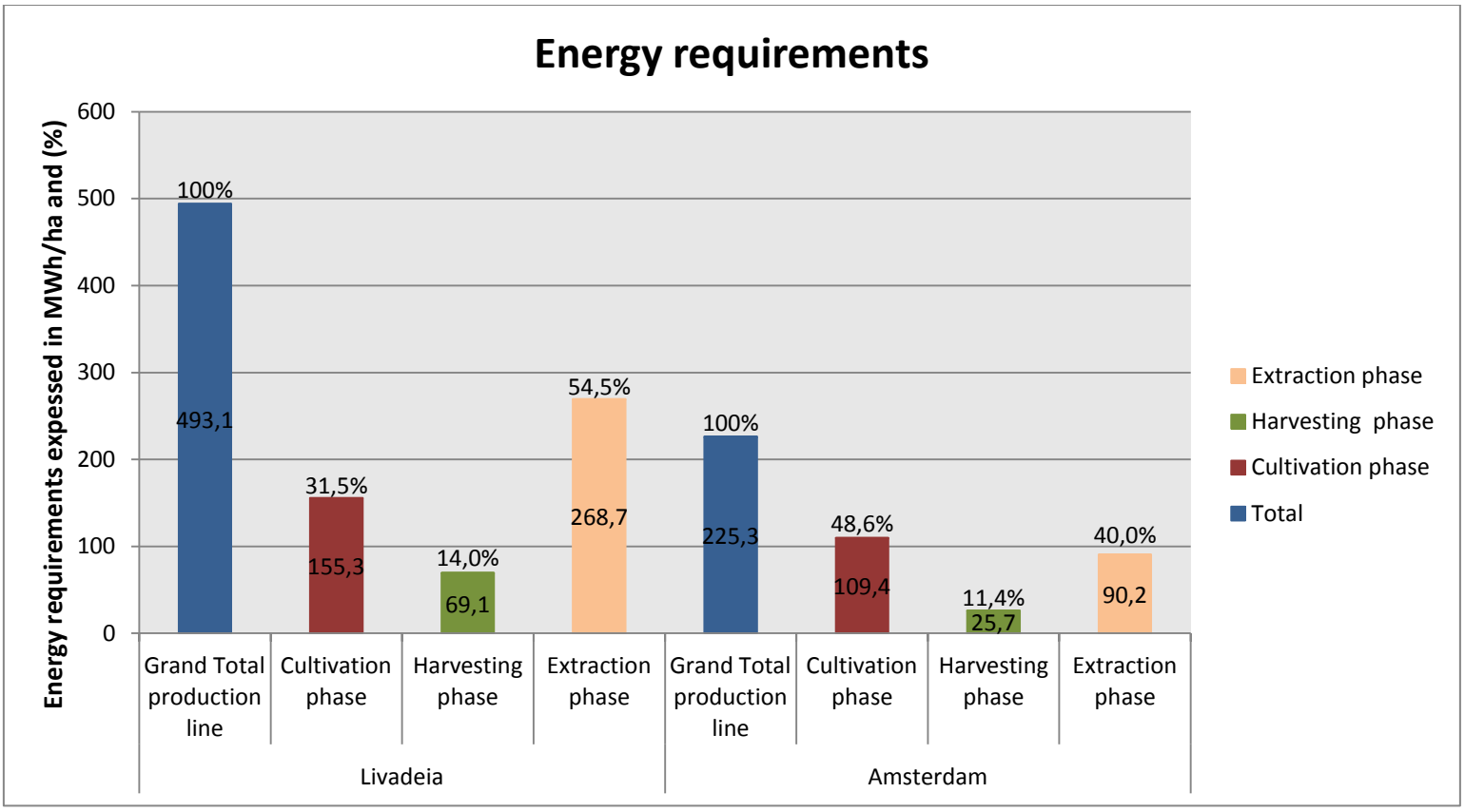

Figure 24: Energy requirements during production process expressed in (MWh/ha) and (%).

In the absence of other studies on the energy requirements during astaxanthin production, the energy requirements for the three phases presented in table 14 were compared with a conventional large scale production line of bio-energy derived by microalgae (cultivated photoautotrophically, exploiting solar radiation). Generally, the methods to cultivate, harvest and extract the desired algal product do not differ significantly, unless different metabolisms or energy carriers are selected (see section 3.2). In section 1.2.3, the results of a net energy balance assessment of large scale raceway open ponds reported by Sudhakar et al. (2012a), are portrayed. The assessment included all three phases of the production line and involved mainly the power requirements of each phase. These correspond to 41.4 (MWh/ha/year), 30.6 (MWh/ha/year) and 51.9 (MWh/ha/year) for cultivation, harvesting and extraction phase respectively[20]. The respective percentages of these values on the total energy needs during production line are: 33.4%, 24.7% and 41.9%. In their study, the dehydration process was included in the harvesting phase. In order to compare the reference values with the energy needs calculated in this thesis on the same basis, it was assumed that spray drying (see section 5.3) is part of harvesting phase. The respective fractions of the three phases in this thesis would then amount: 31.5%, 23.9% and 44.6% for Livadeia and 48.6%, 18.6% and 32.8% for

[20] The power requirements reported from Sudhakar et al. (2012a) are expressed in (MJ/ha/year). The values were translated into (MWh/ha/year) in order to facilitate comparison between the reference energy values and those calculated in this thesis.

Amsterdam. Regarding Livadeia, the results resemble significantly with the literature values, while these from Amsterdam have a deviation of approximately 25% (see figure 25)[21]. This can be attributed to the fact that the net energy balance assessment conducted by Sudhakar et al. (2012a) assumed Indian environmental conditions (2850 (h/year) sunshine time, 6100 (MJ/ m^2) annual solar radiation and 23°C annual average temperature), which are closer to these of Livadeia (2500 (h/year), 5400 (MJ/ m^2) and 17°C), Greece than Amsterdam (1840 (h/year), 3890 (MJ/ m^2) and 10°C), the Netherlands (Theoharis, 2014; Greenstream Publishing, 2015; KNMI, 2015; Panetas, 2015; Zednik, 2015)[22]. Furthermore, the fact that, regarding Amsterdam, the distribution of light was assumed the same as calculated from valid data for Livadeia, the actual productivity calculated by the model and consequently mass-energy flows are certainly affected to some extent. Further discussion on this aspect is presented in section 11.2.

Figure 25 portrays the energy requirements all through production process adjusted for comparison with the study of Sudhakar et al. (2012a).

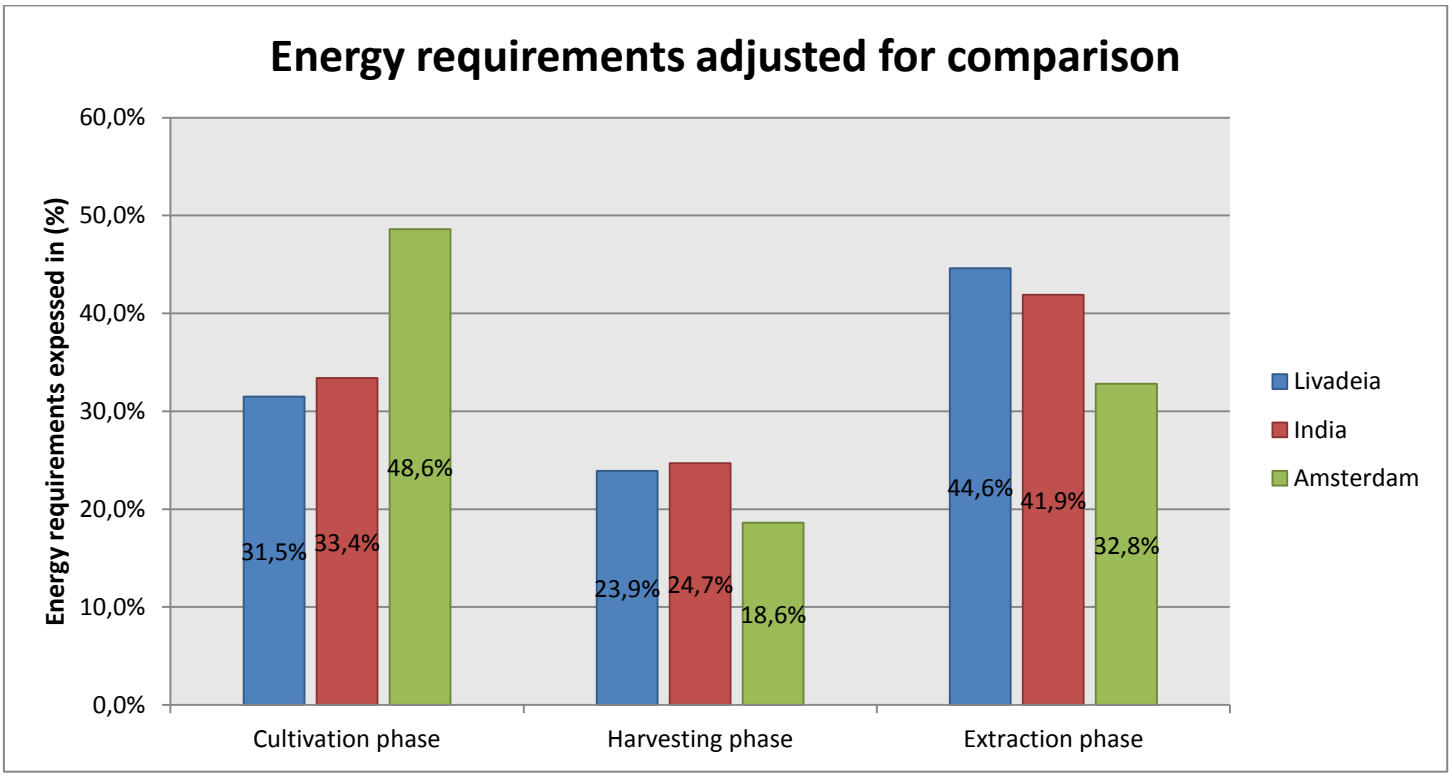

Figure 25: Energy requirements during production process adjusted for comparison with the study of Sudhakar et al. (2012a).

[21] The energy needs between the system of Sudhakar et al. (2012a) and the one of this study are not compared in a numerical point of view. However, the fractions of energy all through production line are of utmost significance and not the absolute values. For instance, although energy fractions in Greece and India resemble each other, the absolute values for each phase are totally different. This is due to the different end products to be extracted (biofuel in the study of Sudhakar et al. (2012a) and astaxanthin in this thesis), which may result in different absolute values of energy, when the latter are calculated using simulation models.

[22] The study of Sudhakar et al. (2012a) did not mention the area, whose environmental data were used for the net energy balance assessment. Thus, the environmental data of Bhopal is mentioned in this study. The energy department of the institute, where the author is a member and conducted his research, exists in this city.

Using the energy requirements presented in table 14 as well as the bio-energy generation through residual biomass gasification (58.2 (MWh/year) and 19.6 (MWh/year) for Livadeia and Amsterdam respectively), the energy balance ratios (EBRs) of the different processes included in the system can be determined for the selected locations. The EBRs illustrate the potential of meeting the energy needs all through production line. The EBR is defined as the total energy input (power requirements) to the total energy output (power generation implementing gasification). However, in this thesis the EBR is expanded to the individual processes of the production line including gasification as well. Thus, the EBR was calculated for each process that consumes power. Figure 26 depicts the detailed EBRs for the selected locations. EBRs that are below 1 show a potential of the respective process's energy needs to be satisfied by the power generated through residual biomass gasification.

Regarding cultivation phase, it is evident that only the energy needs all through the 'red stage' (i.e. raceway pond) for the both locations can be compensated by the power generated through residual biomass gasification. The total energy requirements during 'green stage' (i.e. tubular PBR) are approximately two- and five times higher compared to the 'red stage' for Livadeia and Amsterdam respectively. This outcome goes in line with the theoretical background presented in section 3.3, that closed cultivation systems are more energy intensive that open cultivation systems. The most energy intensive processes during 'green stage' are mixing/circulation and O_2 removal for both cities. The latter reflects the significance to remove the molecular oxygen (waste product) from the system. Regarding harvesting and extraction phases, the respective EBRs prove that only harvesting's energy needs can be compensated adequately by power generated through residual biomass gasification: 84% and 76% for Livadeia and Amsterdam respectively. Admittedly, EBR for the gasification plant is low, since the net electricity efficiency of the process should be high (97%, see section 9.5) in order it to constitute a reliable method for bio-energy production. Overall, nonetheless, the total EBRs for both cities show that the energy requirements associated with astaxanthin production accompanied by residual biomass gasification cannot be covered by residual bio-energy. More specifically, the fractions of compensation for Livadeia and Amsterdam amount to only 12% and 9% respectively. Thus, building a gasification plant for the utilization of residual biomass would not constitute a cost-efficient solution since it is proven that the combination of astaxanthin production and power compensation all through production line employing residual algal biomass gasification for power generation is not feasible yet. This outcome led to the decision to exclude the construction of the gasification plant into the economic performance analysis presented in section 10.

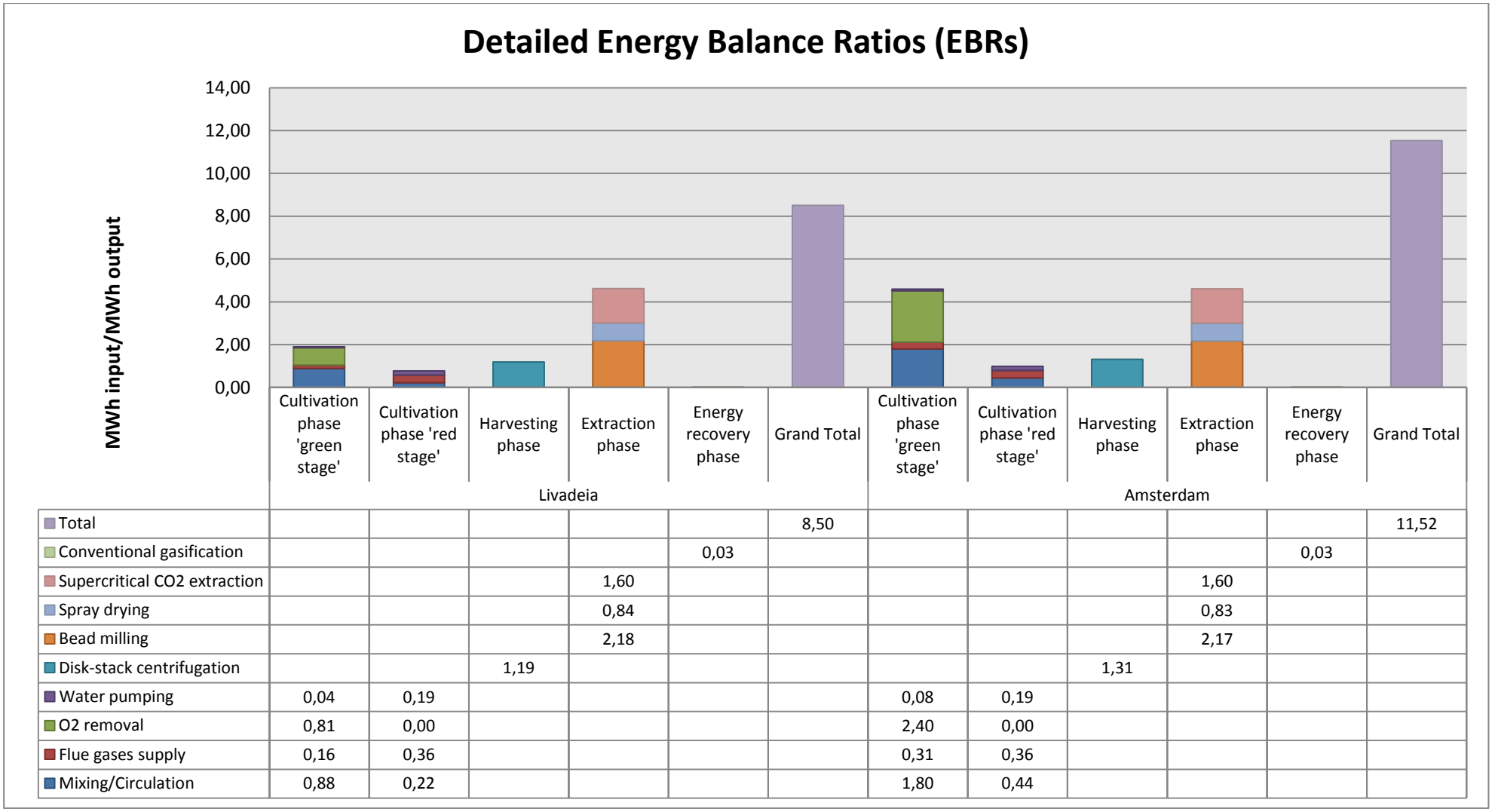

	Livadeia						Amsterdam					
	Cultivation phase 'green stage'	Cultivation phase 'red stage'	Harvesting phase	Extraction phase	Energy recovery phase	Grand Total	Cultivation phase 'green stage'	Cultivation phase 'red stage'	Harvesting phase	Extraction phase	Energy recovery phase	Grand Total
Total						8,50						11,52
Conventional gasification					0,03						0,03	
Supercritical CO2 extraction				1,60						1,60		
Spray drying				0,84						0,83		
Bead milling				2,18						2,17		
Disk-stack centrifugation			1,19						1,31			
Water pumping	0,04	0,19					0,08	0,19				
O2 removal	0,81	0,00					2,40	0,00				
Flue gases supply	0,16	0,36					0,31	0,36				
Mixing/Circulation	0,88	0,22					1,80	0,44				

Figure 26: Detailed energy balance ratios (EBRs) all through production line.

10 Economic performance

10.1 Introduction

In order to assess the potential viability of a company that targets to astaxanthin production, the annual economic performance has to be investigated. In this study, the economic performance all through production line involves a profit and loss (P&L) analysis. A P&L analysis is a financial statement that summarizes the revenues, costs and expenses incurred during a specific period of time. This statement provides information that shows the ability of a company to generate profits by reducing costs and increasing revenues. The costs involve the capital expenditures (CAPEX) and the operational expenditures (OPEX). In this study, the cornerstone of the P&L statement refers to the return of investment (ROI), which shows in the form of percentage the potential to offset the CAPEX and constitutes a valuable tool that assesses the viability of a microalgae production company from a business point of view.

10.2 Capital and operational expenditures

CAPEX is divided into two categories: 1) Equipment costs and 2) fixed capital costs. The former refers to the equipment that builds the bio-refinery and the latter refers to all processes needed in order to construct the bio-refinery. There are only a few studies that include a detailed statement with the capital expenditures of an algal bio-refinery. These statements constituted the basis in order to calculate CAPEX for the selected locations[23]. Literature values were either selected as reported to the various researches or adjusted to the different outcomes presented all through this thesis. For instance, costs of harvesting equipment (disk-stack centrifuge, centrifuge feed pump) were determined by calculating equipments' capacity. In Appendix D a detailed presentation of this calculation can be found. Last but not least, some studies have calculated CAPEX in $US. However, this thesis investigates the potential of viability for cities located in the European Union. Thus, when needed costs in $US were translated into Euros, using the exchange rate for June 2015. This amounts to 0.88 (€/$US) (X-Rates, 2015). Table 15 presents the outcomes for CAPEX.

[23] CAPEX was determined using reference values reported from Molina-Grima et al. (2003), Li et al. (2011), Jonker & Faaij (2013) and Slade & Bauen (2013).

CAPEX	Livadeia		Amsterdam		Source
€2015/ha	Tubular PBR	Raceway pond	Tubular PBR	Raceway pond	
	Equipment costs				
Medium supply station	21120	[-]	21120	[-]	adjusted by Li et al. (2011)
Medium feed pumps	23060	[-]	23060	[-]	(Molina-Grima et al., 2003)
Medium filter unit	15840	[-]	15840	[-]	(Molina-Grima et al., 2003)
Photobioreactors	633600	[-]	633600	[-]	adjusted by Li et al. (2011)
Airlift system	37400	[-]	37400	[-]	(Slade & Bauen, 2013)
Raceway pond	[-]	17700	[-]	17700	(Slade & Bauen, 2013)
Paddlewheel	[-]	7000	[-]	7000	(Jonker & Faaij, 2013)
CO_2 supply system	2640	3900	2640	3900	(Molina-Grima et al., 2003; Slade & Bauen, 2013)
CO_2 storage tank	35200		35200		Li et al. (2011)
Disk-stack centrifuge	58000		50000		(Alibaba Group, 2015a), see Appendix D
Centrifuge feed pump	12610		4800		adjusted by Molina-Grima et al. (2003), see Appendix D
Harvest biomass conveyor belt	12500		12500		(Molina-Grima et al., 2003)
Harvesting storage tank	17600		17600		(Slade & Bauen, 2013)
Bead miller	60000		60000		(Alibaba Group, 2015b)
Spray dryer	26400		26400		(Li et al., 2011)
Supercritical CO_2 extraction facility	85000		85000		(Alibaba Group, 2015c)
Packaging line	20000		20000		(Alibaba Group, 2015d)
Total equipment costs	**1089570**		**1073760**		[-]
	Fixed capital costs				
Land acquisition	25000	25000	45000	45000	(XE, 2015; Boerderij, 2015)
Land preparation	1000	1000	1000	1000	(Jonker & Faaij, 2013)
Piping	232670	9100	232670	9100	(Molina-Grima et al., 2003; Slade & Bauen, 2013)
Electrical	77550	3030	77550	3030	(Molina-Grima et al., 2003; Slade & Bauen, 2013)
Buildings	114060	3030	114060	3030	(Slade & Bauen, 2013)
Installation	228100	6070	228100	6070	(Slade & Bauen, 2013)
Instrumentation and control	77550	6070	77550	6070	(Molina-Grima et al., 2003; Slade & Bauen, 2013)
Engineering & Supervision	199930		199930		(Molina-Grima et al., 2003; Slade & Bauen, 2013)
Total fixed capital costs	**1009160**		**1049160**		[-]
Contractor's fee[24]	209870		212290		[-]
Grand total CAPEX	**2308600**		**2335210**		[-]

Table 15: Capital expenditures of the bio-refinery.

[24] The contractor's fee is usually estimated at 10% of the total equipment and fixed capital costs (Reppas, 2015).

OPEX involves all these costs in order the bio-refinery to operate. For the nutrients, water and power all through production line, reference cost values per unit found in the literature (translated to Euros when $US was the reference value) were simply multiplied with outcomes for mass-energy flows presented in tables 13 and 14 in sections 8.4 and 9.6 respectively. The costs associated with industrial power amounts to €0.13/kWh and €0.089/kWh for Livadeia and Amsterdam respectively (Eurostat, 2015). Regarding CO_2 as a substrate, zero costs were assumed. This decision lies on the fact that CO_2 was supplied into the system exploiting flue gases. Thus, since CO_2 from flue gases is a waste product that is associated with pollution issues, a company that exploits this greenhouse gas from being emitted to the atmosphere would not pay for distribution. This decision goes also in line with the study of Wang et al. (2008), who mention that CO_2 from flue gases is free or even result in revenues if a financial scheme for the prevention of greenhouse gas emissions exists. The manpower was assumed to include five workers, two supervisors and two marketing experts. The salary of this people was adjusted to the basic salaries of each expertise for the selected locations. Table 16 presents the outcomes for OPEX.

OPEX	Livadeia		Amsterdam		Source
€2015/ha/year	Tubular PBR	Raceway pond	Tubular PBR	Raceway pond	
	Cultivation phase				
KNO_3[25]	133320	[-]	96000	[-]	adjusted by Li et al. (2011)
Na_2HPO_4[26]	59980	[-]	43160	[-]	adjusted by Li et al. (2011)
$NaHCO_3$[27]	11090	[-]	7980	[-]	adjusted by Li et al. (2011)
$MgSO_4$[28]	1800	[-]	1300	[-]	(Alibaba Group, 2015e)
Micronutrients[29]	10910	[-]	7740	[-]	adjusted by Li et al. (2011)
CO_2 (from flue gases)	0	0	0	0	[-]
Water[30]	10200	55940	8630	25650	(EYATH, 2015; Vitens, 2015)
Power mixing/circulation	6695	1690	3142	765	adjusted by Eurostat (2015)
Power flue gases supply	1222	2704	543	623	adjusted by Eurostat (2015)
Power O_2 removal	6110	0	4183	0	adjusted by Eurostat (2015)
Power water pumping	299	1469	142	338	adjusted by Eurostat (2015)
Total power cultivation	**20189**		**9736**		[-]
	Harvesting phase				
Power disk-stack centrifugation	**8983**		**2287**		adjusted by Eurostat (2015)
	Extraction phase				
Power bead milling	16484		3791		adjusted by Eurostat (2015)
Power spray drying	6331		1451		adjusted by Eurostat (2015)
Power supercritical CO_2 extraction	12116		2786		adjusted by Eurostat (2015)
Total power extraction	**35126**		**8081**		[-]
Workers	51000		112500		(Trading Economics, 2015; PayScale, 2015)
Supervisors	60000		90000		(Trading Economics, 2015; PayScale, 2015)
Marketing	45000		75000		(Trading Economics, 2015; PayScale, 2015)
Maintenance	20000		20000		adjusted by Li et al. (2011)
Other repairs	5000		5000		[-]
Grand total OPEX	**528343**		**513011**		[-]

Table 16: Annual operational expenses of the bio-refinery.

[25] The costs of KNO_3 per metric ton amount to $500/ton or €440/ton (Li et al., 2011).
[26] The costs of Na_2HPO_4 per metric ton amount to $800/ton or €704/ton (Li et al., 2011).
[27] The costs of $NaHCO_3$ per metric ton amount to $250/ton or €220/ton (Li et al., 2011).
[28] The average costs of $MgSO_4$ per metric ton were found to correspond to €100/ton (Alibaba Group, 2015e).
[29] The costs of other micronutrients per metric ton were estimated by Li et al. (2011) at $2000/ton or €1760/ton.
[30] The costs of water for industrial purposes amount to €0.81/m^3 and €1.00/m^3 for Livadeia and Amsterdam respecrively (EYATH, 2015; Vitens, 2015).

10.3 Profit and Loss Statement

Using the calculated CAPEX and annual OPEX for the selected locations, the Profit and Loss (P&L) statement can be created. In order to assess in depth the economic viability of a potential company, the return of investment (ROI) was calculated for different market prices of astaxanthin. In section 1.2.2.2 the different market prices of astaxanthin found in the literature are mentioned. The global market for 2014 amounted to $447 million for 280 metric tons of both synthetic and natural astaxanthin (Industry Experts, 2015). This means that for 2014 the average market price of both synthetic and natural astaxanthin was $1600/kg. However, other studies mention market prices of natural astaxanthin at $2500-7000/kg (Milledge, 2010; Borowitzka, 2013; Koller et al., 2014; Pérez-López et al., 2014. Therefore, in this thesis the the ROI was calculated for values that cover the whole range. These values are 1600, 2000, 3000, 4000, 5000, 6000 and 7000 ($/$kg_{ASTAXANTHIN}$).

Besides channeling astaxanthin into the market, the residual biomass could be exploited from an economic point of view as well. Since it was decided not to construct a gasification plant in order to meet the energy needs of the production process, the residual biomass could be channeled to the market for nutricional and feeding purposes. This study did not investigate the other metabolites existed in the intracellular environment of *Haematococcus pluvialis*. Thus, an average market price of the biomass for nutrition ($40-50/kg) and of biomass for feeding ($10/kg) was assumed. This price amounted to $35/$kg_{BIOMASS}$.

From the market prices of astaxanthin and residual biomass the gross revenues can be calculated. Applying value added tax (VAT) for the two cities (23% and 21% for Livadeia and Amsterdam respectively) as well as annual operational expenditures the EBITDA can be calculated (European Commission, 2015). EBITDA is one of the most important indicators of a company's financial performance. EBITDA is essentially net income before interest, taxes, depreciation, and amortization, and can be used to analyze and compare profitability between companies and industries because it eliminates the effects of financing and accounting decisions. In this thesis, it is assumed that no loan was taken, but an external investor provided the company with the capital needed. Thus, there are no interests. Subtracting annual depreciation of the capital costs (the depreciation was calculated fot a time span of 10 years, which means 10% annually) and the corporate income taxes (26% and 25% for Livadeia and Amsterdam), the earnings after taxes (EAT) and the cash available for distribution to shareholders (CAD) can be determined (NFIA, 2015). CAD is the subtraction between EBITDA and corporate taxes and constitutes one of the two indicators in order to calculate ROI. The other refers to CAPEX. In section 2.5, calculation of ROI is given by formula 2. Tables 17 and 18 present the P&L statement for the selected locations, using different market prices of astaxanthin which were translated into Euros.

Livadeia

Price(€)/kg	Astaxanthin	1,408	1,760	2,640	3,520	4,400	5,280	6,160
kg	Astaxanthin	471	471	471	471	471	471	471
Price(€)/kg	Biomass	30	30	30	30	30	30	30
kg	Biomass	18,950	18,950	18,950	18,950	18,950	18,950	18,950
GROSS REVENUE		**1,231,668**	**1,397,460**	**1,811,940**	**2,226,420**	**2,640,900**	**3,055,380**	**3,469,860**
VAT		283,284	321,416	416,746	512,077	607,407	702,737	798,068
Net Revenues		**948,384**	**1,076,044**	**1,395,194**	**1,714,343**	**2,033,493**	**2,352,643**	**2,671,792**
OPEX		**528,343**	**528,343**	**528,343**	**528,343**	**528,343**	**528,343**	**528,343**
EBITDA		**419,846**	**547,506**	**866,656**	**1,185,805**	**1,504,955**	**1,824,105**	**2,143,254**
Depreciation		230,860	230,860	230,860	230,860	230,860	230,860	230,860
EBIT		**188,986**	**316,646**	**635,796**	**954,945**	**1,274,095**	**1,593,245**	**1,912,394**
Interest expense debt								
Interest income on cash								
EBT		**188,986**	**316,646**	**635,796**	**954,945**	**1,274,095**	**1,593,245**	**1,912,394**
Tax		49,136	82,328	165,307	248,286	331,265	414,244	497,222
EAT		**139,850**	**234,318**	**470,489**	**706,660**	**942,830**	**1,179,001**	**1,415,172**
CAD		**370,710**	**465,178**	**701,349**	**937,520**	**1,173,690**	**1,409,861**	**1,646,032**
CAPEX		**2,308,600**	**2,308,600**	**2,308,600**	**2,308,600**	**2,308,600**	**2,308,600**	**2,308,600**
ROI		**16.06%**	**20.16%**	**30.39%**	**40.62%**	**50.85%**	**61.08%**	**71.31%**

Table 17: P&L statement for Livadeia.

Amsterdam

Price(€)/kg	Astaxanthin	1,408	1,760	2,640	3,520	4,400	5,280	6,160
kg	Astaxanthin	158	158	158	158	158	158	158
Price(€)/kg	Biomass	30	30	30	30	30	30	30
kg	Biomass	6,370	6,370	6,370	6,370	6,370	6,370	6,370
GROSS REVENUE		**413,564**	**469,180**	**608,220**	**747,260**	**886,300**	**1,025,340**	**1,164,380**
VAT		86,848	98,528	127,726	156,925	186,123	215,321	244,520
Net Revenues		**326,716**	**370,652**	**480,494**	**590,335**	**700,177**	**810,019**	**919,860**
OPEX		**513,011**	**513,011**	**513,011**	**513,011**	**513,011**	**513,011**	**513,011**
EBITDA		**-186,348**	**-142,412**	**-32,570**	**77,271**	**187,113**	**296,955**	**406,796**
Depreciation		233,521	233,521	233,521	233,521	233,521	233,521	233,521
EBIT		**-419,869**	**-375,933**	**-266,091**	**-156,250**	**-46,408**	**63,434**	**173,275**
Interest expense debt								
Interest income on cash								
EBT		**-419,869**	**-375,933**	**-266,091**	**-156,250**	**-46,408**	**63,434**	**173,275**
Tax[31]		0	0	0	0	0	15,858	43,319
EAT		**-419,869**	**-375,933**	**-266,091**	**-156,250**	**-46,408**	**47,575**	**129,956**
CAD		**-186,348**	**-142,412**	**-32,570**	**77,271**	**187,113**	**281,096**	**363,477**
CAPEX		**2,335,210**	**2,335,210**	**2,335,210**	**2,335,210**	**2,335,210**	**2,335,210**	**2,335,210**
ROI		**-7.98%**	**-6.10 %**	**-1.39%**	**3.31%**	**8.01%**	**12.04%**	**15.57%**

Table 18: P&L statement for Amsterdam.

[31] For negative earnings before taxes (EBT) taxes are zero.

Comparing the different values of ROI for the selected locations, it can be noticed that only in Livadeia a potential microalgae company is viable for the whole range of astaxanthin market prices. Furthermore, ROI is particular high for this city at the whole range of market prices (>15%), introducing that way a high economic potential. This means that purity of astaxanthin does not constitute a constraint for a viable company in Livadeia. On the other hand, ROI in Amsterdam is positive only for astaxanthin market prices that are higher than $4000/kg or €3520/kg (see also figure 27). This can be attributed to the lower biomass productivity, which in turn resulted in a lower astaxanthin yield compared to the one of Livadeia. Under a specific threshold of astaxanthin yield, viability of the company cannot be achieved for all market prices.

The biomass productivity calculated by the process model is highly dependent on the environmental conditions and more specifically on solar radiation and temperature. In fact, as all other parameters in the process model were assumed as constants and were the same all through calculation of biomass productivity for the two cities, it can be inferred that variations in solar radiation and temperature define the final 'red' biomass productivity and consequently astaxanthin yield. Since Livadeia is associated with higher solar radiation and average temperature values than Amsterdam on an annual basis, it can be concluded that the lower these values are, the less the biomass productivity and consequently astaxanthin yield. In other words, it is proven that in Amsterdam economic viability for the whole range of astaxanthin market prices can be achieved only if solar radiation and temperature are further enhanced, using for instance artificial illumination and temperature control devices. Nevertheless, if high purity astaxanthin can be achieved in Amsterdam, in order to channel it into the market at prices higher than €3520/kg, establishing a company in the Dutch city is an attractive option as well. Even if, for high market prices, ROI remains low compared to Livadeia, Amsterdam and by extension the Netherlands constitute a safe 'harbor' for such innovative ventures. The Netherlands has a very promising and flourishing economy, well-structured governance and an internationally recognized workplace that highly stimulates and supports 'green' solutions, subsidizing and protecting them.

Figure 27 portrays the development of ROI for the selected locations as function of different astaxanthin market prices.

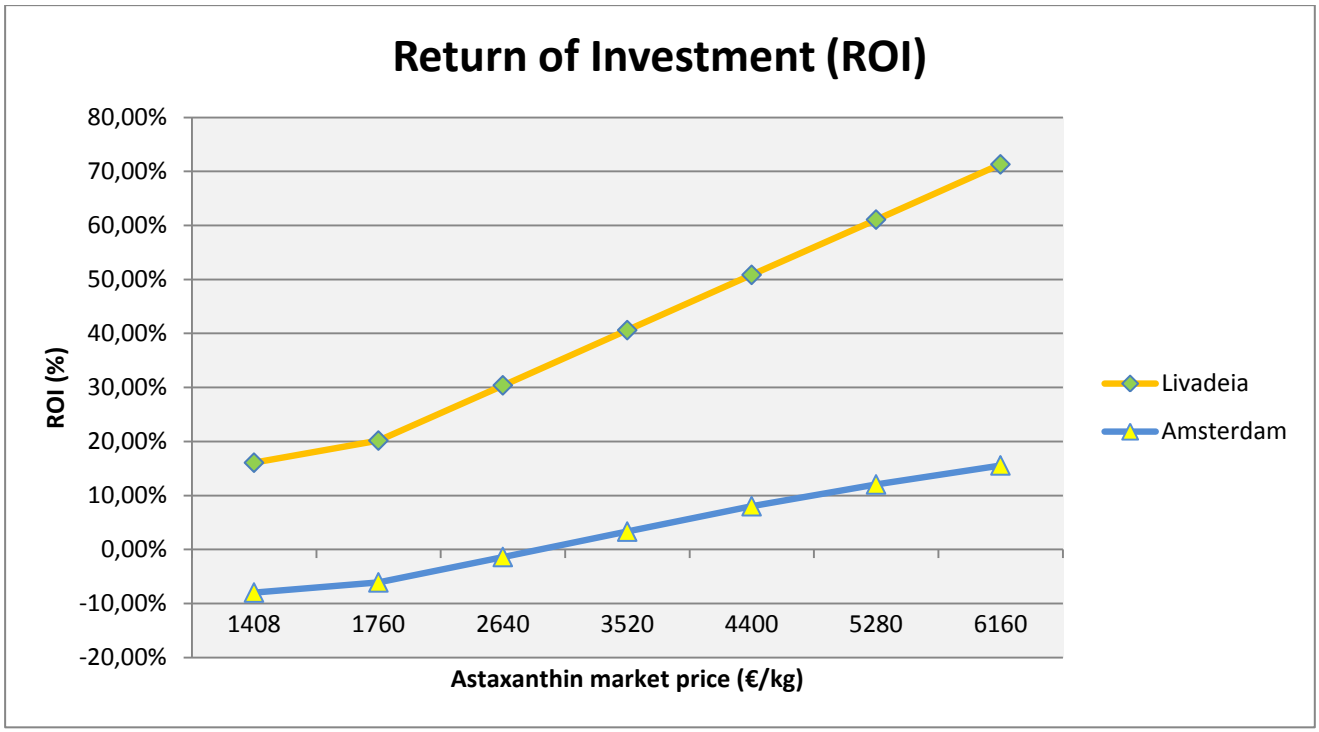

Figure 27: Development of ROI for the selected locations as function of the different astaxanthin market prices.

The last part of the economic performance refers to the costs per kg of astaxanthin. There is not a specific formula for this calculation. One could use only the OPEX or the OPEX summed with depreciation or even all costs that result in EAT (earnings after taxes). For instance, Li et al. (2011) calculated a value of $718/kg or €632/kg taking into account the OPEX and the depreciation as the total costs. For the sake of comparison, the same was done in this thesis. The respective costs for Livadeia and Amsterdam correspond to €1612/kg and €4725/kg. It can be noticed that the calculated values, especially the one from Amsterdam, are significantly higher than the reference value calculated by Li et al. (2011). This can be attributed to the fact that in the study of Li et al. (2011), CAPEX and OPEX were determined based on the financial environment of China. China is an attractive country for industries, since labor, land and utilities costs are significantly lower than the ones from the Western countries. For instance, Li et al. (2011) included in their conceptually scaled up financial statement 19 workers with an annual salary of $5000/worker and 4 supervisors with an annual salary of $8000/supervisor. They did not include marketing experts. In total they assumed a labor capacity of 23 people, which resulted in an expenditure of $127000/year or €111760/year. In this thesis, only 9 people (5 workers, 2 supervisors and 2 marketing experts) were assumed for the selected locations. The respective expenditure amounts to €156000/year and €277500/year for Livadeia and Amsterdam. In other words, employing in Western countries less than half of labor reported for China, workforce costs are higher and may be even double as much than the respective ones from China.

Furthermore, the cost of industrial water in China amounts to only $0.3/$m^3$ or €0.26/m^3, while the respective costs for Livadeia and Amsterdam correspond to €0.81/m^3 and €1.00/m^3, posing a significant difference in water demand costs (Li et al., 2011; EYATH, 2015; Vitens, 2015). Last but not least, CAPEX in this thesis was calculated using mainly capital costs reported from studies that conducted experiments in Europe. This resulted in a CAPEX of €2308600 and €2335210 for Livadeia and Amstedam respectively. The respective value in the study of Li et al. (2011) was $1468500 or

€1292280. This CAPEX is approximately half of the respective ones for Livadeia and Amsterdam. From the CAPEX the depreciation (10%) is calculated. Since it was assumed that costs per kg of astaxanthin involved depreciation besides OPEX, a higher value of depreciation increases the costs per kg of astaxanthin. These are the main reasons that justify the big variation of the costs/kg between China and the selected locations in this thesis.

Besides comparing the costs per kg of natural astaxanthin for the selected locations with the respective values reported in the literature, it is worthier comparing them with the costs associated with synthetic astaxanthin. Costs for synthetic astaxanthin have been estimated at $1000/kg or €880/kg (see section 1.2.2.2). However, it is not reported, of what kind these costs are (e.g. only OPEX, or OPEX summed with depreciation etc.). Thus, it is assumed that these costs refer only to OPEX. Considering this assumption, the annual costs per kg of natural astaxanthin would then amount to €1122/kg and €3247/kg for Livadeia and Amsterdam respectively. It can be noticed that for Livadeia, the annual costs per kg of natural astaxanthin compete with the ones for synthetic astaxanthin adequately. This is not the case for Amsterdam, where the respective costs are four times bigger than the costs of synthetic astaxanthin. As already mentioned, this is due to low algal biomass productivity incurred in the Dutch city.

11 Discussion and recommendations

11.1 Introduction

This thesis examined four aspects of large scale natural astaxanthin production using the algal strain *Haematococcus pluvialis*, which will strongly influence viability of the whole process in the future, competing synthetic astaxanthin as well: 1) The mass- 2) energy flows during production process; 3) the compensation of energy needs associated with the production process, employing residual biomass gasification and 4) economic performance of the production process. The tool in order to provide answers to the abovementioned aspects was the construction of a process model, which simulated the three phases involved in a natural astaxanthin production line: Cultivation, harvesting and extraction. The model was based on previous attempts to simulate microalgae growth mainly for the production of algal biofuels, adjusted to the needs of astaxanthin production. In the following sections, limitations of the research, theoretical implications and recommendations for industry and policy makers are discussed in detail.

11.2 Limitations

One of the biggest limitations of this thesis refers to the distribution of light that was used in the process model. Calculating biomass productivity and consequently astaxanthin yield using hourly irradiance data enhances validity of the results, since a more detailed approach is followed. In fact, this is also proposed by a plethora of studies that have simulated microalgae growth (Sukenik et al., 1991; Sudhakar et al., 2012b; Jonker & Faaij, 2013). Nonetheless, hourly irradiance data are not easily accessible and in most cases they even cost significant amount of money, since their detailed collection constitutes a demanding challenge. Detailed hourly irradiance was provided confidentially for Livadeia by ETHER. From this data an average monthly distribution solar radiation was calculated, which was applied for Amsterdam as well. It can be claimed that this assumption for light distribution does not result in the most accurate results for the Dutch city. In fact, considering that the Amsterdam is built at higher latitude than Livadeia, which means that during summer length of daytime is longer than the Greek city, it is expected that biomass productivity and consequently astaxanthin yield would be bigger.

Furthermore, proposed microalgae process models by the different studies do not take into account the impact of CO_2, O_2, pH, nutrients and mixing on biomass productivity calculation. In section 8, where mass flows are discussed, most of these factors are accompanied by utilization efficiency. However, this efficiency should not be confused with the impact of these factors on the biomass productivity calculation formula. Since in this thesis the central idea of the model is to translate incident solar irradiation into biomass productivity using HHV, the abovementioned factors do not play any direct role on the amount of solar energy absorbed by the algal cells, but they facilitate other parts of cultivation. Thus, their impact was translated into an efficiency factor, which was determined at will. This is a limitation that may affect final results for biomass productivity.

11.3 Theoretical implications

From a sustainability point of view, cultivating freshwater microalgae such as *Haematococcus pluvialis* for the recovery of various high valued metabolites such as astaxanthin encloses an increased consumption of freshwater. In fact, it is calculated that for Livadeia and Amsterdam a supply of 81662 (m^3/year) and 34281 (m^3/year) is required (see section 8.4). These values correspond to the water volume of 22 and 9 Olympic pools respectively. This constitutes significant water

consumption, especially if we take into account that usual large scale microalgae facilities are bigger than 10 hectares. Thus, as Tredici (2012) claims, microalgae cultivation is all about water management. In this realm, the idea of wastewater treatment appeared. Organic and inorganic substances which were released into the environment as a result of domestic, agricultural and industrial water activities resulting in organic and inorganic pollution constitute important nutrient sources for aquatic plants and especially algae (Abdel-Raouf et al., 2012). In other words, instead of supplying the growth medium with macro- and micronutrients in order to facilitate cultivation, wastewater could serve the environment of cultivation. Nevertheless, the resulted algal biomass could be utilized only for bio-energy production and for animal feeding supplements, since wastewater algae may be associated with contamination issues (Cheunbarn & Peerapornpisal, 2010; Abdel-Raouf et al., 2012). Astaxanthin constitutes a feed targeted to salmonids, shrimps, lobsters and crayfishes, but it is also considered as the most powerful antioxidant for humans (see section 1.2.2.2). Most of natural astaxanthin derived by microalgae is channeled to the pharmaceutical and food & beverage sectors. Thus, wastewater treatment is a risky option for cultivating *Haematococcus pluvialis*. Hence, more research is needed in order to combine wastewater treatment with algae products (among them is astaxanthin) that could be destined for human consumption.

In this study, the viable combination of natural astaxanthin production and bio-energy that could offset the energy requirements during production process in two European cities was examined. The bio-energy referred to power generation from residual biomass gasification, after astaxanthin is recovered. We have shown that the total EBR is too low and that only 12% and 9% of the total energy needs could be compensated for Livadeia and Amsterdam respectively. Pérez-López et al. (2014) report in their study that stress conditions, which trigger astaxanthin accumulation in the intracellular environment of *Haematococcus pluvialis*, result in low growth rates as well. The latter means that algal biomass quantity is confined when astaxanthin is the targeted product compared to biomass productivity when lipids for biofuels are desired, for example. The smaller the volume of algal biomass is, the less the power generation from residual biomass generation. This aspect poses the need of further investigation on how high astaxanthin concentrations could be combined with high biomass productivities.

In this thesis, we utilized the different microalgae growth models existed in the literature in order to create an astaxanthin production process model, which incorporated all three phases of the production line. In section 11.2, the limitation of the impact of CO_2, O_2, pH, nutrients and mixing on biomass productivity calculation is discussed. The determination of these factors at will, may affect the performance of the process model. Although the validity of the model was confirmed comparing the results with two different sources, further investigation on the role of these factors in the process model should be conducted. All parameters of the model should be scientifically certified.

The technical part linked with the astaxanthin production involved the detailed presentation of the energy requirements all through production process. However, this study did not include indirect energy consumption. Quite simply, any energy consumption is labeled as ‘indirect’ if the actual burning of the fossil fuel or consumption of the energy is off-site. For instance, gasoline consumption for transportation of the consumables needed in the production line or the energy associated with the production of macro- and micronutrients needed for cultivation, constitute indirect energy consumption. An investigation on this technical aspect would be very interesting, in order to acquire

a rounded view of all energy needs that accompany a microalgae facility. This would examine the actual sustainable profile of this 'green' solution.

Regarding mass flows, this thesis investigated the in- and outflows of all substrates needed for a successful production process. Nevertheless, recycling was not taken into account. For instance, water removed after disk-stack centrifugation and spray drying along with excessive macro- and micronutrients existed in this water could be channeled back to the selected cultivation system. The same goes for the unutilized CO_2 (Milledge, 2013). This aspect is of particular importance, since in this way costs will be reduced, while sustainable development and circular economy is strongly enhanced. A potential research on substrate recycling during astaxanthin production process would result in a more detailed mass balance statement and would constitute certainly an added value to the scientific community.

From the economic point of view, this thesis presents a detailed P&L statement that assesses the viability of a company should it is established in the selected locations. It is evident, that a company located in Livadeia is associated with a higher economic potential than a company established in Amsterdam. We have concluded that environmental conditions (solar radiation and temperature) are parameters that determine astaxanthin yield (see sections 6.3 and 10.3). Since climatic conditions in Amsterdam do not favor microalgae growth adequately, artificial lights and control temperature devices could be employed. Undoubtedly, these devices are accompanied with extra power consumption among others. An increased power consumption compared to the one calculated in this thesis will increase the costs and may hamper further the viability of the company. However, biomass productivity and consequently astaxanthin yield would be higher as well, something that may not only compensate the extra costs but also result in higher revenues and ROI than the current situation. Pérez-López et al. (2014) have calculated a power consumption of artificial lighting at 1924 (kWh/kg) of the carotenoid. Assuming that the astaxanthin yield from Livadeia (i.e. 471) is a satisfying goal, the energy requirements for artificial bulbs would amount to 906 (MWh/year). This seems to be a high power demand, which will lead to high operational costs. However, this value refers to microalgae cultivation implementing only artificial lighting as the energy carrier for algal growth. Therefore, more research should be conducted on the combination of solar energy and artificial light as well as energy requirements and economic performance associated with this action.

Last but not least, the P&L analysis, conducted in this thesis, assesses the economic performance only for the first year. However, projections of this performance show the actual potential of the company in the global market. Projections are not an easy task, especially for business plans. Valid long-run business forecasts involve an abundance of variables that their gathering and interaction analysis not only demand a considerable amount of time but even corporate finance experts may be unable to provide valid answers. For instance, the price per kWh or the fraction of the VAT may change in the near future, especially for 'green' solutions. Detailed long-run business forecasts, regarding astaxanthin production, constitute the cornerstone of the scientific background presented in this study and would be a great asset for future viability of microalgae ventures.

11.4 Recommendations for Industry and Policy Makers

Two of the biggest constraints for commercialization of microalgae products refer to the increased capital and operational costs, especially for photobioreactors. Although this thesis proved that astaxanthin production from microalgae is attractive from an energy and economic perspective, this

is not applicable for all locations that cultivate microalgae photoautotrophically. For Amsterdam, for example, only for high astaxanthin market prices, this venture is considered viable. Consequently, conducting research on energy efficiency during the production line as well on lower costs for materials and equipment would boost this industry to be established in the market. In such way, industry would also open the gates for commercialization of algal biofuels that are not cost-efficient yet.

Furthermore, although costs per kg of natural astaxanthin calculated for Livadeia (€1122/kg) may compete adequately with the ones for synthetic astaxanthin reported by different studies (€880/kg), it cannot outcompete totally the synthetic astaxanthin market. Since astaxanthin is mainly channeled as feed for salmonids shrimps, lobsters and crayfishes, the more expensive natural astaxanthin would result in overpriced fishes in the market. However, the public mostly does not appear to demand and is not willing to pay a higher price for naturally pigmented salmonids. Most consumers probably do not realize that most of the salmonids, shrimps, lobsters and crayfishes found in the supermarkets nowadays are farmed, that astaxanthin is introduced to their diets and that this pigment is a synthetic product derived by petrochemicals at a rate that exceeds 99% (see section 1.2.2.2). As long as public stays uninformed on the advantages of natural astaxanthin over the synthetic one, natural astaxanthin is condemned to remain at <1% of the global market. Therefore, future policies should support research and marketing initiatives regarding natural astaxanthin, in order to educate public on the beneficial properties of this powerful antioxidant, gaining the place it deserves in the market.

12 Conclusions

In this thesis, we answered the following question: *What are the expected mass-energy flows as well as economic performance involved in large scale production of astaxanthin derived by microalgae?*

In order to provide a valid answer on the abovementioned research question, a process model that simulated all phases (i.e. cultivation, harvesting and extraction) involved in the production process, was created. The model calculated the annual astaxanthin yield. The model assumed a hybrid system for photoautotrophic cultivation of the strain *Haematococcus pluvialis*. The hybrid system comprised by a fence of horizontal tubular PBRs and a raceway pond. The model was based on solar radiation and temperature data for two European cities: Livadeia, Greece and Amsterdam, the Netherlands. This yield was calculated at 471 (kg/year) and 158 (kg/year) for the Greek and the Dutch city respectively. Taking into account saturation intensities of illumination for optimal alga growth and accumulation of the pigment into the intracellular environment, we proved the higher solar radiation and temperature is, the higher the astaxanthin yield. This is due to the fact that astaxanthin accumulation is facilitated by increased solar radiation. It can be inferred, consequently, that equator countries are more suitable for astaxanthin production. This statement is also enhanced by the locations, where the most important natural astaxanthin producers have built their facilities. Cyanotech has its facilities in Hawaii, while Algaetechnologies in the south part of Israel. Validity of the model was assessed in two ways: 1) By comparing the astaxanthin yields with the ones achieved by an actual production facility; 2) by comparing the energy requirements with the net energy balance assessment found in the literature. It was found that astaxanthin yield between Livadeia and the one from an actual facility in Shenzhen, China resemble significantly. Furthermore, power consumption distribution during the different phases between Livadeia and Bhopal, India match to a high extent. Taking into account that the three cities share similar environmental conditions, it can be deduced that the process model can be rendered as a valid tool for biomass productivity calculation of every microalgal strain, if adjustments on model inputs are made. For instance, other algae species may involve different saturation intensities for optimal growth than the ones chosen for *Haematococcus pluvialis.*

Based on the biomass productivity calculated by the process model, the mass- and by extension energy flows all through production process were calculated. Regarding mass flows, it is evident that microalgae cultivation is associated with high fresh water consumption. More specifically, 81662 (m^3/year) and 34281 (m^3/year) without recycling are needed within the production process in Livadeia and Amsterdam respectively. Furthermore, 462.8 (t/year) and 333.2 (t/year) of fertilizers are required during the cultivation phase for the Greek and the Dutch city respectively. In order to proliferate, microalgae need CO_2 as well. This thesis assumed a CO_2 supply by exploiting flue gases. It was calculated that 150.9 (t/year) and 65.6 (t/year) of flue gases CO_2 are needed during cultivation for Livadeia and Amsterdam respectively. Furthermore, CO_2 demand for supercritical CO_2 extraction is also assumed that is facilitated by flue gases and amounts to 354 (t/year) and 119 (t/year) for Livadeia and Amsterdam respectively. These high values of CO_2 show that in the near future large scale microalgae cultivation facilities may strongly contribute on mitigating the excess of industrial CO_2 emissions, stimulating that way sustainable development. However, water consumption during cultivation constitutes a significant issue towards a sustainable profile and should be tackled either by recycling or wastewater treatment.

As for energy flows, the total energy requirements all through the production process were calculated at 494.6 (MWh/year) and 225.9 (MWh/year) for Livadeia and Amstedam respectively. The highest energy needs were associated with the process of bead milling during extraction phase, where 126.8 (MWh/year) were calculated for Livadeia, while the respective value for Amsterdam amounted to 42.6 (MWh/year). In order to encourage energy self-sufficiency of the whole system, the compensation of the energy needs implementing residual biomass gasification, was investigated. Only 12% and 9% of the total energy needs could be offset by electricity generated from syngas (the outcome of biomass gasification) for Livadeia and Amsterdam respectively.

Regarding economic performance, a Profit and Loss (P&L) analysis was conducted. In this analysis the associated CAPEX and OPEX for the two cities were calculated, which facilitated the construction of the P&L statement. The P&L statement ended with the return of investment (ROI) for the different market prices of astaxanthin. It was found that only in Livadeia viability of a microalgae company would be ensured, for all market prices. This highlights the significance of a warm climate, when cultivating microalgae photoautotrophically. ROI for the Greek city ranges from 16.06-71.31% for the different market prices. Regarding Amsterdam, viability of a microalgae production company starts at €3520/kg of astaxanthin, while positive values of ROI range from 3.31-15.57%. Furthermore, one of the most important aspects of economic performance revolves around the costs per kg of natural astaxanthin. It was found that for Livadeia these costs amount to €1122/kg, which competes adequately with the costs of synthetic astaxanthin (€880/kg). On the other side, the respective costs of natural astaxanthin for Amsterdam were calculated at €3247/kg. This value cannot compete with the one reported for synthetic astaxanthin, rendering Amsterdam an inappropriate location for natural astaxanthin production from this point of view.

In retrospect, natural astaxanthin production derived by *Haematococcus pluvialis* that was cultivated in sites characterized generally by high solar radiation and high temperatures is an attractive option from a business point of view, and a competitive alternative to synthetic astaxanthin. Looking ahead, as society stimulates a transition towards ‘green’ solutions and taking into account that the global market is estimated to skyrocket from $447 million in 2014 to over 1.5 billion dollars by 2020, it is worth investigating further the different possibilities to produce this metabolite naturally focusing in energy efficiency within the different production stages and/or considering the use of renewable energy. Potential domination of natural astaxanthin over the synthetic alternative will offer high quality fisheries that metabolize this pigment in their nutrition and will expand the applications in the pharmaceutical/cosmetics sector as well.

Bibliography

Abdel-Raouf, N., Al-Homaidan, A. A., Ibraheem, I. B. M. (2012). Microalgae and wastewater treatment. Saudi Journal of Biological Sciences, 19(3), 257–275.

Acién, F. G., Fernández Sevilla, J. M., Sánchez Pérez, J. A., Molina Grima, E., & Chisti, Y. (2001). Airlift-driven external-loop tubular photobioreactors for outdoor production of microalgae: Assessment of design and performance. Chemical Engineering Science, 56(8), 2721–2732.

Acién, F. G., Fernández, J. M., Magán, J. J., Molina, E. (2012). Production cost of a real microalgae production plant and strategies to reduce it. Biotechnology Advances, 30(6), 1344–1353.

Aflalo, C., Meshulam, Y., Zarka, A., Boussiba, S. (2007). On the relative efficiency of two- vs. one-stage production of astaxanthin by the green alga Haematococcus pluvialis. Biotechnol Bioeng; 98:300–5.

Alam, F., Date, A., Rasjidin, R., Mobin, S., Moria, H., & Baqui, A. (2012). Biofuel from Algae- Is It a Viable Alternative? Procedia Engineering, 49, 221–227.

Alibaba Group. (2015a). Dhc730 High Speed Disc Stack Centrifuge Separator For Bioengineering Broth. Retrieved June 15, 2015, from http://www.alibaba.com/product-detail/DHC730-High-Speed-Disc-Stack-Centrifuge_1985975426.html?s=p

Alibaba Group. (2015b). Wsc Horizontal Bead Mill/sand Mill For Paint And Ink. Retrieved June 15, 2015, from http://www.alibaba.com/product-detail/WSC-horizontal-bead-mill-sand-mill_60107452537.html?s=p

Alibaba Group. (2015c). Supercritical Co2 Extraction Machine. Retrieved June 15, 2015, from http://www.alibaba.com/product-detail/supercritical-CO2-extraction-machine_60112458662.html?s=p

Alibaba Group. (2015d). Powder Filling Packing Machine - Buy Powder Packing Machine,Powder Filling Machine,Powder Packaging Machine Product on Alibaba.com. Retrieved June 18, 2015, from http://www.alibaba.com/product-detail/Powder-Filling-Packing-Machine_60196968246.html

Alibaba Group. (2015e). White Crystal Magnesium Sulphate Mgso4 (purity 99.5%). Retrieved June 15, 2015, from http://www.alibaba.com/product-detail/White-Crystal-Magnesium-Sulphate-MgSO4-Purity_60087677691.html?s=p

Alzate, M. E., Muñoz, R., Rogalla, F., Fdz-Polanco, F., & Pérez-Elvira, S. I. (2014). Biochemical methane potential of microalgae biomass after lipid extraction. Chemical Engineering Journal, 243, 405–410.

Aragon, A. B., Padilla, R. B. and Ros de Ursinos, J. A. F. (1992). Experimental study of the recovery of algae cultured in effluents from the anaerobic biological treatment of urban wastewaters. Resources Conserv. Recycling, 6: 293-302.

Arnold, M. (2013). Sustainable algal biomass products by cultivation in waste water flows. *VTT Technology*, *147*, 1–84.

Azadi, P., Brownbridge, G., Mosbach, S., Kraft, M., Street, P., & Street, P. (2014). Simulation and Life-cycle Assessment of Algae Gasification Process in Dual Fluidized Bed Gasifiers. Cambridge Centre for Computational Chemical Engineering, (144).

Azarian, G. H., Mesdaghinia, A. R., Vaezi, F., Nabizadeh, R., & Nematollahi, D. (2007). Algae removal by electro-coagulation process application for treatment of the effluent from an industrial wastewater treatment plant. Iranian Journal of Public Health, 36(4), 57–64.

Bahnasawy, A. H., Okasha, A. E., & Gonbeej, E. E. (2010). Performance evaluation of a laboratory scale spray dryer. Process Engineering, 27(January), 326–346.

Barros, A. I., Gonçalves, A. L., Simões, M., & Pires, J. C. M. (2014). Harvesting techniques applied to microalgae: A review. Renewable and Sustainable Energy Reviews, 41, 1489–1500.

Ben-Amotz, A. (2008) Presentation: "Large scale open algae ponds" NREL-AFOSR workshop algae workshop February. Arlington, Virginia.

Beychok, M. (2012). Fossil fuel combustion flue gases. Retrieved April 20, 2015, from http://www.eoearth.org/view/article/171355/

Bilanovic, D., Andargatchew, A., Kroeger, T., Shelef, G. (2009). Freshwater and marine microalgae sequestering of CO2 at different C and N concentrations—response surface methodology analysis. Energy Conversion and Management; 50(2): 262–7.

Boerderij. (2015). Grondprijzen Waterland en Noord-Hollandse Droogmakerijen. Retrieved June 18, 2015, from http://www.boerderij.nl/Home/grondmarkt/Grondprijzen/?gebied=2706

Borowitzka, M. (2013). High-value products from microalgae - their development and commercialization. J Appl Phycol; 25:743–56.

Boussiba, S., Vonshak, A. (1991). Astaxanthin accumulation in the green alga Haematococcus pluvialis. Plant Cell Physiol; 32:1077–82.

Boussiba, S., Vonshak, A., Cohen, Z., Richmond, A. (2000). Procedure for large-scale production of astaxanthin from Haematococcus. Google Patents.

Brennan, L., Owende, P. (2010). Biofuels from microalgae-A review of technologies for production, processing, and extractions of biofuels and co-products. Renewable and Sustainable Energy Reviews, 14, 557–577. doi:10.1016/j.rser.2009.10.009

Bucy, H. B., Baumgardner, M. E., & Marchese, A. J. (2012). Chemical and physical properties of algal methyl ester biodiesel containing varying levels of methyl eicosapentaenoate and methyl docosahexaenoate. Algal Research, 1(1), 57–69.

Cardozo, K. H. M., Guaratini, T., Barros, M. P., Falcão, V. R., Tonon, A. P., Lopes, N. P., … Pinto, E. (2007). Metabolites from algae with economical impact. Comparative Biochemistry and Physiology - C Toxicology and Pharmacology, 146, 60–78.

Chang, R. L., Ghamsari, L., Manichaikul, A., Hom, E. F. Y., Balaji, S., Fu, W., Shen, Y., Hao, T., Palsson, B., Salehi-Ashtiani, K., Papin, J. A. (2011). Metabolic network reconstruction of Chlamydomonas offers insight into light-driven algal metabolism. Mol. Syst. Biol 7; Article number 518.

Chen, C. Y., Yeh, K. L., Aisyah, R., Lee, D. J., Chang, J. S. (2011). Cultivation, photobioreactor design and harvesting of microalgae for biodiesel production: a critical review. Bioresource Technology, 102(1), 71–81.

Cheng, L., Zhang, L., Chen, H., Gao, C. (2006). Carbon dioxide removal from air by microalgae cultured in a membrane-photobioreactor. Sep. Purif. Technol. 50, 324–329.

Cheunbarn, S., & Peerapornpisal, Y. (2010). Cultivation of Spirulina platensis using Anaerobically Swine Wastewater Treatment Effluent, 586–590.

Chisti, Y. (2007). Biodiesel from microalgae. Biotechnol. Adv. 25, 294–306.

Chojnacka, K., Marquez-Rocha, F. J. (2004). Kinetic and stoichiometric relationships of the energy and carbon metabolism in the culture of microalgae. Biotechnology 3, 21–34.

Christenson, L., Sims, R. (2011). Production and harvesting of microalgae for wastewater treatment, biofuels and bioproducts. Biotechnol Adv ; 29: 686–702.

Clarens, A. F, Resurreccion, E. P, White, M. A, Colosi, L. M. (2010). Environmental life-cycle comparison of algae to other bioenergy feedstocks. Environ Sci Technol; 44:1813–9.

Conover, C. A., Poole, R. T., & Henley, R. W. (1991). Light and Fertilizer Recommendations for the Interior Maintenance of Acclimatized Foliage Plants. University of Florida IFAS. Retrieved April 13, 2015, from http://mrec.ifas.ufl.edu/foliage/resrpts/rh_91_7.htm

Cooney, M., Young, G., Nagle, N. (2009). Extraction of Bio-oils from Microalgae. Separation & Purification Reviews, 38(4), 291–325.

Costa, J. A. V., & de Morais, M. G. (2013). An Open Pond System for Microalgal Cultivation. Biofuels from Algae (pp. 1–22). Elsevier B.V.

Cuellar-Bermudez, S. P., Aguilar-Hernandez, I., Cardenas-Chavez, D. L., Ornelas-Soto, N., Romero-Ogawa, M. a., & Parra-Saldivar, R. (2014). Extraction and purification of high-value metabolites from microalgae: essential lipids, astaxanthin and phycobiliproteins. Microbial Biotechnology, 190–209.

Cyanotech. (2015). BioAstin - Natural Astaxanthin. Retrieved June 17, 2015, from http://www.cyanotech.com/bioastin.html

Danquah, M. K., Ang, L., Uduman, N., Moheimani, N., Forde, G. M. (2009). Dewatering of microalgal culture for biodiesel production: exploring polymer flocculation and tangential flow filtration. J Chem Technol Biotechnol; 84: 1078–83.

Del Campo, J. A, Rodríguez, H., Moreno, J., Vargas, M. Á, Rivas, J., Guerrero, M. G. (2004). Accumulation of astaxanthin and lutein in Chlorella zofingiensis (Chlorophyta). Appl Microbiol Biotechnol; 64:848–54.

Del Rio, E., Acién, F. G., García-Malea, M. C., Rivas, J., Molina-Grima, E., & Guerrero, M. G. (2005). Efficient one-step production of astaxanthin by the microalga Haematococcus pluvialis in continuous culture. Biotechnology and Bioengineering, 91(7), 808–815.

Del Rio, E., Acien, F. G., Garcia-Malea, M. C., Rivas, J., Molina-Grima, E., & Guerrero, M. G. (2007). Efficiency assessment of the one-step production of astaxanthin by the microalga Haematococcus pluvialis. Biotechnology and Bioengineering, 100(2), 397–402.

Delrue, F., Setier, P. a., Sahut, C., Cournac, L., Roubaud, a., Peltier, G., & Froment, a. K. (2012). An economic, sustainability, and energetic model of biodiesel production from microalgae. Bioresource Technology, 111, 191–200.

Demirbas, A. (2001). Biomass resource facilities and biomass conversion processing for fuels and chemicals. Energy Conversion and Management, 42,(11), 1357-1378.

Dominguez-Bocanegra, a. R., Guerrero Legarreta, I., Martinez Jeronimo, F., & Tomasini Campocosio, A. (2004). Influence of environmental and nutritional factors in the production of astaxanthin from Haematococcus pluvialis. Bioresource Technology, 92, 209–214.

Doucha, J., Straka, F., & Lívanský, K. (2005). Utilization of flue gas for cultivation of microalgae (Chlorella sp.) in an outdoor open thin-layer photobioreactor. Journal of Applied Phycology, 17, 403–412.

Doucha, J., & Lívanský, K. (2008). Influence of processing parameters on disintegration of Chlorella cells in various types of homogenizers. Applied Microbiology and Biotechnology, 81(3), 431–440.

Dragone, G., Fernandes, B., Vicente, A.A. and Teixeira, J.A. (2010), Third generation biofuels from microalgae in Current Research, Technology and Education Topics in Applied Microbiology and Microbial Biotechnology, Mendez-Vilas A (ed.), Formatex, 1355-1366.

Dragos, N., Bercea, V., Bica, A., Drugă, B., Nicoară, A., & Coman, C. (2010). Astaxanthin production from a new strain of haematococcus pluvialis grown in batch culture. Annals of the Romanian Society for Cell Biology, 15(2), 353–361.

Duan, P., Savage, P.E. (2010). Hydrothermal liquefaction of a microalga with heterogeneous catalysts. Industrial and Engineering Chemistry Research 50, 52–61.

EAE, Eijkelkamp Agrisearch Equipment. (2009). Evaporation Pan (Operating Instructions). The Netherlands.

(DEA). Danish Energy Agency, Energinet. (2012). Technology data for energy plants-Generation of Electricity and District Heating, Energy Storage and Energy Carrier Generation and Conversion.

Erdman, J. (2014). June 2014 Is Earth's Hottest June on Record: NOAA. Retrieved March 26, 2015, from http://www.weather.com/science/environment/news/june-2014-worlds-record-hottest-warmest-june-noaa-20140721

Eriksen, N. (2008). The technology of microalgal culturing. Biotechnology Letters; 30(9):1525–36.

Evens, T. J., Niedz, R. P., & Kirkpatrick, G. J. (2008). Temperature and irradiance impacts on the growth, pigmentation and photosystem II quantum yields of Haematococcus pluvialis (Chlorophyceae). Journal of Applied Phycology, 20, 411–422.

European Commission. (2015). VAT rates-Applied in the Member States of the European Union. Situation at 1st January 2015:1-29

Eurostat. (2015). File:Half-yearly electricity and gas prices, second half of year, 2012–14 (EUR per kWh) YB15.png - Statistics Explained. Retrieved June 15, 2015, from http://ec.europa.eu/eurostat/statistics-explained/index.php/File:Half-yearly_electricity_and_gas_prices,_second_half_of_year,_2012%E2%80%9314_(EUR_per_kWh)_YB15.png

EYATH. (2015). Invoice prices - Greece. Retrieved June 19, 2015, from http://www.eyath.gr/swift.jsp?CMCCode=060202

Fábregas, J., Otero, A., Maseda, A., & Domínguez, A. (2001). Two-stage cultures for the production of astaxanthin from Haematococcus pluvialis. Journal of Biotechnology, 89(1), 65–71.

García-Camacho, F., Gallard- Rodríguez, J., Sánchez-Mirón, A., Cerón-García, MC., Belarbi, EH., Chisti, Y., Molina-Grima, E. (2007). Biotechnological significance of toxic marine dinoflagellates. Biotechnol Adv; 25:176–94.

Garcia-Malea, M. C., Brindley, C., Del Rio, E., Acién, F. G., Fernández, J. M., & Molina, E. (2005). Modelling of growth and accumulation of carotenoids in Haematococcus pluvialis as a function of irradiance and nutrients supply. Biochemical Engineering Journal, 26(2-3), 107–114.

GEA Westfalia Separator Group. (2015). Separator GSE 300-06-777. Retrieved May 5, 2015, from http://www.westfalia-separator.com/products/product-finder/product/separator-gse-300-06-777.html

Giannelli, L., Yamada, H., Katsuda, T., & Yamaji, H. (2015). Effects of temperature on the astaxanthin productivity and light harvesting characteristics of the green alga Haematococcus pluvialis. Journal of Bioscience and Bioengineering, 119(3), 345–350.

Goodwin, T.W. (1984) The Biochemistry of the Carotenoids (Vols 1,2), Chapman & Hall

Goyal, H. B., Seal, D., & Saxena, R. C. (2008). Bio-fuels from thermochemical conversion of renewable resources: A review. Renewable and Sustainable Energy Reviews, 12(2), 504–517.

Greenstream Publishing. (2015). Solar Irradiance - calculate the solar energy available on your site. Retrieved March 28, 2015, from http://solarelectricityhandbook.com/solar-irradiance.html

Greenwell, H.C., Laurens, L.M.L., Shields, R.J., Lovitt, R.W., Flynn, K.J. (2010). Placing Microalgae on the Biofuels Priority List: A Review of the Technological Challenges. Journal of the Royal Society Interface, 7,(46), 703-726.

Gu, W., Xie, X., Gao, S., Zhou, W., Pan, G. (2013). Comparison of Different Cells of Haematococcus pluvialis Reveals an Extensive Acclimation Mechanism during its Aging Process: From a Perspective of Photosynthesis. PLoS ONE 8(7): e67028.

Guan, Q., Savage, P. E., & Wei, C. (2012). Gasification of alga Nannochloropsis sp. in supercritical water. Journal of Supercritical Fluids, 61, 139–145.

Guschina, I.A., Harwood, J.L. (2006). Lipids and lipid metabolism in eukaryotic algae. Prog. Lipid. Res. 45, 160–186.

Heasman, M., Diemar, J., O' Connor, W., Sushames, T., Foulkes, L., Nell, J.A. (2000) Development of extended shelf-life microalgae concentrate diets harvested by centrifugation for bivalve molluscs—a summary. Aquacult Res; 31(8 – 9):637– 59.

Hanotu, J., Bandulasena, H.C.H., Zimmerman, W.B. (2012). Microflotation performance for algal separation. Biotechnol Bioeng; 109:1663–73

He, P., Duncan, J., Barber, J. (2007). Astaxanthin accumulation in the green alga Haematococcus pluvialis: effects of cultivation parameters. J Integr Plant Biol; 49:447–51.

Harun, R., Singh, M., Forde, G., Danquah, M. (2010). Bioprocess engineering of microalgae to produce a variety of consumer products. Ren. Sustain. Energy Rev. 14, 1037–1047.

Huntley, M. E., & Redalje, D. G. (2007). CO2 mitigation and renewable oil from photosynthetic microbes: A new appraisal. Mitigation and Adaptation Strategies for Global Change (Vol. 12, pp. 573–608).

Iersel, S. van, Gamba, L., Rossi, A., Alberici, S., Dehue, B., Staaij, J. van de, & Flammini, A. (2009). Algae-based Biofuels: A Review of Challenges and Opportunities for Developing Countries, 1–50.

Imamoglu, E., Dalay, M. C, Sukan, F. V (2009). Influences of different stress media and high light intensities on accumulation of astaxanthin in the green alga Haematococcus pluvialis. New Biotechnol; 26:199–204.

Industry Experts. (2015). Global Astaxanthin Market – Sources, Technologies and Applications.

James, S. C., & Boriah, V. (2010). Modeling algae growth in an open-channel raceway. Journal of Computational Biology : A Journal of Computational Molecular Cell Biology, 17(7), 895–906.

Jannsen, M. (2002). "Cultivation of microalgae: effect of light/dark cycles on biomass yield" (PhD thesis). Wageningen University. Wageningen, the Netherlands, ISBN: 90-5808-592-9, 184 pages

Janssen, M., Tramper, J., Mur, L.R., Wijffels, R.H. (2003). Enclosed outdoor photobioreactors: light regime, photosynthetic efficiency, scale-up, and future prospects. Biotechnol. Bioeng. 81, 193–210.

Jonker, J. G. G., & Faaij, a. P. C. (2013). Techno-economic assessment of micro-algae as feedstock for renewable bio-energy production. *Applied Energy*, *102*, 461–475.

Jorquera, O., Kiperstok, A., Sales, E. a., Embiruçu, M., & Ghirardi, M. L. (2010). Comparative energy life-cycle analyses of microalgal biomass production in open ponds and photobioreactors. Bioresource Technology, 101(4), 1406–1413.

Kadirjo, A. (2011). Equipment used in cosmetics production. Retrieved May 15, 2015, from https://andriantoangkadirjo85.wordpress.com/tag/bead-mill/

Khoo, H. H., Koh, C. Y., Shaik, M. S., & Sharratt, P. N. (2013). Bioenergy co-products derived from microalgae biomass via thermochemical conversion - Life cycle energy balances and CO2 emissions. Bioresource Technology, 143, 298–307.

Kitsara, G., Floros, J., Papaioannou, G., & Kerkides, P. (2008). Spatial and Temporal Analysis of Pan Evaporation in Greece. Athens.

Kleinegris, D., Barbosa, M., Bosma, R., & Wijffels, R. (2014). Microalgae for energy.

KNMI. (2015). KNMI - Daily weather data for the Netherlands - Download. Retrieved March 06, 2015, from http://www.knmi.nl/climatology/daily_data/selection.cgi

Koller, M., Muhr, A., & Braunegg, G. (2014). Microalgae as versatile cellular factories for valued products. *Algal Research*, *6*, 52-63.

Kong, W.B., Song, H., Hua, S.F., Yang, H., Yang, Q.i., Xia, C.G. (2012). Enhancement of biomass and hydrocarbon productivities of Botryococcus braunii by mixotrophic cultivation and its application in brewery wastewater treatment. African Journal of Microbiology Research 61489–61496.

Leach, G., Oliveira, G., & Morais, R. (1998). Spray-drying of Dunaliella salina to produce a β-carotene rich powder. Journal of Industrial Microbiology and Biotechnology, 20(2), 82–85.

Lee, J.Y., Yoo, C., Jun, S.Y., Ahn, C.Y., Oh, H.M. (2010). Comparison of several methods for effective lipid extraction from microalgae. Bioresour. Technol. 101, 75–77.

Li, Y., Horsman, M., Wu, N., Lan, C., Dubois-Calero, N. (2008). Biofuels from microalgae. Biotechnology Progress; 24(4): 815–20.

Li, J., Zhu, D., Niu, J., Shen, S., & Wang, G. (2011). An economic assessment of astaxanthin production by large scale cultivation of Haematococcus pluvialis. Biotechnology Advances, 29(6), 568–574.

Liu, J.C., Chen, Y.M., Ju, Y.H. (1999). Separation of algal cells from water by column flotation. Sep Sci Technol; 34:2259–72.

Lohrey, C., & Kochergin, V. (2012). Biodiesel production from microalgae: Co-location with sugar mills. Bioresource Technology, 108(August), 76–82.

Lorenz, R. T., & Cysewski, G. R. (2000). Commercial potential for Haematococcus microalgae as a natural source of astaxanthin, 18(April), 160–167.

Ma, R.Y-N., Chen, F. (2001) Enhanced production of free trans-astaxanthin by oxidative stress in the cultures of the green microalga Chlorococcum sp. Process Biochem; 36:1175–9.

Maity, J. P., Bundschuh, J., Chen, C.-Y., & Bhattacharya, P. (2014). Microalgae for third generation biofuel production, mitigation of greenhouse gas emissions and wastewater treatment: Present and future perspectives – A mini review. Energy.

Marker, M., Tsavalos, A. J., & Young, A. J. (1996). Autotrophic growth and carotenoid production of Haematococcus pluvialis in a 30 liter air-lift photobioreactor. Journal of Fermentation and Bioengineering, 82(2), 113–118.

Markou, G., & Nerantzis, E. (2013). Microalgae for high-value compounds and biofuels production: a review with focus on cultivation under stress conditions. Biotechnology Advances, 31(8), 1532–42.

Mata, T. M., Martins, A. a., & Caetano, N. S. (2010). Microalgae for biodiesel production and other applications: A review. *Renewable and Sustainable Energy Reviews*, *14*(1), 217–232.

Mazzuca-Sobczuk, T., García-Camacho, F., Molina-Grima, E., Chisti, Y. (2006). Effects of agitation on the microalgae Phaeodactylum tricornutum and Porphyridium cruentum. Bioprocess Biosyst Eng; 28: 243–50.

McKendry, P. (2002). Energy production from biomass (part 1): Overview of biomass. Bioresource Technology, 83(1), 37–46.

Mendes-Pinto, M. M., Raposo, M. F. J., Bowen, J., Young, a. J., & Morais, R. (2001). Evaluation of different cell disruption processes on encysted cells of Haematococcus pluvialis: Effects on astaxanthin recovery and implications for bio-availability. Journal of Applied Phycology, 13(1), 19–24.

Mendes, R. L., Nobre, B. P., Cardoso, M. T., Pereira, A. P., & Palavra, A. F. (2003). Supercritical carbon dioxide extraction of compounds with pharmaceutical importance from microalgae. Inorganica Chimica Acta, 356, 328–334.

Mendiola, J. a., Jaime, L., Santoyo, S., Reglero, G., Cifuentes, a., Ibañez, E., & Señoráns, F. J. (2007). Screening of functional compounds in supercritical fluid extracts from Spirulina platensis. Food Chemistry, 102(4), 1357–1367.

Mercer, P., & Armenta, R. E. (2011). Developments in oil extraction from microalgae. European Journal of Lipid Science and Technology, 113(5), 539–547.

Milledge, J.J. (2010) Commercial application of microalgae other than as biofuels: a brief review. Rev Environ Sci Biotechnol: 1-11.

Milledge, J.J. (2012) Microalgae—commercial potential for fuel, food and feed, Food Sci. Technol. 26, 28–30.

Milledge, J. J. (2013). Energy Balance and Techno-economic Assessment of Algal Biofuel Production Systems.

Milledge, J., Smith, B., Dyer, P., & Harvey, P. (2014). Macroalgae-Derived Biofuel: A Review of Methods of Energy Extraction from Seaweed Biomass. Energies, 7(11), 7194–7222.

Mohan, S. V., Devi, M. P., Subhash, G. V., & Chandra, R. (2014). *Biofuels from Algae*. *Biofuels from Algae* (pp. 155–187). Elsevier.

Molina-Grima, E., Acién, F.G., García Camacho, F., Chisti, Y. (1999). Photobioreactors: light regime, mass transfer, and scaleup. J Biotechnol; 70:231–47.

Molina-Grima, E., Fernández, J., Acién, F. G., & Chisti, Y. (2001). Tubular photobioreactor design for algal cultures. Journal of Biotechnology, 92, 113–131.

Molina-Grima, E., Belarbi, E.H., Acién-Fernández, F.G., Robles-Medina, A., Chisti, Y. (2003). Recovery of microalgal biomass and metabolites: process options and economics. Biotechnol Adv; 20: 491–515.

Mollah, M. Y. a, Morkovsky, P., Gomes, J. a G., Kesmez, M., Parga, J., & Cocke, D. L. (2004). Fundamentals, present and future perspectives of electrocoagulation. Journal of Hazardous Materials, 114(1-3), 199–210.

Montagnes, D.J.S., and Franklin, D.J. (2001). Effect of temperature on diatom volume, growth rate, and carbon and nitrogen content: reconsidering some paradigms. Limnol. Oceanogr. 46, 2008–2018.

Murphy, C. F., & Allen, D. T. (2011). Energy-water nexus for mass cultivation of algae. Environmental Science & Technology, 45(13), 5861–8.

(NFIA). Netherlands Foreign Investment Agency. (2015). Business Environment & Taxation. Retrieved June 22, 2015, from http://nfia.com/businessenvironment.html

Nguyen, K. (2013). Astaxanthin: a comparative case of synthetic vs. natural production. Chemical and Biomolecular Engineering Publications and Other Works, 1(1), 1–11.

NOA. (2015). Weather Forecast. Retrieved March 06, 2015, from http://cirrus.meteo.noa.gr/forecast/bolam/index.htm

Nobre, B., Marcelo, F., Passos, R., Beirão, L., Palavra, A., Gouveia, L., & Mendes, R. (2006). Supercritical carbon dioxide extraction of astaxanthin and other carotenoids from the microalga Haematococcus pluvialis. European Food Research and Technology, 223(6), 787–790.

Nobre, B. P., Villalobos, F., Barragán, B. E., Oliveira, a. C., Batista, a. P., Marques, P. a S. S., … Gouveia, L. (2013). A bio-refinery from Nannochloropsis sp. microalga - Extraction of oils and pigments. Production of biohydrogen from the leftover biomass. Bioresource Technology, 135, 128–136.

Olaizola, M. (2003). Commercial development of microalgal biotechnology: From the test tube to the marketplace. Biomolecular Engineering, 20(4-6), 459–466.

Olguin, E.J., Giuliano, G., Porro, D., Tuberosa, R., Salamin, F. (2012). Biotechnology for a more sustainable world. Biotechnol. Adv. 30 (5), 931–932.

Orosa, M, Franqueira, D, Cid, A, Abalde, J. (2005). Analysis and enhancement of astaxanthin accumulation in Haematococcus pluvialis. Bioresource Technol 96:373–378.

Orosz, M. S., Forney, D. (2008). A comparison of algae to biofuel conversion pathways for energy storage off-grid (pp. 1–31).

Park, J. B. K., Craggs, R. J., & Shilton, a. N. (2011). Wastewater treatment high rate algal ponds for biofuel production. Bioresource Technology, 102(1), 35–42.

Panetas, G. (2015). Solar irradiation data of a 7500 m^2 photovoltaic park in Livadeia. Excel sheet. Athens.

PayScale. (2015). Average Salary in Netherlands. Retrieved June 19, 2015, from http://www.payscale.com/research/NL/Country=Netherlands/Salary

Perez-Garcia, R.O., Bashan, Y., Puente, M.E. (2011). Organic carbon supplementation of municipal wastewater is essential for heterotrophic growth and ammonium removing by the microalgae Chlorella vulgaris. J. Phycol., 190–199.

Pérez-López, P., González-García, S., Jeffryes, C., Agathos, S. N., McHugh, E., Walsh, D., … Moreira, M. T. (2014). Life-cycle assessment of the production of the red antioxidant carotenoid astaxanthin by microalgae: From lab to pilot scale. Journal of Cleaner Production, 64, 332–344.

Prime, J., Khan, S., & Wilkes, E. (2014). Energy Consumption in the UK (2014): Domestic energy consumption in the UK between 1970 and 2013. Department of Energy & Climate Change, (July).

Qin, S., Liu, G. X, Hu, Z. Y. (2008). The accumulation and metabolism of astaxanthin in Scenedesmus obliquus (Chlorophyceae). Process Biochem; 43:795–802.

Ramanathan, G., Rajarathinam, K., Boothapandi, M., Abirami, D., Ganesamoorthy, G., Duraipandi. (2011). Construction of vertical tubular photobioreactor for microalgae cultivation. J. Algal Biomass Utln. 2, 41–52.

Rawat, I., Ranjith-Kumar R., Mutanda, T., Bux, F. (2011). Dual role of microalgae: phycoremediation of domestic wastewater and biomass production for sustainable biofuels production. ApplEnergy; 88: 3411–24.

Razon, L. F., & Tan, R. R. (2011). Net energy analysis of the production of biodiesel and biogas from the microalgae: Haematococcus pluvialis and Nannochloropsis. Applied Energy, 88(10), 3507–3514.

Reppas, G. (2015). Vice president of R^2 Strom GmbH/R Energy SA. Personal communication.

Richmond, A. (2004) Handbook of microalgal culture: biotechnology and applied phycology. Blackwell Science Ltd;

Robert, M.H., Christina, E.C., Tom, N.K., Stephen, L.F., Oybek, K., David, R.S., et al. (2012). Evaluation of environmental impacts from microalgae cultivation in open-air raceway ponds: Analysis of the prior literature and investigation of wide variance in predicted impacts. Algal Research 1, 83–92.

Rodolfi, L., Zittelli, GC., Bassi, N., Padovani, G., Biondi, N., Bonini, G., Tredici, MR. (2008). Microalgae for oil: strain selection, induction of lipid synthesis and outdoor mass cultivation in a low-cost photobioreactor. Biotechnology and Bioengineering; 102(1):100–12.

Rogers, J. N., Rosenberg, J. N., Guzman, B. J., Oh, V. H., Mimbela, L. E., Ghassemi, A., … Donohue, M. D. (2013). A critical analysis of paddlewheel-driven raceway ponds for algal biofuel production at commercial scales. Algal Research, 4, 76–88.

Rubio, J., Souza, M.L., Smith, R.W. (2002). Overview of flotation as a wastewater treatment technique. Miner Eng; 15:139–55.

Rubio-Camacho, F., García Camacho, F., Fernández Sevilla, J. M., Chisti, Y., & Molina Grima, E. (2003). A mechanistic model of photosynthesis in microalgae. Biotechnology and Bioengineering, 81(4), 459–473. doi:10.1002/bit.10492

Sahena, F., Zaidul, I. S. M., Jinap, S., Karim, a. a., Abbas, K. a., Norulaini, N. a N., & Omar, a. K. M. (2009). Application of supercritical CO2 in lipid extraction - A review. Journal of Food Engineering, 95(2), 240–253.

Saidur, R., Abdelaziz, E. a., Demirbas, a., Hossain, M. S., & Mekhilef, S. (2011). A review on biomass as a fuel for boilers. Renewable and Sustainable Energy Reviews, 15(5), 2262–2289.

Salim, S., Bosma, R., Vermue, M.H., Wijffels R.H. (2011). Harvesting of microalgae by bioflocculation. J Appl Phycol; 23: 849–55.

Sánchez-Mirón, A., Contreras-Gómez, A., García-Camacho, F., Molina-Grima, E., Chisti, Y. (1999). Comparative evaluation of compact photobioreactors for large-scale monoculture of microalgae. J Biotechnol; 70:249–70.

Sarada, R., Tripathi, U., & Ravishankar, G. (2002). Influence of stress on astaxanthin production in Haematococcus pluvialis grown under different culture conditions. Process Biochemistry, 37(6), 623–627.

Sazdanoff, N., (2006) “Modeling and simulation of the algae to biodiesel fuel cycle” undergraduate Thesis, The Ohio State University.

Schenk, P. M., Thomas-Hall, S. R., Stephens, E., Marx, U. C., Mussgnug, J. H., Posten, C., Kruse, O., Hankamer, B. (2008). Second Generation Biofuels: High-Efficiency Microalgae for Biodiesel Production. BioEnergy Research, 1, 20–43.

Semerjian, L., Ayoub, G. M. (2003). High-pH-magnesium coagulation-flocculation in wastewater treatment. Advances in Environmental Research, 7(2), 389–403.

Shirvani, T., Yan, X., Inderwildi, O.R., Edwards, P.P., King, D.A. (2011). Life cycle energy and greenhouse gas analysis for algae-derived biodiesel. Energy Environ. Sci. 4, 3773–3778.

Show, K. Y., Lee, D. J., Chang, J. S. (2013). Algal biomass dehydration. Bioresource Technology, 135, 720–729.

Singh, A., & Olsen, S. I. (2011). A critical review of biochemical conversion, sustainability and life-cycle assessment of algal biofuels. Applied Energy, 88(10), 3548–3555.

Skjånes, K., Rebours, C., Lindblad, P. (2012). Potential for green microalgae to produce hydrogen, pharmaceuticals and other high value products in a combined process. Crit Rev Biotechnol:1–44.

Slade, R., & Bauen, A. (2013). Micro-algae cultivation for biofuels : cost , energy balance , environmental impacts and future prospects – Supplementary Information Life Cycle assessment meta-model approach and assumptions, (1), 1–28.

Spolaore, P., Joannis-Cassan, C., Duran, E., & Isambert, A. (2006). Commercial applications of microalgae. Journal of Bioscience and Bioengineering, 101(2), 87–96.

Stepan, D.J., Shockey, R.E., Moe, T.A., Dorn R. (2002). Carbon dioxide sequestering using microalgae systems. Pittsburgh, PA: U.S. Department of Energy.

Sukenik, a., Levy, R. S., Levy, Y., Falkowski, P. G., & Dubinsky, Z. (1991). Optimizing algal biomass production in an outdoor pond: a simulation model. Journal of Applied Phycology, 3, 191–201.

Sudhakar, K., Premalatha, M., Sudharshan, K. (2012a). Energy Balance and Exergy analysis of large scale algal biomass production, 66–69.

Sudhakar, K., Premalatha, M., & Rajesh, M. (2012b). Large-scale open pond algae biomass yield analysis in India: a case study. International Journal of Sustainable Energy, (March 2015).

Suh, I. S., & Lee, C.-G. (2003). Photobioreactor engineering: Design and performance. Biotechnology and Bioprocess Engineering, 8, 313–321.

Sun, A., Davis, R., Starbuck, M., Ben-Amotz, A., Pate, R., Pienkos, P.T. (2011). Comparative cost analysis of algal oil production for biofuels, Energy 36 (8) 5169–5179.

Sung, K.D., Lee, J.S., Shin, C.S., Park, S.C., Choi, M.J. (1999). CO2 fixation by Chlorella sp. KR-1 and its cultural characteristics. Biores. Technol. 68, 269–273.

Thana, P., Machmudah, S., Goto, M., Sasaki, M., Pavasant, P., & Shotipruk, A. (2008). Response surface methodology to supercritical carbon dioxide extraction of astaxanthin from Haematococcus pluvialis. Bioresource Technology, 99(8), 3110–3115.

The Engineering Toolbox. (2015). Gases - Densities. Retrieved April 21, 2015, from http://www.engineeringtoolbox.com/gas-density-d_158.html

Theoharis, M. (2014). Laboratory excercises on agricultural and greenhouse constructions. Arta, Greece: Technological Institue of Epirus.

Tomaselli, L. (2004), The microalgal cell. In: Richmond A, eds. Handbook of Microalgal Culture: Biotechnology and Applied Psychology. Oxford: Blackwell Publishing Ltd, 3-19.

Trading Economics. (2015). Greece Minimum Monthly Wage | 1999-2015 | Data | Chart | Calendar. Retrieved June 19, 2015, from http://www.tradingeconomics.com/greece/minimum-wages

Tredici, M. R. (2010). Photobiology of Microalgae Mass Cultures: Understanding the Tools for the Next Green Revolution. Biofuels, 1,(1), 143-162.

Tredici, M. R. (2012). Energy balance of microalgae cultures in photobioreactors and ponds. EU Workshop:Life Cycle Analysis of Algal Based Biofuels.

UCSB ScienceLine. (2015). Why does carbon dioxide in a solid state sublime? Retrieved May 27, 2015, from http://scienceline.ucsb.edu/getkey.php?key=4120

Uduman, N.,Qi, Y., Danquah, M.K., Forde, G.M., Hoadley, A. (2010). Dewatering of microalgal cultures: a major bottleneck to algae-based fuels. J Renew Sustain Energy; 2: 012701–15.

Ugwu CU, Aoyagi H, Uchiyama H. (2008). Photobioreactors for mass cultivation of algae. Bioresource Technology; 99(10):4021–8.

Valderrama, J. O., Perrut, M., Majewski, W., & Serena, L. (2003). Extraction of Astaxantine and Phycocyanine from Microalgae with Supercritical Carbon Dioxide Extraction of Astaxantine and Phycocyanine from Microalgae with Supercritical Carbon Dioxide, 827–830.

Van Den Hende, S., Vervaeren, H., Desmet, S., Boon, N. (2011). Bioflocculation of Microalgae and Bacteria Combined with Flue Gas to Improve Sewage Treatment. New Biotechnology, 29,(1), 23-31.

Vandamme, D., Foubert, I., Muylaert, K. (2013). Flocculation as a low-cost method for harvesting microalgae for bulk biomass production.TrendsBiotechnol; 31:233–9.

Vanthoor-Koopmans, M., Wijffels, R.H., Barbosa, M.J., Eppink, M.H.M. (2013). Bio-refinery of microalgae for food and fuel. Bioresour Technol; 135:142–9.

Venkata Subhash, G., Chandra, R., Venkata Mohan, S. (2013). Microalgae mediated bio-electrocatalytic fuel cell facilitates bioelectricity generation through oxygenic photomixotrophic mechanism. Bioresour. Technol.

Vitens (2015). Industrial water price in the Nethelands. Personal communication.

Wang, B., Li, Y., Wu, N., Lan, C.Q. (2008). CO2 bio-mitigation using microalgae. Applied Microbiology and Biotechnology; 79(5):707–18.

Weissman, J., Raymond, P.G., Benemann, J.R. (1988). Mixing, carbon utilization and oxygen accumulation. Biotechnology and Bioengineering; 31:336–44.

Weissman, J., Tillet, D., & Goebel, R. (1989). Design and Operation of an Outdoor Microalgae Test Facility, (October), 25.

Wijffels, R., & Barbosa, M. (2013). Smart solutions to optimize biodiesel production in green microalgae. AlgaePARC, Wageningen University.

Wijffels, R.H., Kruse, O., Hellingwerf, K.J. (2013). Potential of industrial biotechnology with cyanobacteria and eukaryotic microalgae, Curr. Opin. Biotechnol. 24, 405–413.

Williams, P. J. L. B., Laurens, L. M. L. (2010). Microalgae as Biodiesel & Biomass Feedstocks: Review & Analysis of the Biochemistry, Energetics & Economics. Energy & Environmental Science, 3,(5), 554-590.

X-Rates. (2015). Exchange Rates. Retrieved June 19, 2015, from http://www.x-rates.com/

XE. (2015). Advertisements for agricultural land in Livadeia. Retrieved June 18, 2015, from http://www.xe.gr/property/poliseis%7Cagrotemaxia%7Clevadeon.html

Xin, L., Hong-ying, H., Ke, G., & Ying-xue, S. (2010). Effects of different nitrogen and phosphorus concentrations on the growth, nutrient uptake, and lipid accumulation of a freshwater microalga Scenedesmus sp. Bioresource Technology, 101(14), 5494–5500.

Zaimes, G. G., Khanna, V. (2013). Microalgal biomass production pathways: evaluation of life-cycle environmental impacts. Biotechnology for Biofuels, 6(1), 88.

Zajonc, A., Roychoudhuri, C., Rajarshi, R., Loudon, R., Finkelstein, D., Muthukrishnan, A., … Schleich, W. P. (2003). On the dual nature of light. Optics & Photonic News, 14(10), 1–35.

Zamalloa, C., Vulsteke, E., Albrecht, J., Verstraete, W. (2011). The Techno-Economic Potential of Renewable Energy through the Anaerobic Digestion of Microalgae. Bioresource Technology, 102,(2), 1149-1158.

Zednik, T. (2015). Weather averages for Bhopal, India |. Retrieved June 30, 2015, from http://weather-averages.com/location/in/1275841-bhopal

Zenouzi, A., Ghobadian, B., Hejazi, M., Rahnemoon, P. (2013). Harvesting of microalgae Dunaliella salina using electroflocculation. J Agric Sci Technol; 15:879–88.

Zhang, X. W., Gong, X. D., & Chen, F. (1999). Kinetic models for astaxanthin production by high cell density mixotrophic culture of the microalga Haematococcus pluvialis. Journal of Industrial Microbiology & Biotechnology, 23(1), 691–696.

Zhang, B. Y., Geng, Y. H., Li, Z. K., Hu, H. J., & Li, Y. G. (2009). Production of astaxanthin from Haematococcus in open pond by two-stage growth one-step process. Aquaculture, 295(3-4), 275–281.

Zhang, W., Wang, J., Wang, J., & Liu, T. (2014). Bioresource Technology. Attached cultivation of Haematococcus pluvialis for astaxanthin production. BIORESOURCE TECHNOLOGY, 158, 329–335.

Zhekisheva M, Zarka A, Khozin-Goldberg I, Cohen Z, Boussiba S. (2005). Inhibition of astaxanthin synthesis under high irradiance does not abolish triacylglycerol accumulation in the green alga Haematococcus pluvialis (Chlorophyceae). J Phycol 41:819–826.

Zhu, X. G., Long, S. P., & Ort, D. R. (2008). What is the maximum efficiency with which photosynthesis can convert solar energy into biomass? Current Opinion in Biotechnology, 19(Figure 1), 153–159.

Appendix A: Weight Analysis of the chemical elements in the initial medium recipe

The initial recipe comprised of various chemical compounds expressed in mM (milimolar) for the macronutrients and in μM (micromolar) for the micronutrients. The SI units for molar concentration are mol/m^3. However, most chemical literature traditionally uses mol/dm^3, which is the same as mol/liter. These traditional units are often denoted by a capital letter M (pronounced "molar"). In order to find the weight percentage of each chemical element presented in table 6, the molar has to be converted into gram/liter. This can be accomplished by using the atomic masses of each chemical element. The results are presented below, in table A:

Compounds		Element	Weight (grams/liter)
10mM KNO_3	**Macronutrients**	Potassium (K)	0.39
		Nitrogen (N)	0.14
		Oxygen (O)	0.48
2mM Na_2HPO_4		Sodium (Na)	0.092
		Hydrogen (H)	0.002
		Phosphorus (P)	0.062
		Oxygen (O)	0.128
2mM $NaHCO_3$		Sodium (Na)	0.046
		Hydrogen (H)	0.002
		Carbon (C)	0.024
		Oxygen (O)	0.096
0.5mM $MgSO_4$		Magnesium (Mg)	0.012
		Sulfur (S)	0.016
		Oxygen (O)	0.032
50μM H_3BO_3	**Micronutrients**	Hydrogen (H)	0.00015
		Boron (B)	0.00055
		Oxygen (O)	0.0024
50μM $C_{10}H_{16}N_2O_8$		Carbon (C)	0.006
		Hydrogen (H)	0.0008
		Nitrogen (N)	0.0014
		Oxygen (O)	0.0064
10μM $MnCl_2$		Manganese (Mn)	0.00055
		Chlorine (Cl)	0.00071
5μM $FeCl_3$		Iron (Fe)	0.00028
		Chlorine (Cl)	0.00053
2μM Na_2MnO_4		Sodium (Na)	0.000092
		Manganese (Mn)	0.00011
		Oxygen (O)	0.00013
1.5μM $NaVO_3$		Sodium (Na)	0.000035
		Vanadium (V)	0.000077
		Oxygen (O)	0.000072
0.8μM $ZnSO_4$		Zinc (Zn)	0.000052
		Sulfur (S)	0.000026
		Oxygen (O)	0.000051
0.4μM $CuSO_4$		Copper (Cu)	0.000025
		Sulfur (S)	0.000013
		Oxygen (O)	0.000026
0.2μM $CoCl_2$		Cobalt (Co)	0.000012
		Chlorine (Cl)	0.000014

Table A: Analysis of the chemical compounds, which the initial medium recipe in the tubular PBR (Li et al., 2011).

Appendix B: Stages of tubes needed for the tubular PBR fence

As mentioned in section 6.1, the volume of broth all through the 'green' and 'red stage' should be the same. In order to find the ratio between the volumes, which will designate the number of stages of tubes needed to build the tubular PBR fence, an area of one hectare for the fence and the raceway pond is assumed. Admittedly, no matter which area is chosen, the ratio does not change, in case this area is the same for both systems. The area of one hectare is assumed to have a length and width of 100 meters. Taking into account the chosen depth for the raceway pond (i.e. 0.3m, see table 11) and assuming that the raceway pond covers the whole area, the total volume of the pond amounts to:

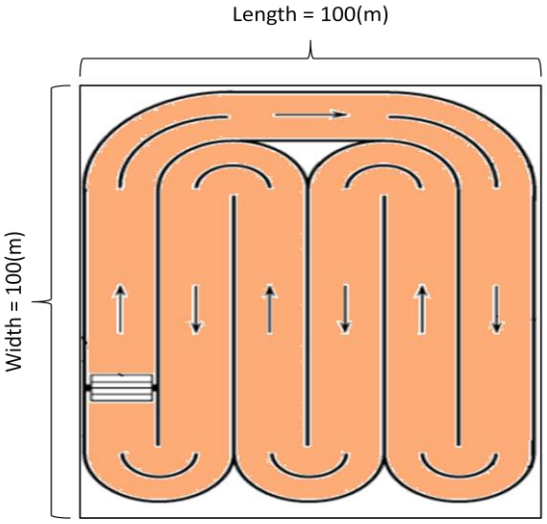

Figure B1: Plot of the cultivation area using a raceway pond.

$$V_{POND} = \text{Length} * \text{Width} * \text{Depth} \Leftrightarrow$$

$$V_{POND} = 100(\text{m}) * 100(\text{m}) * 0.3(\text{m}) \Leftrightarrow$$

$$V_{POND} = 3000\ (\text{m}^3)$$

Regarding the horizontal tubular PBR, it is assumed that the distance between the tubes is 0.05 meters. Taking into account the depth of the tubes, which is simultaneously the diameter of the cylinder (i.e. 0.05m, see table 11), the amount of tubes that constitute the first stage and cover the area of one hectare can be calculated at follows:

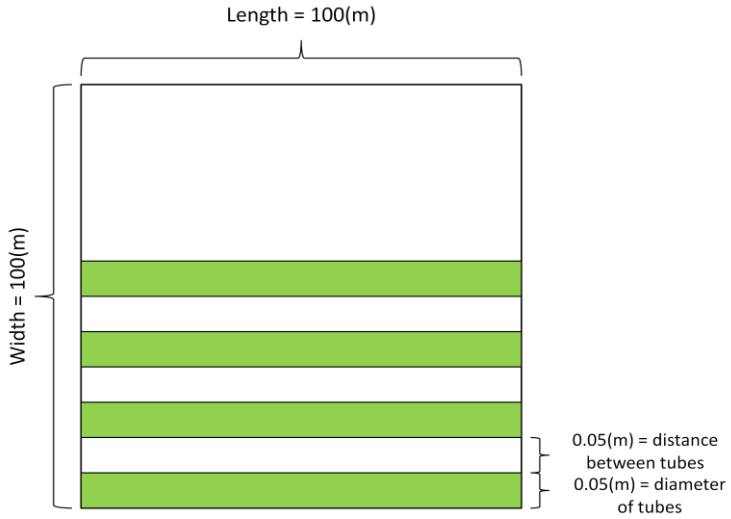

Figure B2: Plot of the cultivation area using a horizontal tubular PBR fence.

$$N_{TUBES} = \frac{\text{Width}}{(\text{Distance between tubes} + \text{Diameter of tubes})} \Leftrightarrow$$

$$N_{TUBES} = \frac{100(m)}{[0.05(m) + 0.05(m)]} \Leftrightarrow$$

$$N_{TUBES} = 1000(\text{tubes})$$

The next step is to calculate the volume of the tubes of the first stage that covers the selected area. The tube is a cylinder and the volume of a cylinder with radius r and length L is given by the following formula:

$$V_{CYLINDER} = \pi * r^2 * L$$

The total volume of the first stage would then amount to:

$$V_{FIRST\ STAGE} = 1000 * \pi * r^2 * L \Leftrightarrow$$

$$V_{FIRST\ STAGE} = 1000 * 3.14 * [0.025(m)]^2 * 100(m) \Leftrightarrow$$

$$V_{FIRST\ STAGE} = 196(m^3)$$

Nevertheless, the volume of the horizontal photobioreactor should be equal with the volume of the raceway pond. The number of stages could then be calculated at follows:

$$V_{POND} = V_{PBR} \Leftrightarrow$$

$$V_{POND} = V_{FIRST\ STAGE} * N_{STAGES} \Leftrightarrow$$

$$N_{STAGES} = \frac{3000(m^3)}{196(m^3)} \Leftrightarrow$$

$$N_{STAGES} = 15$$

In retrospect, all through 'green stage' a 15-stage horizontal tubular PBR fence should be selected for stimulating *Haematococcus pluvialis* cultivation.

Appendix C: Mass Balances

C1: Nutrients

The weight analysis in appendix A led to the weight concentration of each chemical element existed in the 'initial medium recipe' (in grams/liter). In order to calculate the initial composition of the macronutrients (KNO_3, Na_2HPO_4, $NaHCO_3$, $MgSO_4$) and taking into account the volume of the horizontal tubular PBR fence as well as the daily medium renewal rate and the nutrient utilization efficiency, the following formula can be used:

$$(\text{Compound Demand}) = (\text{days}) * \frac{V_{PBR} * (\text{Compound Concentration}) * (\text{Daily renewal rate})}{\eta_{\text{Utilization}}}$$

The days in an annual basis correspond to 360. The volume of the horizontal tubular PBR fence amounts to 3000(m^3), while the compound concentration is the sum of the elemental weight concentrations of each macronutrient depicted in table A (see Appendix A). Regarding the daily medium renewal rate, the value of 25% was assumed for Livadeia, which is the same as the one mentioned by Li et al. (2011) using the same hybrid system as selected in this study. The reason for this decision was explained in detail in section 8.1. In order to find the renewal rate for Amsterdam, the interaction between nutrients uptake and solar intensity is taken into account. As goes for all plants, nutrients uptake by algal cells and solar intensity have a proportionate linear behavior. In other words, the higher the solar intensity, the higher the ability of microalgae to metabolize the inoculated fertilizers (Conover et al., 1991; Wijffels & Barbosa, 2013). Since Amsterdam experiences lower solar intensities all-year than Livadeia, the daily medium renewal rate for Amsterdam can be calculated using the renewal rate of Livadeia as a benchmark: Dividing the annual solar intensity of Amsterdam with the respective value of Livadeia, the conversion factor between the annual solar intensities of the two cities can be determined. Table 9 provides the appropriate data for calculation. The conversion factor amounts to 0.72. Multiplying this value with the daily medium renewal rate of Livadeia (i.e. 25%), the daily medium renewal rate of Amsterdam can be calculated; this is 18%. The $\eta_{\text{Utilization}}$ amounts to 75% for raceway ponds and 90% for tubular PBRs (see section 8.1). Regarding the micronutrients, their weight concentration as a whole in the 'initial medium recipe' was used in order to calculate the demand. Last but not least, all through 'red stage' the algal cells were subjected to complete nutrient starvation, which means that nutrient demand for this stage equals to zero (see section 8.1).

C2: Carbon Dioxide & Oxygen

In order to calculate the CO_2 demand for the horizontal tubular PBR as well as the raceway pond during cultivation, it would be sufficient to multiply biomass productivity with the multiplication factor of 1.8 (tons CO_2/ton biomass) (see sections 3.6.4 and 8.2). Nonetheless, carbon is introduced into the system from the injection of some nutrients that contain carbon, such as $NaHCO_3$. This carbon is in a soluble form and can be absorbed from the algal cells. Therefore, since in this thesis, the demand of nutrients is determined separately and multiplication factor of 1.8 (tons CO_2/ton biomass) includes all the carbon needed during cultivation, the amount of the soluble carbon, existed in the fertilizers and which was metabolized by the algal cells should be excluded. The quota of C

existed in the 'initial medium recipe' amounts to 1.95% (see table 6). Thus, CO_2 demand can be calculated at follows:

$$CO_2 = \frac{(\text{Biomass Productivity} * 1.8) - [(\text{annual Carbon in fertilizers}) * (\frac{44}{12})]}{\eta_{\text{Utilization}}}$$

The $\eta_{Utilization}$ amounts to 35% for the raceway pond ('red stage') and 75% for the horizontal tubular PBR ('green stage'). During 'red stage', it was assumed that the *Haematococcus pluvialis* cells were subjected into complete nutrient starvation (see section 8.1), meaning that no fertilizers including carbon were inoculated in the raceway pond. As a consequence, the subtractive factor in the abovementioned formula that describes the volume of soluble carbon in the growth medium equals zero.

The second inflow of CO_2 in the production line refers to supercritical CO_2 extraction during extraction phase. In order to calculate the amount of solvent (CO_2 enhanced with ethanol as co-solvent at 9.4%) per kg of feed (i.e. 'red' biomass) at 2.5% astaxanthin content needed to recover astaxanthin successfully a linear trend-line using data from Valderrama et al. (2003) was created. Figure C1 depicts this trend-line:

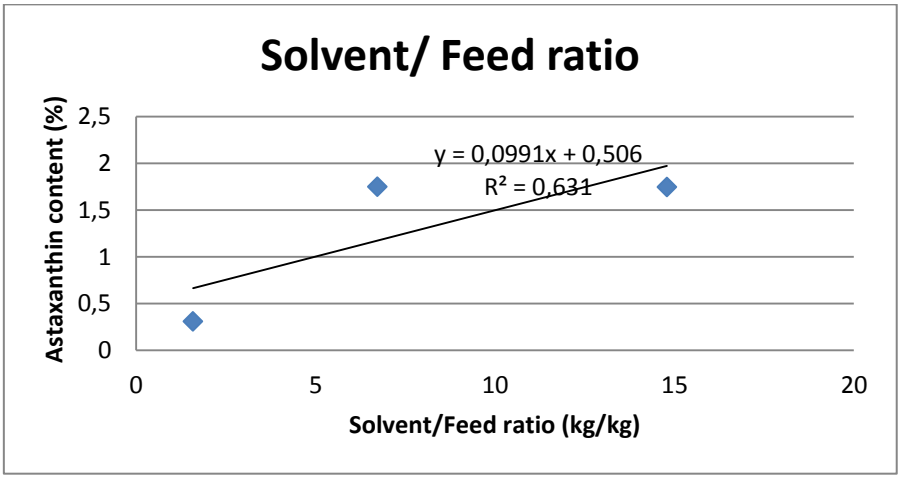

Figure C1: Solvent/feed ratio as function of astaxanthin content.

Using the formula corresponding to the linear trend-line, the solvent/feed ratio (kg/kg) can be calculated for the desired astaxanthin content. At 2.5% astaxanthin content (the assumed value for this study), the solvent/feed ratio was calculated 20.12. Admittedly, supercritical CO_2 extraction is implemented only on 'red' biomass (after 'red stage' cultivation) and not after 'green stage'.

The in- and outflows of molecular oxygen (O_2) in our system during cultivation involve the following parts: First, using CO_2 demand as a benchmark, the amount of oxygen existed in the flue gas is determined. Carbon dioxide corresponds to 10% v/v of the total flue gases (see section 3.6.4). Having calculated the demand of CO_2 in tons and using the density of CO_2, the total volume of flue gases for each stage and consequently the amount of O_2 can be calculated. An example is presented: The demand of CO_2 for the 'green stage' in Livadeia amounts to 46.9 tons. The density of CO_2 in normal

conditions[32] corresponds to ρ=1.84 (kg/m^3) (The Engineering Toolbox, 2015). The annual volume of CO_2 would then amount to:

$$V_{CO2} = \frac{m_{CO2}}{\rho_{CO2}} = \frac{46.9 * 10^3 (kg)}{1.84 \left(\frac{kg}{m^3}\right)} = 25489 (m^3)$$

This volume suggests 10% of the total volume of flue gases. This means that the total amount of flue gases supplied into the PBR for Livadeia equals to 254890 (m^3) annually. The fraction of oxygen in the flue gases corresponds to 3% v/v (see section 3.6.4), which leads to an annual volume of 358700*3%= 7647 (m^3). The density of O_2 equals to ρ=1.33 (kg/m^3) in normal conditions. Consequently, the annual mass uptake of O_2 for 'green stage' in Livadeia amounts to:

$$m_{O2 \text{ from flue gases}} = V_{O2} * \rho_{O2} = 10760 (m^3) * 1.33 \left(\frac{kg}{m^3}\right) = 10.2 (t)$$

The same calculation was followed for the two stages in the selected cities. Regarding utilization efficiency the abovementioned calculation includes the utilization efficiency used in the CO_2 demand determination. Thus, it is assumed that the utilization efficiency of O_2 coincides with the one of CO_2; namely, 35% for the raceway pond ('red stage') and 75% for the horizontal tubular PBR ('green stage'). Indisputably, the rest is degassed respectively.

The second part of O_2 mass balance involves the amount of molecular oxygen inoculated via the medium recipe. In Appendix C1 the annual demand of fertilizers was calculated. In table 6 the weight fraction of O in the medium recipe is presented; this amounts to 48.32%. Using this percentage and the total demand of fertilizers the annual amount of O_2 existing in the growth medium due to inoculation of macro- and micronutrients can be calculated for the 'green stage'. Since no fertilizers were inoculated all through 'red stage', the mass of O_2 for this stage equals to zero. The formula to calculate the annual mass of O_2 inoculated in the PBR ('green stage') via the medium recipe is given below:

$$O_{2 \text{ in nutrients}} = \frac{(\text{annual total Nutrients demand}) * (\%\ O \text{ in Nutrients})}{2}$$

The third part refers to the amount of oxygen inside the algal cell. The determination of this mass can be achieved by multiplying the concentration of oxygen in microalgae (27% and 29% for the 'green' and the 'red stage' respectively) with the annual biomass productivity of each stage. In other words using the following formula:

$$O_{2 \text{ in algal cell}} = \frac{(\text{annual Biomass Productivity}) * (\%\ O \text{ in algal cells})}{2}$$

The fourth and last part of the molecular oxygen's mass balance revolves around microalgae's tolerance of O_2 levels inside the growth medium. In section 3.6.4 these levels were mentioned; namely, the O_2 limit, above which microalgae suffer, ranges from 25-40 (mg/liter of water). Knowing the volume of water needed in the two parts of the hybrid system annually and taking into account the average value of this range (i.e. 32 mg/liter of water), the suffering limit in an annual basis can be

[32] Normal conditions refer to normal temperature and pressure for gases, which correspond to 20°C and 1 (atm) respectively (The Engineering Toolbox, 2015).

determined. Excluding the amount of O_2 trapped in the algal cells, the rest amount of O_2 that exists in the broth has to be extracted. In PBRs this process is accomplished using an exhaust, while in raceway ponds it happens naturally since raceways are open to the atmosphere. The amount of O_2 to be extracted can be calculated by just subtracting this limit from the sum of all inflows.

C3: Water

The demand of water is one of the most important parameters to be taken into account during cultivation. As mentioned in section 8.3, the suspended solids of microalgae amount to 0.035% and 0.3% for raceway ponds and PBRs respectively. Considering that density of water is 1000 (kg/m^3), the volume of water (in m^3) needed can be calculated; admittedly cubic meters of water equal tons. However, hydrogen can be introduced into the system when inoculating the fertilizers (see table 6). This chemical compartment is in a soluble form and therefore it has to be excluded from water demand calculation. Last but not least, the loss of water due to evapotranspiration has to be also considered. This loss must be replaced by adding fresh water, something that increases water demand. The formula for calculating water demand in an annual basis for the two stages is given below:

$$\text{Water Demand} = \frac{\frac{\text{Productivity}}{\%\text{ suspended solids}} * (1 - \%\text{ suspended solids})}{\rho_{\text{WATER}}} - \left[(\text{H in fertilizers}) * \left(\frac{18}{2}\right)\right] + \text{Evapotraspiration losses}$$

It is assumed that there are no evapotranspiration losses during the 'green stage', since the tubular PBR fence is a closed system. The evapotranspiration losses all through the 'red stage' (i.e. raceway pond) were calculated adjusting local annual evapotranspiration data for the selected cities. More specifically, Kitsara et al. (2008) have calculated the annual evapotranspiration for Livadeia, using 'class A' evaporation pan. The dimensions of this round pan are 54mm in height and 1206mm in diameter (EAE, 2009). The annual reference height of evapotranspiration for Livadeia was calculated 1131(mm/y) (Kitsara et al., 2008). We can adjust these data to the needs of the raceway pond in Livadeia as follows: First, it is assumed that the reference evapotranspition calculated during 2008 by Kitsara et al. (2008) stands for 2014 as well. The annual reference volume of evapotranspirated water can be calculated using the following formula:

$$\text{V}_{\text{REFERENCE}} = \text{Area}_{\text{PAN}} * \text{Height of Evapotranspiration} \Leftrightarrow$$

$$\text{V}_{\text{REFERENCE}} = \pi * \text{radius}^2 * 1.131(\text{m/y}) \Leftrightarrow$$

$$\text{V}_{\text{REFERENCE}} = \pi * [\frac{1.206(\text{m})}{2}]^2 * 1.131(\text{m/y}) \Leftrightarrow$$

$$\text{V}_{\text{REFERENCE}} = 1.29(\text{m}^3/\text{y})$$

In an area of 1.14(m^2) (i.e. the area of the evaporation pan) the annual reference volume of evapotraspiration amounts to 1.29(m^3). For 1 ha (i.e. 10000 m^2), which is the cultivated area in this study, the annual evapotranspirated water in Livadeia would then amount to 11316(m^3) or 11316(tons) of water. The same calculation was done for Amsterdam. The annual reference height of evapotranspiration for 2014 was calculated 625(mm/y), using data from KNMI (2015). Thus, the annual reference volume of evapotranspirated water mounts to 0.71(m^3). Consequently, the annual evapotranspirated water for 1 ha in Amsterdam would then amount to 6228(m^3) or 6228(tons) of

water. The evapotranspiration losses, all through 'green stage', were assumed as zero (see section 8.3).

Furthermore, as during 'red stage' no fertilizers were inoculated, the subtractive factor that describes the volume of soluble Hydrogen in the growth medium was not considered for this stage.

Last but not least, regarding harvesting phase, taking into account the fraction of suspended solids in the algal cake (i.e. 12%) after applying disk-stack centrifugation (recovery efficiency RE_{CENTR}=98%), the water in the cake can be calculated. The formula is given below:

$$\text{Water in cake after centrifucation} = \frac{\frac{\text{Productivity} * \text{RE}_{\text{CENTR}}}{\%\ \text{suspended solids}} * (1 - \%\ \text{suspended solids})}{\rho_{\text{WATER}}}$$

The moisture content in the 'red' biomass, after implementing spray drying, amounts to 5%. Using the productivity after centrifugation (i.e. applying recovery efficiency of 98%), and taking into account the recovery efficiencies for bead milling (RE_{BEAD}=100%) and spray drying (RE_{SPRAY}=98%) and moisture content (i.e. 5%) after spray drying, the water in the dried powder can be determined using the following formula:

$$\text{Water in powder} = \text{Productivity}_{\text{after centrifugation}} * \text{RE}_{\text{BEAD}} * \text{RE}_{\text{SPRAY}} * \%\ \text{moisture}$$

Admittedly, disk-stack centrifugation and spray drying were applied only after accumulation of astaxanthin in the raceway pond (i.e. only after 'red stage') and not after 'green stage'.

Appendix D: Capacity and costs of harvesting equipment

In order to determine the capital costs of the harvesting equipment (i.e. disk-stack centrifuge and centrifuge feed pump) its capacity has to be calculated. The capacity of the harvesting equipment depends on the amount of broth (m^3) that has to be processed in a time span of one hour. Taking into account the specific 'wet' productivity after 'red stage' for each month (calculated by the process model) as well as the active production hours per month and the concentration of microalgae all through 'red stage' (0.35g/l or $3.5*10^{-4}$ ton/m^3) the capacity of the harvesting equipment per month for each of the selected location can be determined:

$$\text{Capacity} = \frac{\frac{\text{'Wet' Productivity per month}}{\text{active hours per month}}}{\%\ \text{suspended solids}}$$

Table D portrays the results centrifuge capacity for the selected locations:

Month	Livadeia	Amsterdam
	Capacity (m^3/hour)	
January	1.43	0
February	2.22	0
March	3.40	1.14
April	6.46	2.02
May	13.52	6.57
June	36.45	13.65
July	50.95	19.43
August	48.48	18.62
September	29.93	14.10
October	9.52	4.76
November	6.20	0
December	2.86	0

Table D: Harvesting equipment capacity.

For the determination of capital costs of the harvesting equipment the highest capacity is taking into account as a benchmark. This is 50.95 (m^3/hour) and 19.43 (m^3/hour) for Livadeia and Amsterdam respectively. The centrifuge that will be purchased has to facilitate the respective capacities. Liaoning Fuyi Machinery Co., Ltd is a manufacturer and trading companies that construct high-end disk-stack centrifuges of different capacities for bioengineering processes. The DHC-730 model (capacity of 50-80 (m^3/hour)) costs $58000. This model is selected for Livadeia. Regarding Amsterdam, the DHC-550 model (capacity of 8-15 (m^3/hour)) is selected. The price of this model was estimated, since the supplier's platform mentions only the range ($15000-58000 for 0.5-80 ($m^3$/hour)). The estimated price for DHC-550 model amounts to $50000 (Alibaba Group, 2015a).

Regarding the centrifuge feed pump, the reference value reported by Molina-Grima et al. (2003) was adjusted to the capacity of the disk-stack centrifuge presented in table D. The reference value amounts to 281.3 ($/$m^3$/h) or 247.5 (€/$m^3$/h). Considering the highest capacity the costs of the centrifuge feed pump can be calculated for the selected locations: 12610 € and 4800 € for Livadeia and Amsterdam respectively.